# Toward a Drug Delivery Coating for Intraocular Lenses



by

Renée Chivon Smith

B.S. Chemistry
University of North Carolina – Chapel Hill, 2005

SUBMITTED TO THE HARVARD-MIT DIVISION OF HEALTH SCIENCES AND TECHNOLOGY IN PARTIAL FULFILLMENT OF THE REQUIREMENTS FOR THE DEGREE OF

DOCTOR OF PHILOSOPHY IN CHEMISTRY AND BIOMEDICAL ENGINEERING

AT THE

MASSACHUSETTS INSTITUTE OF TECHNOLOGY

May 2010
[June 2010]





Signature of Author:_____
Harvard-M.I.T Division of Health Sciences and Technology
May 3, 2010

Certified by:_____
Paula T. Hammond, Ph.D.
Bayer Chair Professor of Chemical Engineering and Executive Officer
Thesis Supervisor

Accepted by:_____
Ram Sasisekharan, Ph.D.
Director, Harvard-MIT Division of Health Sciences and Technology
Edward Hood Taplin Professor of Health Sciences & Technology and Biological Engineering

This page was intentionally left blank.

# Toward a Drug Delivery Coating for Intraocular Lenses

by

Renée Chivon Smith

Submitted to the Harvard-M.I.T Division of Health Sciences and Technology
on May 3, 2010, in partial fulfillment of the requirements for the degree of
Doctor of Philosophy in Chemistry and Biomedical Engineering

ABSTRACT

Layer-by-layer assembly has become a quintessential tool for the creation of versatile, dynamic nanostructured materials able to dictate cellular behavior through exquisite surface functionality and delivery of bioactive agents. The primary aim of this work was to use layer-by-layer assembly to advance ophthalmic drug delivery modalities post cataract surgery to overcome the challenges of traditional postoperative therapy. Hydrolytically degradable multilayer films were used to create a multi-drug delivery coating for intraocular lenses (IOL). The establishment of a drug delivery coating for intraocular lenses required key advances in ultrathin film technology.

This thesis focused on rational polymer design for tailored release, incorporation of hydrophobic small molecule therapeutics, and controlled multi-agent release. Fabrication rules and design tools necessary to create hydrolytically degradable polyelectrolyte multilayer films with preprogrammed advanced engineered release kinetics were investigated. A correlation between polycation hydrophobicity, as determined using octanol:water coefficients, allowed for the reliable prediction of release dynamics. A novel ultrathin system able to produce programmable zero order release kinetics of uncharged or hydrophobic small molecule therapeutics was developed. Charged cyclodextrin polymers were essential for the trapping of cyclodextrin–drug complexes in stable, surface eroding films capable of sustained drug release without altering therapeutic activity.

*In vitro* investigation of cellular interactions with hydrolytically degradable multilayer films containing anti-inflammatory agents was conducted. These anti-inflammatory films controlled inflammation over physiologically relevant timescales and maintained the transparency and optical clarity of the IOL. Lastly, the first multilayer thin film system able to address the demands of both infection and inflammation, using small molecule pharmaceutics is described. The power, versatility, and utility of this multi-functional system were highlighted by the creation of functional drug coatings on intraocular lenses, bandage, and sutures. These combination devices effectively prevented bacterial growth while suppressing the production of

inflammatory cytokines. Combined, these efforts surmounted key challenges toward the development of intraocular lenses able to prevent complications of cataract surgery and enhanced the fundamental understanding of layer-by-layer systems.

Thesis Supervisor: Paula T. Hammond
Title: Bayer Chair Professor of Chemical Engineering and Executive Officer

*For my grandmother, Mamie L. Coefield,*

"Unless the LORD builds the house,
its builders labor in vain.
Unless the LORD watches over the city,
the watchmen stand guard in vain.

In vain you rise early
and stay up late,
toiling for food to eat—
for he grants sleep to those he loves."

Psalm 127:1-2

## Acknowledgements

*"For the LORD God is a sun and shield; the LORD bestows favor and honor; no good thing does he withhold from those whose walk is blameless."* – Psalm 84:11

First and foremost, I would like to thank Jesus Christ, my Lord and Savior. So many people have contributed to the success of this work and my personal and professional development. Please know that if you are not listed here, I have not forgotten your impact.

There have been a number of faculty members who have been indispensible. I would like to thank my advisor, Paula T. Hammond, for giving me scientific freedom, support, encouragement, mentorship, and confidence. I would also like to thank my thesis committee, Prof. Robert Langer and Prof. Alex Klibanov, for their time, energy, and sound advice. Prof. Tim Swager and Prof. Kristala Jones Prather have been supportive throughout my tenure. I thank you for taking the time to listen and for your wonderful advice. In my undergraduate, I was honored to work in the lab of Prof. Joe DeSimone. It is his influence that led me to MIT and I continue to draw confidence from his continued faith in my abilities. I would like to thank my collaborators Dr. Joe Rizzo III, Dr. Ken Mandell, and Aurolabs.

I have been blessed to work in a lab full of superstars! I thank you for all your advice, kindness, and collaborative spirit. I would be remissed if I did not thank by name Mara MacDonald, Ray Samuel, and Anita Shukla. This work would not have been possible without you. I have had the opportunity to work with wonderful undergraduate students: Alia Carter, Vanessa Eveon, Amy Leung, and Mariawy Riollano. Thank you for your input.

I have had the privilege of being a part of organizations that have served as my local family and support network. Thank you Black Graduate Ministries, Beacon City Church, Office of the Dean of Graduate Students, ACME, and Baker House. I would especially like to thank Loreal Andrews, Ugochi Ofoh, Pastor Sharon Mitchell, Dean Blanche Staton, and Dean Christopher Jones for their continual love and support.

Finally, I would like to thank my family and friends who have guided and supported me along this path. Thanks mom (Dean Mable Smith). Your love, support, and selflessness have made all of this possible. Dad (Freddie Smith) thank you for love, support, and establishing a strong work ethic in me. Thanks sis (Nakia Smith), your energy, uniqueness, love, and support, have brought balance and joy to my life. Thank you Ajay Watson, my nephew. You are my favorite stress reliever. Pierre Fuller, my fiancé, thank you for walking this road with me. Your presence has changed my life and allowed me to overcome so many obstacles.

# Table of Contents

# List of Figures

# List of Tables

# Chapter 1 : Introduction

Cataracts, the clouding of the eye's natural lens, are the leading cause of visual disability worldwide, accounting for approximately 50 % of global blindness.[1-3] Treatment requires the surgical removal and replacement of the opaque lens with an artificial intraocular lens (IOL). Postoperative side effects include pain, swelling, infection, inflammation, and bleeding. If left untreated these conditions could result in the formation of secondary cataracts, reduced vision, or irreversible blindness.[3] To avoid these complications, patients are required to administer a complex schedule of anti-inflammatory and antibiotic eye drops daily for 6-8 weeks. For this to be effective there must be efficient drug delivery to intraocular tissue and high patient compliance. However, both the efficacy of topical drug delivery and patient compliance is low. Research indicates that even with proper administration less than the 5% of active drug reaches the site of physiological need.[4] Moreover, the majority of cataract patients, especially those suffering from arthritis, experience extreme difficulty in correctly dispensing eye drops, further lowering efficacy. The associated difficulty and frequency of administration exacerbates patient noncompliance, thus increasing the risk of ocular pathology.[4, 5] The shortcomings of the current treatment regimen are exemplified by the high incidence of secondary cataracts. At least forty percent of all cataract patients will develop a secondary cataract and as a result require additional specialized surgery.[6, 7] Cost and availability of preventative medication often preclude its use altogether in many developing nations. A practical solution is to coat the IOLs for immediate and concurrent release of the antibiotic and anti-inflammatory. A self-dosing IOL will

eliminate the need for patient compliance and increase the therapeutic efficacy by maintaining a constant release at the surgical site. The goal of this work is to utilize layer-by-layer (LBL) assembly to create a multi-drug delivery coating for intraocular lens.

## Layer-by-Layer Assembly

Layer-by-layer has emerged as a powerful tool in the creation of dynamic thin films system that imparts exquisite surface functionality. Layer-by-layer assembly, first introduced in 1992 by Decher, is a directed assembly technique based on complementary chemical interaction.[8, 9] In 1966, Iler described the sequential absorption of two oppositely charged metal oxides in solution and laid the foundation for layer-by-layer assembly.[10] However, the impact of the molecular design of thin films through Langmuir Blodgett deposition and self assembled monolayers, must have influenced Decher.[9, 11, 12] In theory, any complementary interaction, including hydrogen bonding, van der Waals forces, and bimolecular recognition can be utilized, but electrostatic interactions have been most extensively investigated.[13-18] Electrostatic LbL deposition utilizes ionic interactions to form stable films with nanometer scale control of composition through the alternating adsorption of oppositely charged species. The driving force behind multilayer formation is a result of both electrostatic complex formation and the gain in entropy due to the release of counterions.[19, 20]

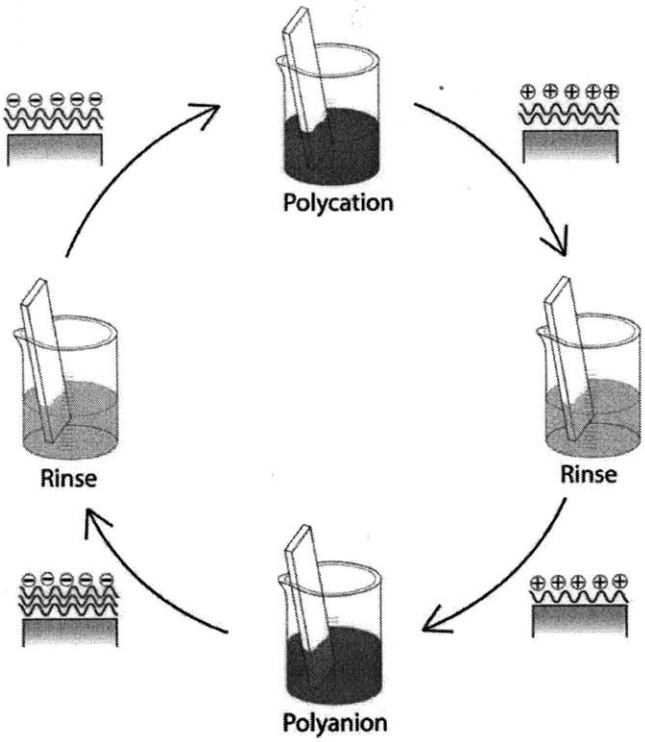


**Figure 1.1 Schematic of electrostatic layer-by-layer assembly**

The schematic shows electrostatic layer-by-layer deposition. Ionic interactions are used to form stable films through the alternating adsorption of oppositely charged species. A charged substrate is placed in a polyelectrolyte solution to functionalize the surface and provide a new charge. Films are rinsed in between each deposition step to remove non-electrostatically bound material.

A schematic of electrostatic LbL can be seen in figure 1.1. In the schematic, a charged substrate is placed in an oppositely charged polyelectrolyte solution. A polyelectrolyte is defined as a molecule containing more than one charge that is often macromolecular in structure. Positively charged polyelectrolytes are referred to as polycations and negatively charged polyelectrolytes are polyanions. Many surfaces including glass and silicon are naturally charged while others can be rendered charged with simple treatment methods such as plasma etching. The oppositely charged

polyelectrolyte absorbs until complete charge reversal occurs. Charge reversal is critical to the success of this process, as it limits layer growth through repulsive forces and provides adequate surface charge for the next deposition step.[20] The newly charged surface is then rinsed to remove non-electrostatically bound material and placed in a polyelectrolyte solution of opposite charge. This polyelectrolyte deposition step results in complete charge reversal, restoration of the original surface charge, and formation of a bilayer.

In this manner polyelectrolyte multilayer films can be built one molecular layer at a time with complete control of film composition and architecture. Top down degradation, through hydrolysis for example, enables release of film components in the inverse order of assembly. Ionic strength, pH, and counterion choice can be used to control the deposition characteristic of each layer and subsequent film morphology.[14] Typically, layer-by-layer is performed in aqueous solutions using dip assembly methods but organic solvents as well as spray and spin coat assembly methods can be utilized.[21, 22] Layer-by-layer is a powerful technique for the creation of diverse nano-engineered material systems able to enhance existing technology or function as standalone devices. These films are unique in their ability to incorporate a diverse set of materials, such as carbon nanotubes, functional polymers, viruses, cells, oligonucleotides, proteins, and inorganics, on virtually any surface through mild aqueous manufacturing at room temperature.[9, 14, 15, 23-32] Since its advent, layer-by-layer has been applied to almost every area of science and technology.

## Cataracts

Cataracts usually develop as an age-related phenomenon caused by protein aggregation in the clear crystalline lens and can be seen in figure 1.1.[1] This clouding, which is usually present in both eyes, disrupts the passage of light through the eye and transmits a blurred image onto the retina. Cataract removal is the only cure for this form of blindness. Today, cataract surgery is performed as an outpatient procedure under local anesthesia. The cataract is usually removed via a high-frequency ultrasonic probe, which is inserted through a single, very small (around 3 mm) incision. The ultrasonic energy liquefies the lens and suction, applied through the same tool, is used to remove the emulsified lens. The artificial intraocular lens provides both a clear optical path and restorative refractive capability for the eye. IOLs are made either of hard plastic or soft, foldable polymers and consists of a central optic, which provides the refractive element, and two haptics, which provide structural support for the IOL. Polymeric materials such as poly(methyl methacrylate), hydrophobic acrylics, poly(2-hydroxyethyl methacrylate), or silicone are most commonly used.[33] A typical IOL design can be seen in figure 1.2

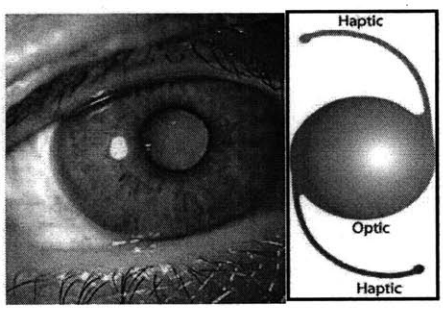


**Figure 1.2 Picture of a cataract and schematic of a typical intraocular lens**

The picture on the left shows a mature cataract.[34] The image on the right shows the design of a typical intraocular lens used for treatment. Intraocular lenses consist of a central optic that provides the refractive element and two haptic which provide structural support for the lens in the lens capsule of the eye.

Cataract surgery is one of the most commonly performed surgical procedures in the world.[7] Though generally safe, the risk of debilitating complications is significant and requires vigilance. Postoperative inflammation always occurs to some extent because surgical trauma induces the release of prostaglandins, the main players in postoperative ocular inflammation. These prostaglandins can cause retinal blood vessels to leak fluid which accumulates in the macula, the part of retina responsible for central vision. The resulting swelling is referred to as cystoid macular edema and is the most common complication that degrades vision. Cystoid macular edema occurs even when surgery is performed well from a technical standpoint and is present in up to 19% of patients.[35, 36] Inflammation can also contribute to the development of posterior capsule opacification (PCO), the most frequent postoperative complication. PCO, or secondary cataract, is caused by lens epithelial cells that as a result of surgical trauma adhere to the lens capsule, proliferate, and migrate across the posterior lens capsule causing opacities.[37, 38] The most serious complication is endophthalmitis, which is ocular inflammation most commonly caused by infection. Endophthalmitis occurs in at least 0.1% of patients and is usually devastating.[39, 40]

To prevent or limit complications, eye drops are always prescribed after surgery. While selection of the postoperative therapy largely depends on ophthalmologist preference, general standards do exist. Corticosteroids and nonsteroidal anti-inflammatory drugs (NSAIDs) are commonly used in the management and prevention of non-infectious ocular inflammation following cataract surgery. However, the complications associated with corticosteroids, such as increased ocular pressure, make NSAIDs the appealing option for prevention of both PCO and cystoid macular edema.[41]

Additionally, ex vivo models have also shown that the pharmacologic activity of NSAIDs can prevent the lens epithelial cell changes that lead to PCO.[42] Vancomycin is commonly used to treat and prevent endophthalmitis due to its potency, broad spectrum gram positive coverage, and low risk of allergic reaction.[2, 43-45] Fluoroquinolones are also commonly used to prevent infection. However, topical administration of eye drops is both imprecise and inefficient and severe limitations exist with this drug delivery modality.[5]

The vast majority of each administered eye drop is washed away by the tear film and drains onto the face or through the tear ducts into the nose.[5] Medication spilled in the tear ducts can be systemically absorbed and lead to allergic reactions, and cardiac or pulmonary compromise.[46, 47] Moreover, penetration through the cornea is highly variable across individuals. It impossible to know *a priori* the precise medicinal dose needed for each patient. Furthermore, the absorption of some eye drops varies with ocular inflammation, which varies markedly across patients.[46, 47] To account for these issues a large bolus of drug is delivered at the ocular surface to achieve doses within the therapeutic window inside the eye. As a result, the amount of drug needed within the eye is about 1/1000 of the amount that is delivered at the surface. In dwelling ophthalmic drug delivery implants have shown that both the time course of treatment and dosage is significantly reduced by local drug delivery.[48] Release of dexamethasone, a corticosteroid, for seven days in the intraocular space was able to successfully prevent and treat ocular inflammation post cataract surgery as well as the 6-8 week traditional eye drop therapy.[48] Low patient compliance and cost also add to the ineffectiveness of eye drops.[6, 49] Physical ailments such as arthritis, stroke and

neuropathies as well as cognitive deficits and visual disorders compromise the ability of patients, especially the elderly, to comply with their postoperative therapy.[7, 36] Since cataract surgery is an outpatient procedure the burden to adhere to the complex eye drop regiment lies solely on the patient. Eye drops also represent a significant financial cost to the patient and healthcare system and in developing nations where eye drops are not available or unaffordable, patients do not receive these medications.[50] Strategies able to maximize therapeutic efficiency while minimizing cost and patient compliance are needed.

## Thesis Overview

In this thesis, a foundation for bioactive coatings able to treat the three most common or severe complications of cataract surgery, while maximizing therapeutic efficacy and eliminating the need for patient compliance was established. Though numerous methods exist to construct drug delivery coatings, only layer-by-layer enables the sophisticated molecular control necessary to achieve complex preprogrammed release of multiple therapeutic at physiological conditions on any substrate via simple aqueous manufacturing. Still, the formation of an effective IOL delivery system hinges upon the ability to selectively control and tailor release kinetics, incorporate appropriate therapeutics, and successfully prevent pathology. In order to create a bioactive coating for IOLs, several obstacles had to be surmounted. An illustration of the technological foundation needed for bioactive coatings can be in figure 1.3. Research, herein, focused on rational polymer design for tailored release, incorporation of hydrophobic small molecule therapeutics, controlled multi-agent release of small molecules, and the *in vitro* efficacy of hydrolytically degradable LbL films.

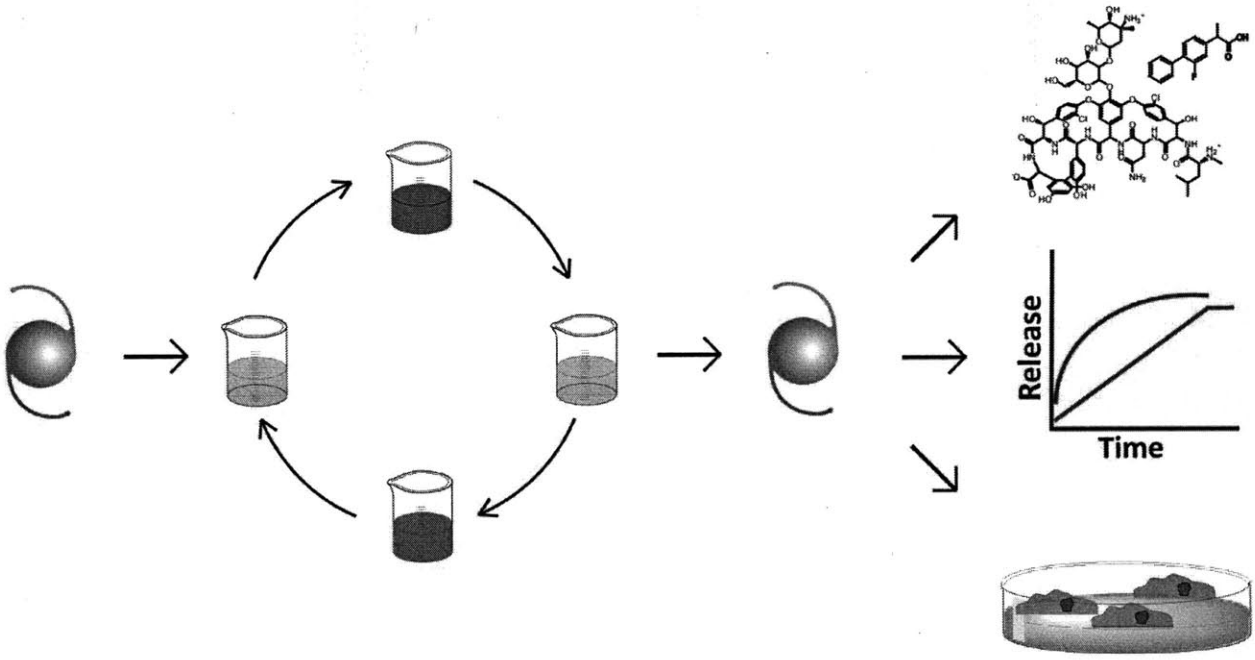


**Figure 1.3 Illustration of the technological foundation necessary for medication dispensing intraocular lenses**

The illustration shows the overarching goal of this work, to create a drug delivery coating for intraocular lenses. In the schematic, an intraocular lens is given a functional coating using layer-by-layer assembly. The coating does not alter the optical properties or overall structure of the intraocular lens. However the lens is equipped with small molecule therapeutics, which can be delivered from the surface with distinct release profiles and can modulate cell behavior.

In chapter two, the fabrication rules and design tools necessary to create hydrolytically degradable polyelectrolyte multilayer films with preprogrammed advanced engineered release kinetics are investigated. In chapter three, a layer-by-layer system able to produce sustained, controlled release of uncharged or hydrophobic small molecule therapeutics is explored. In chapter four, the cellular interactions with a hydrolytically degradable layer-by-layer system containing anti-inflammatory agents and its ability to control pathological processes are assessed. Lastly, in chapter five, the

construction, release dynamics, and *in vitro* efficacy of multi-agent films containing antibiotic and anti-inflammatory drugs is examined. Combined these efforts enable the creation of a multi-agent layer-by-layer film designed to prevent the postoperative complications of cataract surgery.

## References


[1] G. Brian, H. Taylor, *Bull World Health Organ* **2001**, *79*, 249.
[2] T. J. Liesegang, *Mayo Clin Proc* **1997**, *72*, 149.
[3] C. Parsons, D. S. Jones, S. P. Gorman, *Expert Review of Medical Devices* **2005**, *2*, 161.
[4] G. Velez, S. M. Whitcup, *British Journal of Ophthalmology* **1999**, *83*, 1225.
[5] D. Ghate, H. F. Edelhauser, *Expert Opin, Drug Deliv.* **2006**, *3*, 275.
[6] R. Balkrishnan, *Clin Ther* **1998**, *20*, 764.
[7] A. P. Rotchford, K. M. Murphy, *Eye (Lond)* **1998**, *12 ( Pt 2)*, 234.
[8] G. Decher, *Science* **1997**, *277*, 1232.
[9] G. Decher, J. B. Schlenoff, Wiley-VCH, Weinheim, **2003**, p. 524.
[10] R. K. Iler, *Journal of Colloid and Interface Science* **1966**, *21*, 569.
[11] K. B. Blodgett, *Journal of the American Chemical Society* **1934**, *56*, 495.
[12] I. Langmuir, *Journal of the American Chemical Society* **1919**, *41*, 868.
[13] X. Q. Cui, R. J. Pei, X. Z. Wang, F. Yang, Y. Ma, S. J. Dong, X. R. Yang, *Biosensors & Bioelectronics* **2003**, *18*, 59.
[14] P. T. Hammond, *Advanced Materials* **2004**, *16*, 1271.
[15] N. A. Kotov, *Nanostructured Materials* **1999**, *12*, 789.
[16] W. B. Stockton, M. F. Rubner, *Macromolecules* **1997**, *30*, 2717.
[17] S. A. Sukhishvili, S. Granick, *Journal of the American Chemical Society* **2000**, *122*, 9550.
[18] S. Y. Yang, M. F. Rubner, *Journal of the American Chemical Society* **2002**, *124*, 2100.
[19] M. Schonhoff, *Journal of Physics-Condensed Matter* **2003**, *15*, R1781.
[20] T. Boudou, T. Crouzier, K. F. Ren, G. Blin, C. Picart, *Advanced Materials* **2010**, *22*, 441.
[21] P. A. Chiarelli, M. S. Johal, J. L. Casson, J. B. Roberts, J. M. Robinson, H. L. Wang, *Advanced Materials* **2001**, *13*, 1167.
[22] K. C. Krogman, N. S. Zacharia, S. Schroeder, P. T. Hammond, *Langmuir* **2007**, *23*, 3137.
[23] M. Campas, C. O'Sullivan, *Analytical Letters* **2003**, *36*, 2551.
[24] F. Caruso, *Advanced Materials* **2001**, *13*, 11.
[25] N. A. Kotov, I. Dekany, J. H. Fendler, *Journal of Physical Chemistry* **1995**, *99*, 13065.
[26] J. L. Lutkenhaus, P. T. Hammond, *Soft Matter* **2007**, *3*, 804.
[27] Y. Lvov, K. Ariga, I. Ichinose, T. Kunitake, *Journal of the American Chemical Society* **1995**, *117*, 6117.
[28] Y. Lvov, K. Ariga, T. Kunitake, *Chemistry Letters* **1994**, 2323.

[29] D. M. Lynn, *Soft Matter* **2006**, *2*, 269.
[30] S. S. Shiratori, M. F. Rubner, *Macromolecules* **2000**, *33*, 4213.
[31] Z. Y. Tang, Y. Wang, P. Podsiadlo, N. A. Kotov, *Advanced Materials* **2006**, *18*, 3203.
[32] V. V. Tsukruk, F. Rinderspacher, V. N. Bliznyuk, *Langmuir* **1997**, *13*, 2171.
[33] A. W. Lloyd, R. G. A. Faragher, S. P. Denyer, *Biomaterials* **2001**, *22*, 769.
[34] D. Marion, in *UpToDate* (Ed.: D. Basow), UpToDate, Waltham, MA, **2010**.
[35] P. G. Ursell, D. J. Spalton, S. M. Whitcup, R. B. Nussenblatt, *J Cataract Refract Surg* **1999**, *25*, 1492.
[36] C. M. Hughes, *Drugs Aging* **2004**, *21*, 793.
[37] I. M. Wormstone, *Experimental Eye Research* **2002**, *74*, 337.
[38] H. Matsushima, H. Iwamoto, K. Mukai, Y. Katsuki, M. Nagata, T. Senoo, *Expert Review of Medical Devices* **2008**, *5*, 197.
[39] D. F. Chang, R. Braga-Mele, N. Mamalis, S. Masket, K. M. Miller, L. D. Nichamin, R. B. Packard, M. Packer, A. C. C. Comm, *Journal of Cataract and Refractive Surgery* **2007**, *33*, 1801.
[40] R. C. Wang, P. L. Lou, E. A. Ryan, A. J. Kroll, *Seminars in Ophthalmology* **2002**, *17*, 153.
[41] J. Colin, *Drugs* **2007**, *67*, 1291.
[42] F. Giuliano, T. D. Warner, *British Journal of Pharmacology* **1999**, *126*, 1824.
[43] Y. Alster, L. Herlin, M. Lazar, A. Loewenstein, *British Journal of Ophthalmology* **2000**, *84*, 300.
[44] J. R. Ferencz, E. I. Assia, L. Diamantstein, E. Rubinstein, *Archives of Ophthalmology* **1999**, *117*, 1023.
[45] N. Mamalis, L. Kearsley, E. Brinton, *Curr Opin Ophthalmol* **2002**, *13*, 14.
[46] T. F. Patton, M. Francoeur, *Am J Ophthalmol* **1978**, *85*, 225.
[47] A. Urtti, *Adv Drug Deliv Rev* **2006**, *58*, 1131.
[48] D. F. Chang, V. Wong, *Trans Am Ophthalmol Soc* **1999**, *97*, 261.
[49] G. Anghel, A. C. Anghel, *Oftalmologia* **2008**, *52*, 32.
[50] J. K. Schmier, M. T. Halpern, M. L. Jones, *Pharmacoeconomics* **2007**, *25*, 287.

# Chapter 2 : Hydrophobic Effects in the Critical Destabilization and Release Dynamics of Degradable Multilayer Films

This chapter has been reproduced in part from: R. C. Smith, A. Leung, B. S. Kim, P. T. Hammond, *Chemistry of Materials* **2009**, *21*, 1108-1115.

## Introduction

The advent of medical prosthetic implants has revolutionized the field of medicine, enabling the treatment of previously debilitating disorders. Surgical implantation of prosthetic devices such as coronary stents, intraocular lenses, and urinary catheters are a few of the most successful medical approaches applied in clinical treatment, to date. Nevertheless, these devices are associated with significant postoperative complications and subsequent morbidity.[1, 2] To lower the incidence of pathology, drug delivery coatings for medical prostheses have emerged as an active area of research and development. While various methods to coat medical implants for localized drug delivery exist, most rely on diffusion based release from a bulk matrix and do not enable the engineering of drug release profiles. Moreover, state-of-the-art coatings are still limited to the elution of a single therapeutic that can withstand the relatively harsh processing conditions necessary for fabrication. The versatility, mild aqueous processing conditions, and compositional diversity of layer by layer (LbL) assembled films represents a powerful means to overcome these limitations and construct superior drug delivery coatings.

Layer-by-layer assembly has enabled the creation of conformal thin films with sequential and controlled release capabilities.[3, 4] To extend the capabilities of this

approach, it is desirable to work with a family of polymers which can be compositionally varied to achieve a broad range of degradation rates, mechanical properties, and biocompatibility with simple modifications in monomer choice. In conventional hydrolytically degradable polymer films, the design rules have been thoroughly explored[5]; however, the parameters which influence the degradation and stability behavior in electrostatically assembled multilayer films have not been closely examined and are not well understood. To date, there has been no systematic study exploring the impact of chemical composition on release dynamics in this promising and rapidly expanding set of new drug carrier systems; therefore, no correlation between hydrolytically degradable polymer structure, charge density, and release exist to allow for rational design. In examining these properties, a framework for understanding the nature of degradation in hydrolytically degradable layer-by-layer films has been created, generating a knowledge base and rubric for fabrication of films uniquely tailored for their given applications. Utilization of these tools will expand the scope of degradable multilayer films to applications such as microreactors, bioMEMs, agriculture, tissue engineering, and basic scientific research.

Electrostatic LbL deposition utilizes ionic interactions to form stable films with nanometer scale control of composition through the alternating adsorption of oppositely charged species.[6] LBL films have the ability to incorporate a wide variety of materials, including functional polymers, inorganic nanoparticles, enzymes, small molecules, proteins, polysaccharides, nucleic acids, and carbon nanotubes.[7-16] The ability to create uniform, conformal coatings at room temperature via a mild aqueous process has fueled the emergence of polyelectrolyte multilayer films in biological applications. A

great deal of research has recently focused on the use of polyelectrolyte multilayers as drug delivery vehicles. Caruso, Voegel, and others have highlighted the ability of these films to serve as effective gene and protein delivery vehicles.[7, 12, 13, 17-23] Moreover, Rubner, Thierry, and coworkers have incorporated small molecule therapeutics into these systems.[13, 24, 25]

Still, most research utilizes non-degradable films, which rely on drug diffusion from the bulk polymer matrix, and do not take advantage of the controlled release associated with top down degradation of LBL films. Unlike traditional polymer-based delivery systems, polyelectrolyte multilayer films are constructed one nanoscale layer at a time, alternating between polymer and therapeutic. In this manner, a drug delivery coating can be constructed with precise control over film architecture such that degradation via surface erosion will enable drug release in the inverse order of assembly. As a result, highly tailored release profiles can be achieved. To address this issue, Hammond and coworkers have created hydrolytically degradable polyelectrolyte multilayer films composed of a poly(β-amino ester) and polyanion.[26] Poly(β-amino ester)s are cationic polymers produced through Michael addition polymerization of diacrylate and amine monomers. These polymers were first introduced by Lynn, et al. and have shown promise in gene delivery and as tissue engineering scaffolds.[27-30] A library of 2,350 poly(β-amino ester) has been constructed[31]. Hydrolytically degradable LbL films, composed of a poly(β-amino ester), and poly(styrenesulfonate) or the anticoagulant, heparin sulfate, were initially studied. Films were shown to undergo surface erosion by the hydrolysis of the poly(β-amino ester) and subsequent release of the polyanion.[32] Wood et al. demonstrated multi-component release from hydrolytically

degradable films by showing that heparin sulfate and the model drug, dextran sulfate, could be released sequentially or concurrently depending on the presence or absence of a cross-linked barrier layer.[3]

Recently, Zhang et al. proved that the release kinetics of hydrolytically degradable LBL films were dependent on the chemical structure of the polycation[33, 34]. Three poly (β-amino esters), varying only in alkyl chain length of the diacrylate monomer, were used to show that increasing hydrophobicity could alter the release kinetics of poly(styrene sulfonate) (SPS). Films composed of each of the three polycations with SPS were found to have unique release profiles and films constructed of multiple polycations were found to have release profiles intermediate between those constructed of a single polycation.[35] While this study demonstrated the versatility of LBL delivery systems, there remains much more to understand to fully utilize chemical composition to tune release. In addition, these studies were performed with high molecular weight poly(styrene sulfonate), which is an inaccurate model for biologically relevant drugs.

Work, herein, sought to understand the extent to which structural manipulation could be used to control release of a model biological drug, dextran sulfate, from hydrolytically degradable LBL films. Dextran sulfate (DS) is an ideal model system due to its similarity to glycosaminoglycans and proteins in macromolecular structure and hydrophobicity. A series of polymers from the poly(β-amino ester) family was investigated by varying the diacrylate monomer used in the polymerization. Diacrylate moieties were altered based on alkyl chain length, steric hindrance, and hydrophobicity. Each polymer was examined for growth, degradation, and release of dextran sulfate

from LbL films. Nine polymers were examined in total. These studies revealed a correlation between release dynamics and the octanol:water coefficient (LogP) of the diacrylate monomer. This correlation indicated that there is actually an optimum in hydrophobicity with respect to sustained release kinetics due to LbL film destabilization at high degrees of hydrophobicity. The destabilization of multilayers beyond the optimum was rapid and marked, and highly reproducible. The finding of a correlation between LogP and sustained release profiles will enable the creation of custom drug delivery coatings specifically designed to address the necessary biological, chemical, and mechanical requirements of a given application. Furthermore, this paper presents an observation of multilayer destabilization as a systematic function of hydrophobic content and charge density for the first time. Lastly, a simple method to overcome the hydrophobicity limit and increase release duration was demonstrated.

## Materials & Methods

***Materials:*** All monomers were purchased from Dajac Laboratories, Inc. (Feasterville, PA), except 1,4 butanediol diacrylate, 1,6 hexanediol diacrylate, and 4,4-trimethylenedipiperidine, which were obtained from Alfa Aesar (Ward Hill, MA). Poly (sodium 4styrenesulfonate) (SPS, $M_n$ = 70,000) and dextran sulfate ($M_n$ = 8,000) were purchased from Sigma Aldrich (St. Louis, MO). Dulbecco's PBS buffer and glass substrates were obtained from VWR Scientific (Edison NJ). Linear polyethyleneimine (LPEI, $M_n$ = 25,000) and $^{14}$C-dextran sulfate sodium salt (100 µCi, 1.5 mCi/g, Mn = 8000) was purchased from Polysciences, Inc (Warrington, PA). and American Radiolabeled Chemicals, Inc, respectively.

***Synthesis:*** Poly(β-amino esters) (PBAE) were synthesized as previously described.[27, 29] Briefly, in a typical experiment, a solution of 4,4-trimethylenedipiperidine ( 34.1mmol) in anhydrous THF (50mL) was added to the diacrylate monomer (34.1mmol) dissolved in anhydrous THF (50mL). The reaction mixture was stirred for 48 hours at 50 °C under nitrogen. After 48 hours, the reaction was cooled to room temperature and precipitated in cold stirring hexanes. Polymers were collected and dried under vacuum prior to NMR and GPC analysis. The resulting polymer molecular weights along with their identification, based on diacrylate monomer, can be viewed in Figure 1. Crosslinked PBAE were synthesized by using a 1:1.2 diamine to diacrylate stoichiometric imbalance to diacrylate endcap the polymers. Crosslinking was performed before film formation by exposing diacrylate endcapped PBAE dissolved in THF to UV light in the presence of a photoinitiator, 2,2 dimethyl-2-phenylacetophenone, for five minutes[27]. The polymer was precipitated as described above. The molecular weight of precrosslinked Poly A3 was $M_n$ = 202,393 and $M_w$ = 402,093. Post-crosslinked films were constructed by exposing films containing diacrylate endcapped Poly A3 to UV light for ten minutes.

***Film Fabrication:*** LBL films were constructed on 1.5 $cm^2$ glass substrates using a Carl Ziess HSM series programmable slide stainer. The glass substrates were plasma etched in oxygen using a Harrick PDC-32G plasma cleaner on high RF power for 5 minutes to generate a uniform, negatively charged surface prior to deposition. After loading onto the robotic arm, the glass substrate was dipped into a 2mM aqueous polycation solutions for 10 minutes and then washed with agitation for 10, 20, and 30 seconds in three different water baths to remove all physically absorbed polymer. This

process was repeated with the 2mM polyanion solution to form a bilayer. All degradable polymer films were constructed on ten bilayers of linear polyethylenimine and poly (styrene sulfonate) to ensure uniform adhesion of degradable layers to the surface. These films were constructed from a pH 4.2 solution of LPEI and pH 4.7 solution of SPS. Degradable films were prepared with 10mM polymer solutions in 100 mM acetate buffer at pH 5.0 to avoid the conditions at which poly (β-amino ester)s degrades rapidly. A similar methodology was used to construct pre-crosslinked films, except crosslinked Poly A3, which required several days to dissolve, was utilized. Post-crosslinked films were assembled just as uncrosslinked films, except endcapped Poly A3 was used for film formation. Following deposition, the films were dried thoroughly under a stream of dry nitrogen. Post crosslinked films received 10 minutes of UV treatment after drying.

***Release Studies:*** Release profiles were investigated by monitoring the release of $^{14}C$-dextran sulfate and the degradation of non-radiolabeled films. For drug release experiments, 20 bilayer radiolabeled films were constructed using $^{14}C$-dextran sulfate solution. The radiolabled deposition solutions were prepared by combining $^{14}C$-dextran sulfate (1.5 mCi/g, Mn = 8,000), unlabeled dextran sulfate ($M_n$ = 8,000), and 100 mM acetate buffer to yield a total concentration of dextran sulfate (unlabeled plus labeled) to 2 mg/mL (1 μCi/mL 14C). After fabrication, each twenty bilayer film was immersed in 30 mL phosphate buffer solution (pH 7.4, 137 mM NaCl, 2.7 mM KCl, 10 mM $Na_2HPO_4$). A 1 mL sample was extracted at various time points and analyzed via scintillation counting. Scintillation counting was performed on a Tri-carb liquid scintillation counter (Model U2200) and the amount of radiolabel in each sample vial was measured using $^{14}C$ protocol. Degradation vials were tightly capped between sample extractions to

prevent evaporation of the buffer solution. Raw data (disintegrations per minute, DPM) were converted to micrograms (μg) of drug released using the conversion factor 2.2 x $10^6$ DPM = 1 μCi, the specific radioactivity of the drug, and knowledge of the ratio of total drug to labeled drug in the deposition solution. Degradation studies were performed with nonradiolabled 20 bilayer films. Films were immersed in 20 mL phosphate buffer solution (PBS) in a screw top glass vial and tightly sealed. At various times, films were removed, dried thoroughly under a stream of dry nitrogen, and thickness was measured using profilometry at five predetermined locations on the film surface. Profilometry measurements were performed on a Tencor 21- profilometer. Following measurements, films were reimmersed in buffer solutions and resealed. All release and degradation studies were performed in triplicate. Surface morphology of LbL film was observed by using Nanoscope IIIa AFM microscope (Digital Instruments, Santa Barbara, CA) in tapping mode in air. Release rate was determined by plotting $1 - \frac{M_t}{M_\infty}$ versus time, where $M_t$ equals the amount of drug released at time *t* and $M_\infty$ is the total amount of drug in the system.

***Calculation of Octanol:Water Coefficient:*** Octanol: water coefficients used in this work were an average of well known computational models based on group contribution approaches[36, 37]. In general, these methods break compounds into atoms/fragments that are associated with a given constant determined from a database of structures. Correction factors are used to account for atom/fragment interactions. These estimated values are summed to produce the octanol:water coefficient in logarithmitic form (LogP). The eight methods utilized differ in both database and computational constants used, which lead to differences in logP values [38]. Since no superior method could be

selected, the average was calculated to provide a "consensus" value (Table 2.1). This has been shown to lead to better stability of prediction[37, 39]. Advanced Chemical Development, Inc., ALOGPS 2.1, and Actelion open access software were used to calculate LogP. The following computational models were used in LogP determination: ALOGPS, IALogP, AB/LogP, miLogP, KOWWIN, XLogP, ACD/LogP, and CLogP[39].

## Results and Discussion

### Effect of Small Changes in Molecular Weight

Poly(β-amino ester)s composed of 4,4-trimethylenedipiperidine and diacrylate monomers varying in alkyl chain length, steric bulkiness, and other modulators of hydrophobicity were synthesized to explore the impact of structure. Polymers were named based on their diacrylate monomer, which were grouped according to the aspect of structural control the monomers were used to explore. All monomers were placed in at least one of three categories: alkyl chain length (A), steric bulkiness (B), and mechanistic character (C). The structure of the diacrylate monomers and the molecular weights of their corresponding polymers can be seen in Figure 2.1.

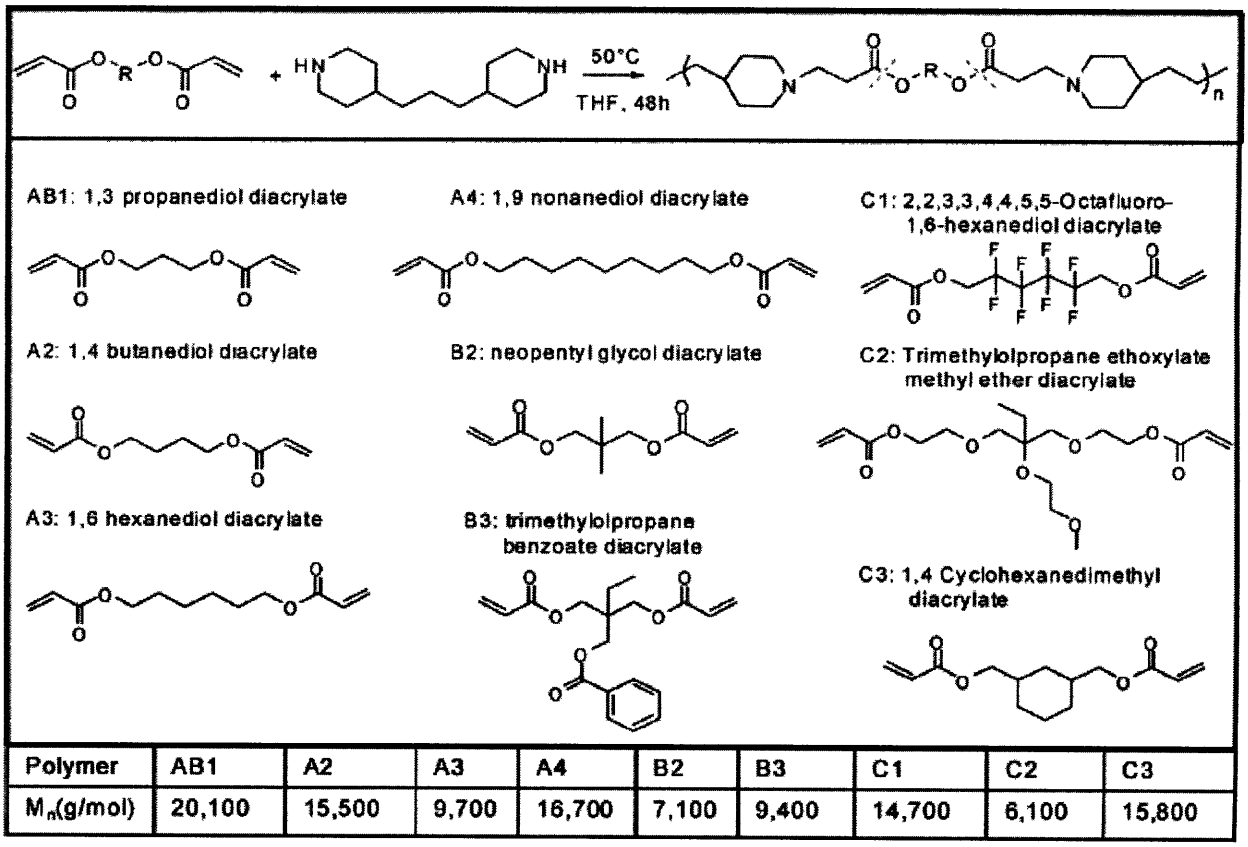


| Polymer | AB1 | A2 | A3 | A4 | B2 | B3 | C1 | C2 | C3 |
|---|---|---|---|---|---|---|---|---|---|
| $M_n$(g/mol) | 20,100 | 15,500 | 9,700 | 16,700 | 7,100 | 9,400 | 14,700 | 6,100 | 15,800 |

**Figure 2.1 Reaction scheme for poly (beta - amino ester) synthesis**

The monomers used in synthesis of the poly (beta – amino esters). Dashed lines indicate hydrolyzable bonds. Letters are used to designate the categories of monomers investigated. All monomers with A were used in the examination of alkyl chain length, B stands for steric bulk, and C for mechanism clarification. In categories A and B, increasing number corresponds to greater alkyl chain length or bulk, respectively. Polymer number average molecular weights ($M_n$) determined via GPC and are included in the table.

The molecular weights of the poly (β-amino esters) range from 6,000- 20,000 g/mol. These differences can be attributed to the fact that molecular weight in step-growth polymerization is highly dependent on stoichiometry and monomer reactivity. Attempts were made to modulate reaction time and stoichiometry to create polymers

with similar molecular weights; however, this could not be achieved for all polymers. To determine the effect of molecular weight differences, release studies were performed on dextran sulfate containing multilayers of Poly A2 with $M_n$ of 6,000 and 16,000 g/mol, as shown in Figure 2.2. Because no differences in release kinetics were observed, it was assumed that small differences in molecular weight between the poly(β-amino ester)s would not substantially affect their degradation and release dynamics; polymers were studied as synthesized.

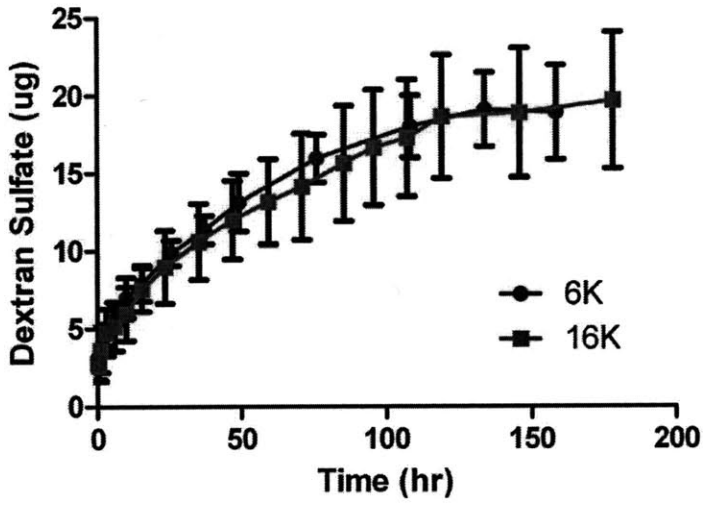


**Figure 2.2 Effect of Poly A2 molecular weight on the release of $^{14}$C-dextran sulfate from (Poly A2/ Dextran Sulfate)$_{20}$ films**

The effect of Poly A2 molecular weight on the release of $^{14}$C-dextran sulfate from (Poly A2/ Dextran Sulfate)$_{20}$ films. PolyA2 with $M_n$s of 6,100 and 16,000 were examined. Release studies were performed at 25°C in PBS buffer.

Although, numerous methods to control degradation of polymers exist, modulation of hydrophobicity has proven to be an effective regulator of degradation rate

for polyesters. Hydrophobicity can control degradation via a number of mechanisms, many of which are a result of reduced exposure to water. In short, the local concentration of water around the scissile bond able to undergo hydrolytic cleavage is decreased with increasing hydrophobicity; because ester hydrolysis is dependent on the effective water concentration, the degradation rate of polyesters can be modulated in this manner. Furthermore, increasing steric bulk around esters can make the bonds less susceptible to hydrolysis. Both methods of controlling degradation rate were utilized to determine the extent to which structural modulation could be used to control degradation of films.

**Effect of Alkyl Chain Length on Release**

To determine the extent to which local hydrophobicity around the ester could be used to control release, four polymers with varying alkyl chain length were investigated. The polymers examined Poly AB1, A2, A3, and A4 contained 3, 4, 6, and 9 methylene units respectively. Drug release and degradation profiles of these polymers can be seen in Figure 2.3. As expected, altering alkyl chain length extends dextran sulfate release; however the most hydrophobic polymer, Poly A4, did not exhibit the longest release as anticipated. $(\text{Poly A4/DS})_{20}$ films were found to be unstable, with 80% of the total amount of dextran sulfate released in less than 10 hours. Currently there are no mathematical drug delivery models for hydrolytically degradable polyelectrolyte multilayer. While it is known that chain hydrolysis is a key factor in degradation rate, the role of other factors such as ionic crosslink density remains largely unknown. It has been experimentally observed that many drug release curves fit linear, segmental linear, or exponential models. If the release data is fit to an exponential the rate of release can be quantitatively compared and seen in table 2.1.

| Polymer | K ( 1/hr)* $10^{-3}$ | $t_{1/2}$ (hr) | Span | $R^2$ |
|---|---|---|---|---|
| a/b1 | 20 ± 10 | 31 ± 2 | 0.94 | 0.998 |
| a2 | 15 ± 0.9 | 48 ± 3 | 0.88 | 0.995 |
| a3 | 6 ± 0.8 | 120 ± 10 | 0.93 | 0.981 |
| a4 | 240 ± 50 | 3 ± 0.6 | 0.65 | 0.968 |
| b2 | 14 ± 1.2 | 48 ± 4 | 0.73 | 0.985 |
| b3 | 430 ± 90 | 2 ± 0.3 | 0.62 | 0.97 |
| c1 | 1000 ± 300 | 0.6 ± 0.2 | 0.65 | 0.945 |
| c2 | 30 ± 10 | 22 ± 7 | 0.55 | 0.932 |
| c3 | 12 ± 3 | 60 ± 10 | 0.84 | 0.973 |
| precrosslinked a3 | 5 ± 0.6 | 150 ± 20 | 0.84 | 0.988 |
| UV treated a3 | 3 ± 0.6 | 220 ± 40 | 0.97 | 0.984 |

**Table 2.1 Constants from exponential fit of release data for (PolyX/Dextran Sulfate)$_{20}$ films**

Release data was plotted as fraction remaining versus time and fit to an exponential decay model: $y = (y_o - plateau)e^{-Kx} + plateau$, where $y_o$ is the y-intercept and plateau is the value at infinite time. The rate constant is K and is expressed in inverse hours. The half life ($t_{1/2}$) was calculated using $t_{1/2} = \ln(2)/K$ and is in hour units. Span is the difference between $y_o$ and plateau and is a dimensionless fraction.

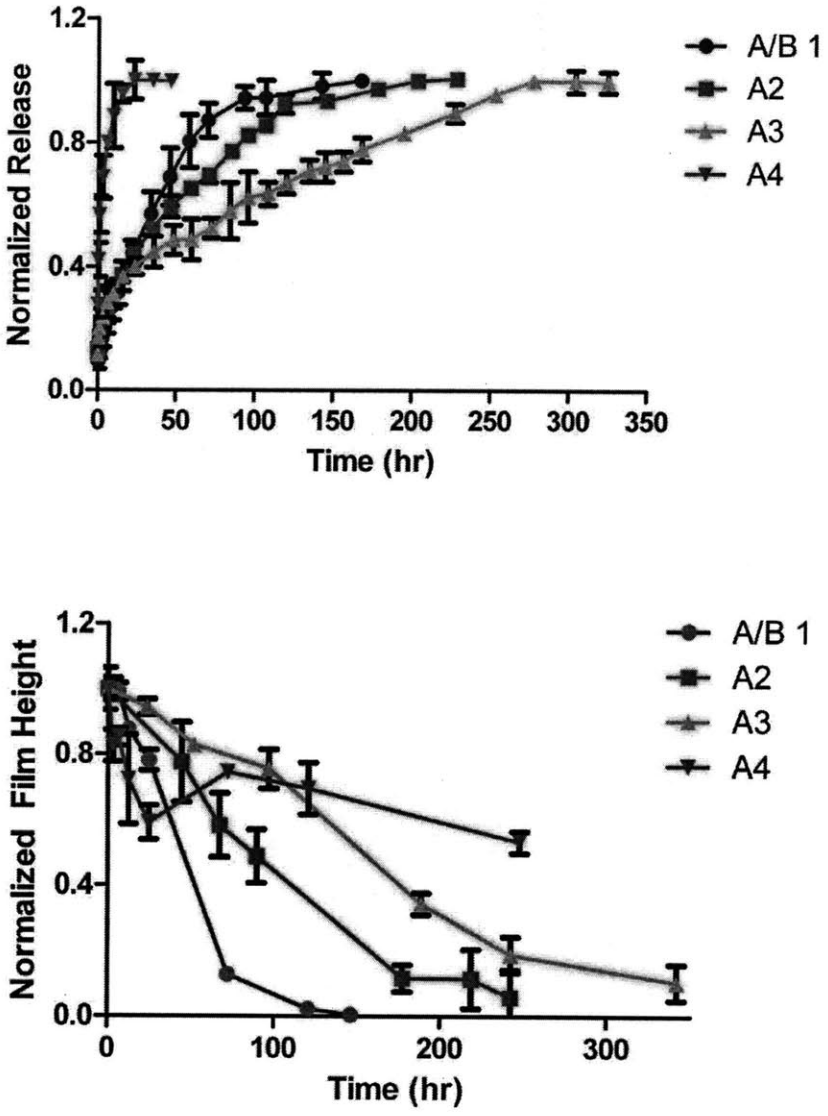


**Figure 2.3 Effect of alkyl chain length on $^{14}$C-dextran sulfate release and film degradation.**

Release and degradation studies were performed on (Poly X/ Dextran Sulfate)$_{20}$ films at 25°C in PBS buffer. A) Normalized release of $^{14}$C-dextran sulfate versus time. Release was normalized by the total amount of dextran sulfate released for each system. B) Normalized film height of (Poly X/ Dextran Sulfate)$_{20}$ over time. Films were normalized by the film height a time zero.

Previous research has highlighted the influence of hydrophobicity on the rate of hydrolysis for poly(β-amino ester)s[33, 40]. Zhong et al. showed that for a series of hyperbranched poly(β-amino ester)s more hydrophobic polymers degrade at a slower rate[40]. Additionally, Lynn showed that erosion of films composed of a poly (β-amino ester) and polystyrene sulfonate was dependent on hydrolysis of the polymer backbone by utilizing polyamide structural analogs of the poly(β-amino ester)s. Films composed of the polyamides, which contained amide linkages instead of esters, did not erode under physiologically relevant conditions[33]. The paper concluded that polymer chain scission via hydrolysis of the ester bonds is necessary for surface erosion of the films; however, Poly A4, which is very hydrophobic, is unlikely to have completely hydrolyzed over the timescale necessary to explain the rapid release of DS from (Poly A4/DS)$_{20}$, especially since more hydrophilic polymers degraded over several days It is improbable that the rapid release kinetics of (Poly A4/DS)$_{20}$ is due to chemical degradation of Poly A4.

Thus to ascertain whether (Poly A4/DS)$_{20}$ films were in fact undergoing an abnormal destabilization phenomenon via bulk erosion or normal surface erosion, film degradation and surface roughness were monitored by profilometry. Here, bulk erosion is defined as degradation that occurs throughout the polymer matrix or includes more than the surface of the film. All films except (Poly A4/DS)$_{20}$ were found to be surface eroding with fairly linear degradation profile and constant roughness profiles (S2). For (Poly A4/DS)$_{20}$ , 60% of total film thickness was removed within 24 hours, while the remaining film did not fully degrade after 240 hours. Reduced film stability may be attributed to reduced ionic interaction resulting from the low charge density of Poly A4. This suggests that alkyl chain modulation can be used to control release within a certain

charge density threshold, at which point it exhibits a maximum release time. If this is the case, chemical control of release via the addition of hydrophobic units is mediated by loss of polymer charge density and the ability of the polymer to form sufficient ionic crosslinks to maintain film stability.

**Effect of Steric Bulk on Release**

To investigate the effect of steric bulk on the release kinetics of hydrolytically degradable LbL films, three polymers, varying only in the substitution on the diacrylate monomers were explored. The effects of bulkiness were studied using poly AB1, B2, and B3. Poly AB1 is composed of 1,3 propanediol diacrylate and trimethylenedipiperidine (diamine used in all polymer) and serves as a control, since it has no substitution on the β-carbon of the diacrylate. Poly B2 has intermediate branching with two methyl groups on the β-carbon, and Poly B3 is the bulkiest of the series, with an ethyl and benzoate moiety. The drug release and degradation profiles of $(\text{Poly AB1/DS})_{20}$, $(\text{Poly B2/DS})_{20}$, and $(\text{Poly B3/DS})_{20}$ can be viewed in figure 2.4. The rates and half lives determined from exponential fitting can be seen in Table 2.1. As anticipated, change in steric bulk does alter release. However, while the release duration increased from Poly AB1 to Poly B2 as expected, the most hindered polymer, Poly B3, had the fastest release rate. In fact, $(\text{Poly B3/DS})_{20}$ films were found to be unstable; more than 80% of the total amount of dextran sulfate was released in ≤ 8 hours.

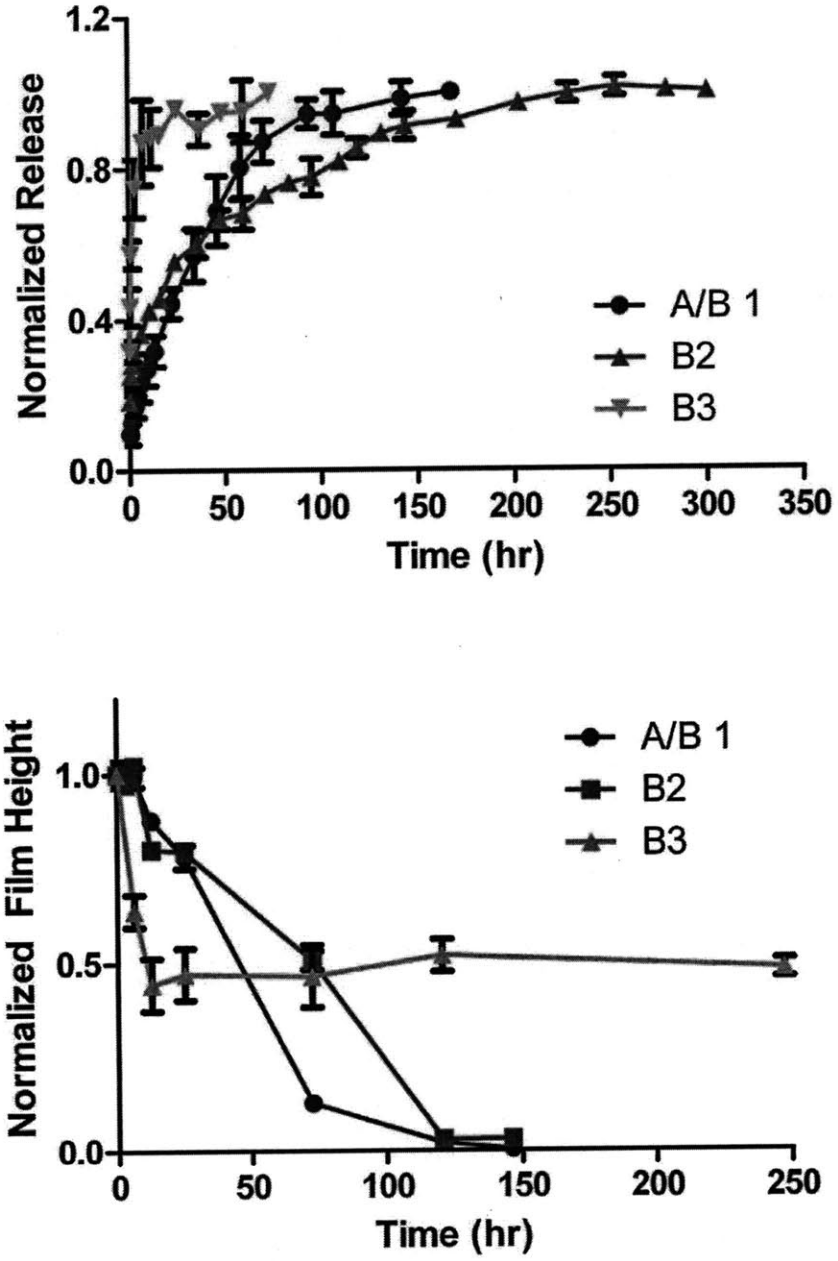


**Figure 2.4 Effect of steric bulk on $^{14}$C-dextran sulfate release and film degradation**

Release and degradation studies were performed on (Poly X/ Dextran Sulfate)$_{20}$ films at 25°C in PBS buffer. A) Normalized release of $^{14}$C-dextran sulfate versus time. Release was normalized by the total amount of dextran sulfate released for each system. B) Normalized film height of (Poly X/ Dextran Sulfate)$_{20}$ over time. Films were normalized by the film height a time zero.

To determine if (Poly B3/DS)$_{20}$ films were undergoing bulk erosion due to destabilization or normal surface erosion, film degradation and surface roughness were monitored. Both (Poly AB1/DS)$_{20}$ and (Poly B2/DS)$_{20}$ had degradation and roughness profiles characteristic of surface erosion.

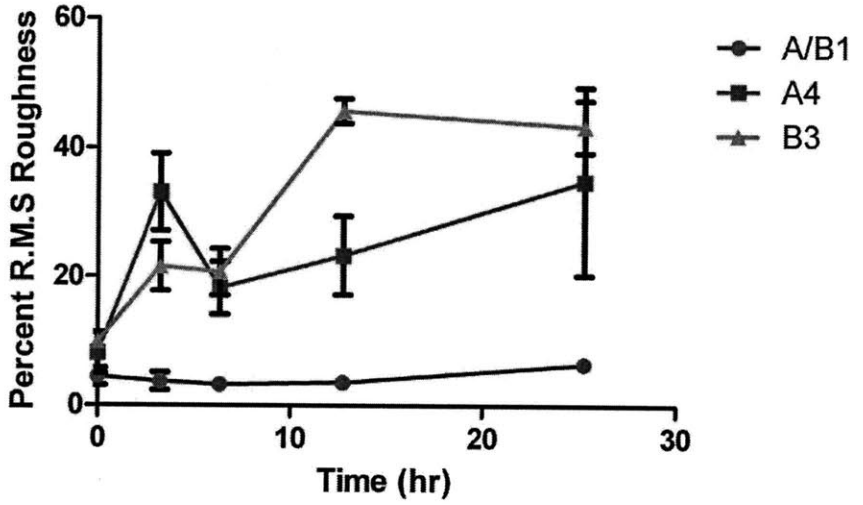


**Figure 2.5 Roughness of hydrolytically degradable films over time**

Analysis of root mean squared (rms) roughness for (Poly AB1/ dextran sulfate), (PolyA4/ dextran sulfate)$_{20}$ , and (PolyB3/dextran sulfate)$_{20}$ over time. Roughness is expressed as the percent of total film height (i.e roughness/ film height).

However, almost 50% of the (Poly B3/DS)$_{20}$ film eroded within the first 4 hours. The remaining film persisted for more than 250 hours indicating that surface erosion was not occurring, since normal surface erosion (top down chemical degradation) would have yielded degradation kinetics similar to those observed in the first four hours. The reduced film stability of Poly B3 may be attributed to its steric bulkiness, which might interfere with the ability to form ionic cross-links. Since ionic crosslinks are noncovalent

in nature, they are subject to exchange with free ions in the solution. Traditionally, polyelectrolyte multilayer films are stabilized by the myriad ionic cross-links that form on each polymer chain; however, in hydrolytically degradable LBL films, which erode via chemical degradation of the polycation, the number of ionic cross-links per chain is constantly being reduced by chain breakdown from ester hydrolysis. If sterics hinder the allowed conformational space of the polymer enough to greatly reduce the number of ionic cross-links formed per repeat unit and the number is further reduced by chain cleavage, the film stability might be compromised. Thus, it appears that the use of steric hindrance to control release rate is limited by the ability of the polymer to form sufficient ionic cross-links to maintain film stability.

Interestingly, in both (Poly A4/DS)$_{20}$ and (Poly B3/DS)$_{20}$ films, a thin slowly degrading film remained after total dextran sulfate release. Based on film degradation profiles, it can be hypothesized that some type of structural rearrangement, such as phase separation, is occurring in these films. The presence of a white precipitant remaining on the substrate after complete release is also suggestive of a phase segregation process in which the dextran sulfate escapes from the film. This analysis suggests that films were immediately destabilized, leading to reorganization of polymer within the film as water-soluble dextran sulfate was released into the bath; presumably, following this rearrangement and major film disruption, the poly(β-amino ester), which is not soluble in pH 7.4 water even at low to moderate molecular weights, remains to a large extent immobilized to the substrate surface as a residue. If phase separation occurred in this setting, charge shielding of the poly(β-amino ester) by ions in solution would allow a dense film to remain on the substrate. The hydrophobic nature of Poly A4

and Poly B3 would result in a very slowly degrading film consisting primarily of the poly(β-amino ester).

**Characterization of Film Destabilization**

To assess the possibility of a phase separation mechanism, AFM measurements of (Poly AB1/DS)$_{20}$, as a control, and (Poly A4/DS)$_{20}$ during degradation in PBS at 25°C were taken over a time course relevant for Poly A4 degradation and can be seen in Figure 5. At time zero, (Poly A4/DS)$_{20}$ films were fairly uniform with slight surface roughness, 8% of the total film thickness; however at six hours, holes on the order of 71 nm - 57% of the total film thickness - formed (figure 2.8). At twelve hours, channels appeared and the film became highly irregular. Then at 24 hours, well after DS release is complete, a relatively smooth film with few holes remained. This same morphology persisted for 48 hours (figure 2.7). In contrast, (Poly AB1/DS)$_{20}$ films start out fairly smooth, 3% of total film thickness, are swollen at six hours, and flatten out as the film continues to degrade. The findings for (Poly A4/ DS)$_{20}$ correlate with a phase segregation mechanism of film destabilization, and are consistent with the analysis of roughness over time. The root mean square roughness of (Poly A4/DS)$_{20}$ and (Poly B3/DS)$_{20}$ films were monitored over the time of complete drug release (figure 2.5). (Poly AB1/DS)$_{20}$ was used as an example of surface erosion more typically observed in these films. Significant changes in roughness were observed for both (Poly A4/DS)$_{20}$ and (Poly B3/DS)$_{20}$, two of the systems which undergo rapid destabilization. After just four hours of immersion in PBS buffer, (Poly A4/DS)$_{20}$ films had a roughness of greater than 30% of the total film thickness and (Poly B3/DS)$_{20}$ films reach a roughness of almost 50% of total film thickness in 12 hours. The gross changes in film morphology probably account for the short drug release times for (Poly A4/DS)$_{20}$ and (Poly

B3/DS)$_{20}$ films, as the soluble DS is released via bulk diffusion from the destabilized films.

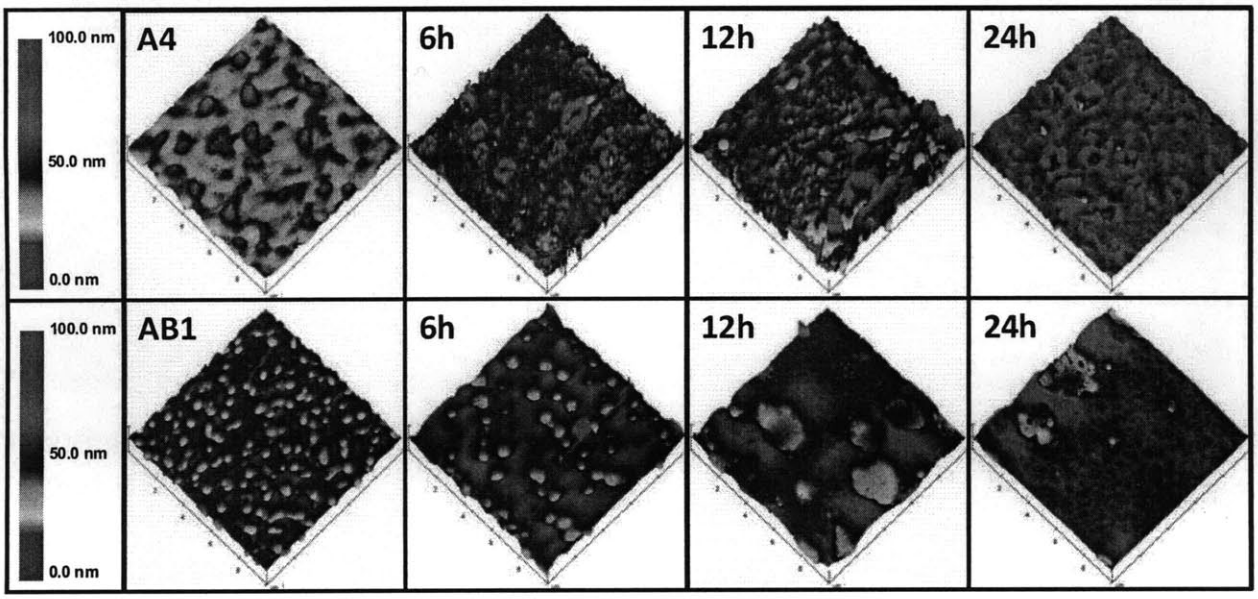


**Figure 2.6 Atomic force microscopy images of (Poly A4/Dextran Sulfate)$_{20}$ (top) and (Poly A/B1 /Dextran Sulfate)$_{20}$ (bottom) films after 0, 6, 12, and 24 hours in PBS buffer at 25°C**

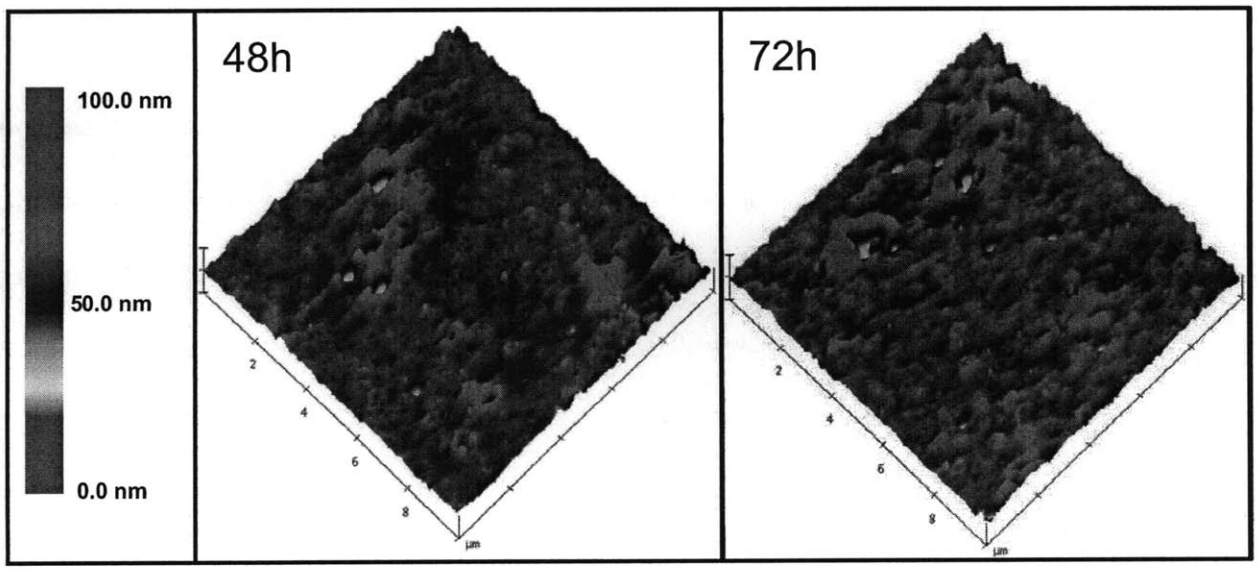


**Figure 2.7 Atomic force microscopy images of (Poly A4/Dextran Sulfate)$_{20}$ (left) and (Poly A/B1 /Dextran Sulfate)$_{20}$ (right) films after 48, and 72 hours in PBS buffer at 25°C**

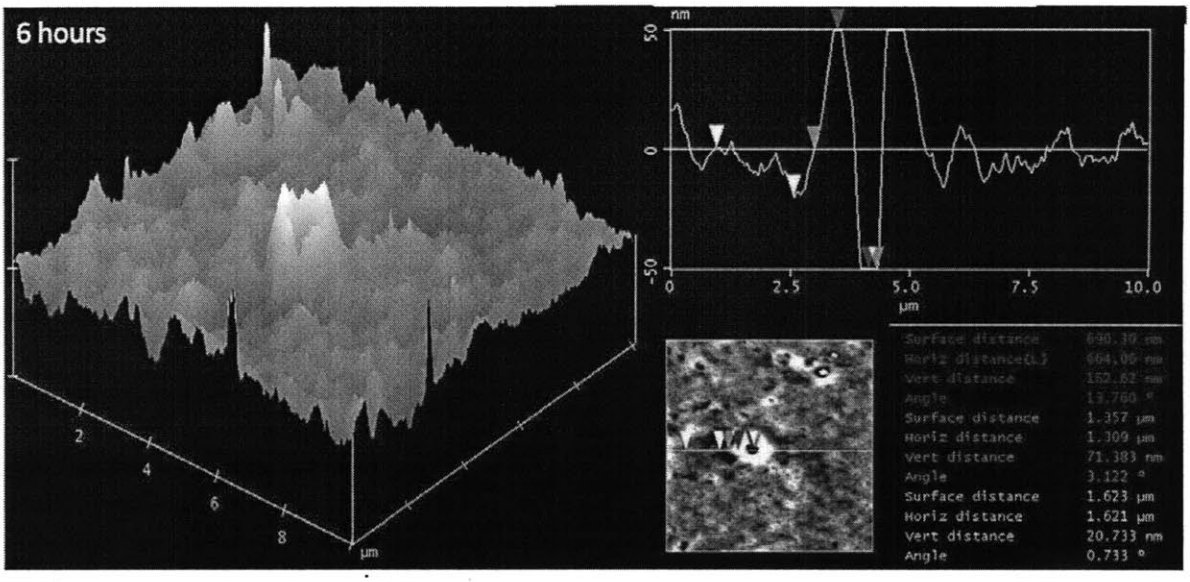


**Figure 2.8 Atomic force microscopy of (Poly A4/Dextran Sulfate)$_{20}$ after 6 hours in PBS at 25°C**

Image on the left shows the hole morphology versus the normal roughness of the film. The Image on the upper right is the section analysis of a line dissecting the hole. Analysis data from the red, green, and white markers show that the hole is 71nm deep and 91nm high (red and green markers). The deep of the deepest valley along the rest on the line is 21nm.

### Extreme Hydrophobicity Destabilizes Films

Investigation of alkyl chain length and steric bulkiness suggest that charge density and hindrance to the formation of ionic crosslinks may serve as limiting phenomena in the structural control of release dynamics. The similar morphological changes observed for both (Poly A4/DS)$_{20}$ and (Poly B3/DS)$_{20}$ suggest a common mechanism for destabilization. In both polymer series, the general hydrophobicity of the polymer is increased. Therefore, it can be hypothesized that film destabilization is caused by a hydrophobicity limit, beyond which film deconstruction and phase segregration occurs. Though the limits of charge density and degree of ionic crosslinks

have been documented in LbL film adsorption, hydrophobic film disruption has yet to be shown[41]. To assess the validity of the hydrophobic effect on multilayers, octanol:water coefficients were calculated for Poly A4 and B3. Octanol: water coefficients are partition coefficients for solutes in octanol versus water, and are often expressed with the logarithmic scale as LogP. The LogP is a distinct physiochemical property of a molecule and used as the standard scale for lipophilicity. In fact LogP calculations are widely used to determine pharmacological endpoints, bioconcentration, soil sorption coefficients, and biodegradation rate. While experimental methods to determine LogP exist, they are often time consuming, expensive, and can be difficult or even impossible to perform for certain molecules[42]. Thus, computational models, which serve as reliable predictive models, are heavily used. In this study, eight widely acclaimed and readily available models of octanol:water coefficients were utilized, to avoid biases that could arise from use of a single method. Using these models, the hydrophobicity of Poly A4 and B3 were found to be similar, indicating that hydrophobicity alone could account for the observed film instability.

**Octanol:Water Coefficient as a Predictor of Release Duration**

To clarify the mechanism of destabilization, and ascertain whether the effect is due to loss in charge density or increase in chain hydrophobicity, polymers C1 and C2 were examined. Poly C1, a fluorinated version of Poly A3 with a LogP similar to Poly A4 and B3, was used to determine if hydrophobicity alone could destabilize the multilayer films. Since $(\text{Poly A3/DS})_{20}$ was found to be stable, and the charge density of A3 and C1 are essentially the same, the destabilization of $(\text{Poly C1/DS})_{20}$ films indicate a mechanism based on hydrophobicity. The release kinetics of multilayers containing Poly C1 can be seen in Figure 2.9. Films constructed of $(\text{Poly C1/DS})_{20}$ were unstable and

released more than 80% of the total amount of the dextran sulfate in less than 8 hours, suggesting that hydrophobicity does cause film instability. Still, the effect of sterics and charge density could not be ruled out, so to determine their role, Poly C2 was also investigated as a component in the multilayer films. Poly C2 has a LogP similar to Poly AB1, but its bulkiness and backbone charge density are similar to Poly A4 and B3 respectively. (Poly C2/DS)$_{20}$ films did not undergo destabilization, as shown in Figure 6. The relative contributions of charge density and alkyl chain length were clarified by investigating the mechanism clarification (C) series of polymers. Specifically, Poly C1 has the same charge density as Poly A3, which forms stable films. However, Poly C1 has a greater octanol:water coefficient and is thus more hydrophobic than Poly A3. Films composed of Poly C1and dextran sulfate were unstable, indicating that hydrophobicity alone can destabilize films. To determine if charge density was responsible for the destabilization of Poly A4, films composed of Poly C2 were constructed. Poly C2 is more hydrophilic than Poly A4, but has a charge density. Poly C2 films were stable, proving that the charge density alone could not disrupt film stability.

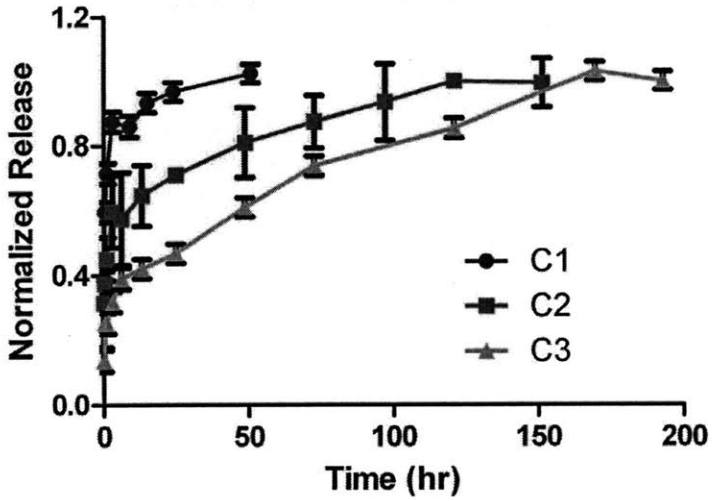


**Figure 2.9 Effect of chemical structure on $^{14}$C-dextran sulfate release**

Release studies were performed on (Poly X/ Dextran Sulfate)$_{20}$ films at 25°C in PBS buffer and release was normalized by the total amount of dextran sulfate released for each system.

Therefore structural manipulation can only be used to alter release in hydrolytically degradable LBL films to the extent that polymer hydrophobicity helps to induce film destabilization.

Since LogP proved to be an important indicator for film instability, release duration versus LogP was plotted for all of the systems to examine the significance of LogP in the release predictions. The resulting graph in Figure 2.10 shows a strikingly clear trend between LogP and release with increasing LogP corresponding to increased release duration until film instability occurs at LogP ≥ 3.8. As illustrated, increasing LogP resulted in a predictive increase in release duration until a certain threshold value. Beyond this point, hydrolysis of the poly(β-amino ester) no longer dominated the erosion process. At values higher than the threshold, the films become destabilized by the

extent of polymer hydrophobicity. The presence of a trend for each computational method was determined. Though slight differences existed, all methods yielded the same general trend; therefore averaged values were used to provide a consensus for logP values and generate a master curve.

To ascertain if Poly A3 served as the true peak of release before destabilization and test the accuracy of the trend, Poly C3 was examined. Poly C3 is composed of a cyclohexanedimethyl diacrylate and has a LogP of 3.1. Films constructed of (Poly C3/DS)$_{20}$ were found to have a release duration lower than (Poly A3/DS)$_{20}$, but did not exhibit film destabilization. Additionally, (Poly C3/DS)$_{20}$ films fell within the trend, suggesting that once a certain logP is reached some degree of hydrophobic destabilization occurs leading to reduced release duration.

| Diacrylate | ALOGPS | IA LogP | AB/LogP | miLogP | KOWWIN | XLOGP | ACD/LogP | ClogP | Average | Std. Dev. |
|---|---|---|---|---|---|---|---|---|---|---|
| AB1 | 1.07 | 1.71 | 1.76 | 1.6 | 1.61 | 1.21 | 1.16 | 1.25 | 1.42 | *0.27* |
| A2 | 1.57 | 2.08 | 2.14 | 1.87 | 2.1 | 1.57 | 2.2 | 1.72 | 1.91 | *0.26* |
| A3 | 2.9 | 2.92 | 3.16 | 2.88 | 3.08 | 2.29 | 2.96 | 2.65 | 2.85 | *0.27* |
| A4 | 3.94 | 4.31 | 4.62 | 4.39 | 4.55 | 3.99 | 4.55 | 4.04 | 4.30 | *0.27* |
| B2 | 2.14 | 2.43 | 2.49 | 2.48 | 2.48 | 1.91 | 1.86 | 2.11 | 2.24 | *0.26* |
| B3 | 3.7 | 3.53 | 4.17 | 4.07 | 3.96 | 3.8 | 4.36 | 3.59 | 3.90 | *0.29* |
| C1 | 3.07 | 3.53 | 4.33 | 3.89 | 4.98 | 4.38 | 4.71 | 3.27 | 4.02 | *0.69* |
| C2 | 1.75 | 1.63 | 1.48 | 1.63 | 0.89 | 0.91 | 1.22 | 1.12 | 1.33 | *0.34* |
| C3 | 2.85 | 2.93 | 3.45 | 3.24 | 3.8 | 2.75 | 3.38 | 2.2 | 3.07 | *0.50* |

**Table 2.2 . LogP values for the eight methods utilized and the average octanol:water coefficients used in analysis.**

The octanol:water coefficients of the diacrylate monomer were calculated using eight different theoretical methods. The eight methods were averaged to provide a consensus value for the diacrylate monomers.

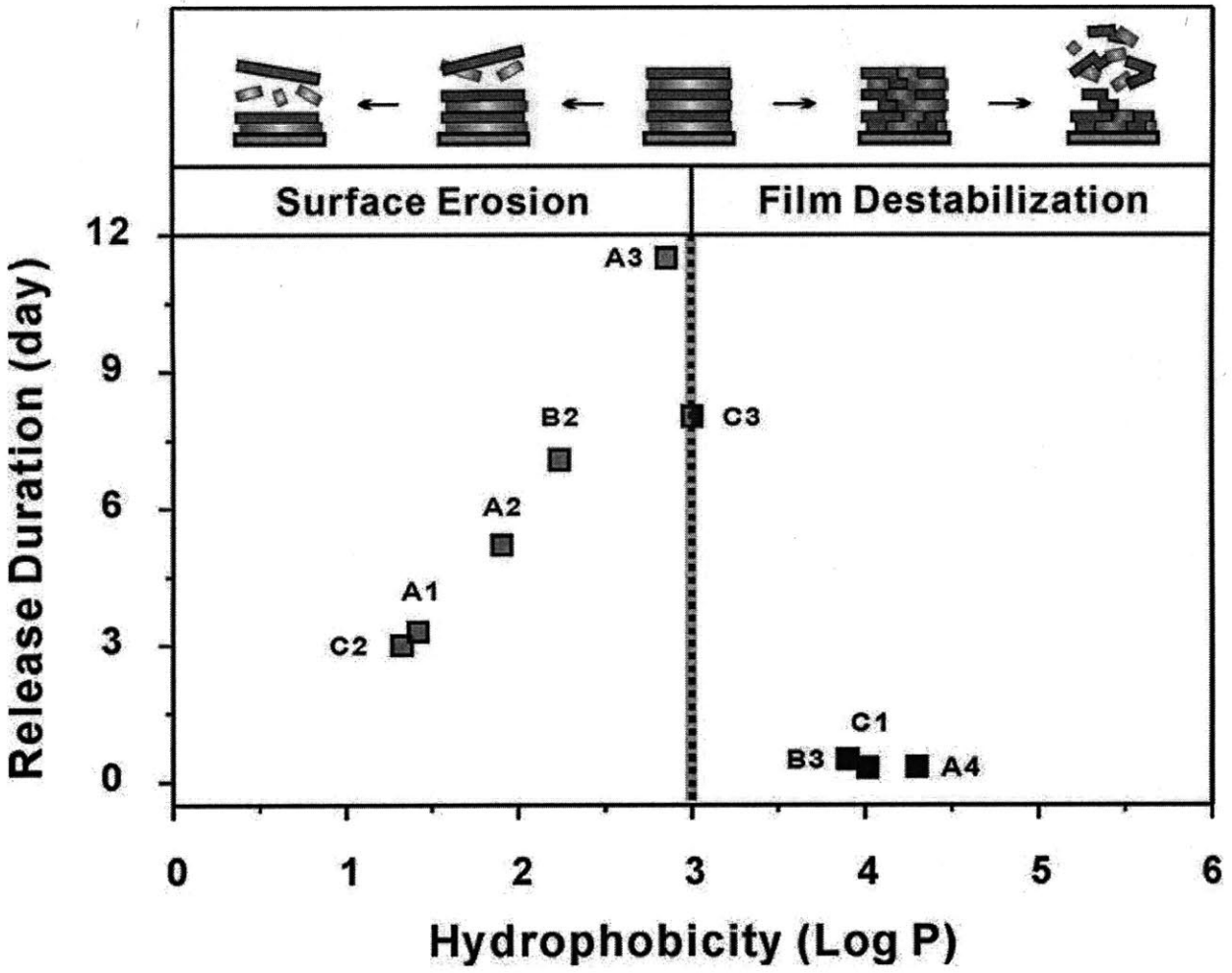


**Figure 2.10 Correlation between octanol:water coefficient (LogP), release duration, and proposed dissolution mechanism in (Poly X/Dextran Sulfate)$_{20}$ films.**

Data labels indicate the corresponding polymer for each observed release time.

This same trend is also observed if the half-lives are used, further validating the utility of LogP in predicting release duration. Ongoing research should focus on elucidating morphological changes in systems with LogP greater than 3.8. The correlations in Figure 2.10 suggest that LogP can be used to predict the release duration of poly (β – amino ester)s in LbL films, irrespective of diacrylate monomer structure, and that these

relationships can potentially be generalized to include a number of different counterpolyanions. Though extreme hydrophobicity represents a barrier to extending release duration through structural manipulation of the polymer backbone, it is not insurmountable. To overcome the hydrophobicity limit and achieve longer release times, crosslinked films were constructed. Diacrylate endcapped Poly A3 was synthesized by creating a stoichiometric imbalance in the monomer ratio. This endcapped polymer was lightly crosslinked using a photoinitiator and assembled in films or films were assembled with endcapped polymer and post-crosslinked by UV exposure after assembly.[27] Figure 2.11 and table 2.1 show that the release duration and half-life is extended with crosslinking. UV treated films had the longest duration and half-life with film release occurring over 600 hr and a $t_{1/2}$ of 222 hours.

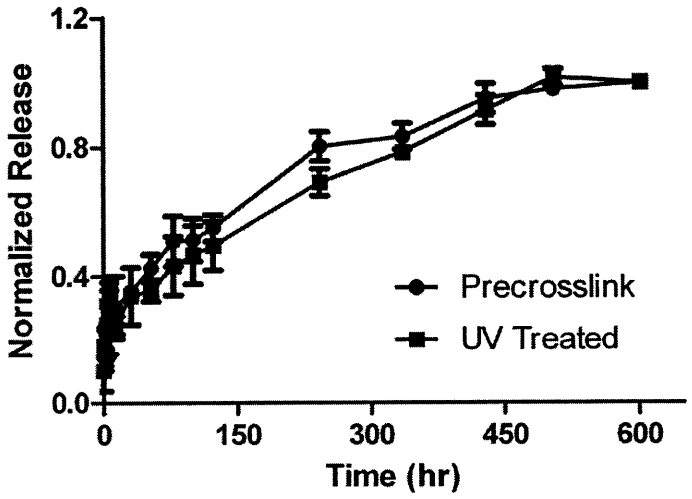


**Figure 2.11 Normalized release from crosslinked (Poly A3/ Dextran Sulfate)$_{20}$ films**

Release studies were performed on crosslinked (Poly X/ Dextran Sulfate)$_{20}$ films at 25°C in PBS buffer and release was normalized by the total amount of dextran sulfate released for each system. Poly (beta – amino esters) were either crossedlinked before film assembly (precrosslink) or crosslinked after assembly (uv treated).

## Conclusions

The fabrication of drug delivery vehicles has emerged as an active area of research due to the complications associated with medical prostheses[1]. Traditional drug delivery coatings are limited by the elution of a single therapeutic, diffusion based release characteristics, and often harsh processing conditions,. Polyelectrolyte multilayer films represent a versatile technology for the creation of simple, conformal drug delivery coatings that enable one to engineer release dynamics based on chemical composition as well as thin film heterostructure. Recent research has highlighted the ability of these films to deliver a broad range of therapeutics and has focused on the creation of hydrolytically degradable films[3, 7, 19]. Hydrolytically degradable polyelectrolyte multilayer films have enabled the attainment of complex release profiles through the selection of film architecture and utilization of top down degradation associated with surface erosion[3]. Still, the formation of an effective delivery system hinges upon the ability to selectively control drug release profiles. Examination of film release dynamics, degradation, and stability as it relates to steric bulk, charge density and hydrophobicity is unprecedented in the literature. Towards establishment of a framework for degradable multilayer film design, the effect of chemical composition on drug delivery properties in hydrolytically degradable, polyelectrolyte multilayer films was investigated. To determine the effect of chemical structure, several poly(β-amino esters) were constructed by varying the diacrylate monomer used in the polymerization. Films containing alternating depositions of the various poly(β-amino esters) and a model drug, dextran sulfate, were used to ascertain the role of hydrophobicity, steric hindrance, and charge density on release dynamics. Small changes in hydrophobicity led to

substantial increases in release duration until a critical hydrophobicity of the degradable polycation was reached, upon which major film destabilization and rapid release occurred.

To clearly understand the boundaries, trends, and limitations associated with chemical control of drug release, a quantitative measure of hydrophobicity, LogP, was used to examine release profiles. This revealed a novel correlation between LogP and release duration. Octanol:water coefficients were found to be a key indicator of release duration and film stability in these systems. Release duration was found to increase proportionally with LogP until a threshold value, at which films becomes rapidly destabilized, was reached. However, the barrier imposed by extreme hydrophobicity could be overcome by other chemical modification such as crosslinking of the film or film components. Destabilization was hypothesized to result from phase segregation of very hydrophobic degradable cation and the hydrophilic polyanion. Thus, release dynamics are not only dependent on hydrolytic susceptibility but a complex balance between hydrophobic composition, charge density, and stability of electrostatic ion pairs. Utilization of LogP as a predictive tool for release duration will allow for the selection of polymers based on biological, chemical, and mechanical properties with an understanding of the effect on drug release. Moreover, issues of biocompatibility including toxicity, immunogenicity, and biofouling can also be addressed. Therefore, polymer selection will no longer be driven by a need for specific release profiles. The determination of a logP:release duration correlation will allow the creation of polymers based on the specific demands of the application and implantation site. In addition, this correlation and in-depth exploration of the interactions that drive hydrophobic instability

in these films may have far reaching implications in electrostatically assembled thin films in general.

## References


[1] P. Wu, D. W. Grainger, *Biomaterials* **2006**, *27*, 2450.
[2] A. Akinc, D. M. Lynn, D. G. Anderson, R. Langer, *Journal of the American Chemical Society* **2003**, *125*, 5316.
[3] K. C. Wood, H. F. Chuang, R. D. Batten, D. M. Lynn, P. T. Hammond, *Proceedings of the National Academy of Sciences of the United States of America* **2006**, *103*, 10207.
[4] K. C. Wood, N. S. Zacharia, D. J. Schmidt, S. N. Wrightman, B. J. Andaya, P. T. Hammond, *Proceedings of the National Academy of Sciences of the United States of America* **2008**, *105*, 2280.
[5] A. Gopferich, *Biomaterials* **1996**, *17*, 103.
[6] G. Decher, *Science* **1997**, *277*, 1232.
[7] J. C. Voegel, G. Decher, P. Schaaf, *Actualite Chimique* **2003**, 30.
[8] N. B. Jessel, P. Schwinte, R. Donohue, P. Lavalle, F. Boulmedais, R. Darcy, B. Szalontai, J. C. Voegel, J. Ogier, *Advanced Functional Materials* **2004**, *14*, 963.
[9] J. T. Zhang, L. S. Chua, D. M. Lynn, *Langmuir* **2004**, *20*, 8015.
[10] P. T. Hammond, *Advanced Materials* **2004**, *16*, 1271.
[11] A. M. Yu, Z. J. Liang, F. Caruso, *Chemistry of Materials* **2005**, *17*, 171.
[12] N. Jessel, M. Oulad-Abdeighani, F. Meyer, P. Lavalle, Y. Haikel, P. Schaaf, J. C. Voegel, *Proceedings of the National Academy of Sciences of the United States of America* **2006**, *103*, 8618.
[13] Z. Y. Tang, Y. Wang, P. Podsiadlo, N. A. Kotov, *Advanced Materials* **2006**, *18*, 3203.
[14] K. J. Loh, J. Kim, J. P. Lynch, N. W. S. Kam, N. A. Kotov, *Smart Materials & Structures* **2007**, *16*, 429.
[15] Y. Zhong, C. F. Whittington, D. T. Haynie, *Chemical Communications* **2007**, 1415.
[16] B. S. Kim, S. W. Park, P. T. Hammond, *Acs Nano* **2008**, *2*, 386.
[17] Y. Lvov, K. Ariga, I. Ichinose, T. Kunitake, *Journal of the American Chemical Society* **1995**, *117*, 6117.
[18] A. P. R. Johnston, H. Mitomo, E. S. Read, F. Caruso, *Langmuir* **2006**, *22*, 3251.
[19] D. M. Lynn, *Soft Matter* **2006**, *2*, 269.
[20] F. Meyer, V. Ball, P. Schaaf, J. C. Voegel, J. Ogier, *Biochimica Et Biophysica Acta-Biomembranes* **2006**, *1758*, 419.
[21] M. A. Borden, C. F. Caskey, E. Little, R. J. Gillies, K. W. Ferrara, *Langmuir* **2007**, *23*, 9401.
[22] A. Dierich, E. Le Guen, N. Messaddeq, J. F. Stoltz, P. Netter, P. Schaaf, J. C. Voegel, N. Benkirane-Jessel, *Advanced Materials* **2007**, *19*, 693.
[23] M. Dimitrova, Y. Arntz, P. Lavalle, F. Meyer, M. Wolf, C. Schuster, Y. Haikel, J. C. Voegel, J. Ogier, *Advanced Functional Materials* **2007**, *17*, 233.

[24] M. C. Berg, L. Zhai, R. E. Cohen, M. F. Rubner, *Biomacromolecules* **2006**, *7*, 357.
[25] B. Thierry, P. Kujawa, C. Tkaczyk, F. M. Winnik, L. Bilodeau, M. Tabrizian, *Journal of the American Chemical Society* **2005**, *127*, 1626.
[26] E. Vazquez, D. M. Dewitt, P. T. Hammond, D. M. Lynn, *Journal of the American Chemical Society* **2002**, *124*, 13992.
[27] D. G. Anderson, C. A. Tweedie, N. Hossain, S. M. Navarro, D. M. Brey, K. J. Van Vliet, R. Langer, J. A. Burdick, *Advanced Materials* **2006**, *18*, 2614.
[28] S. R. Little, D. M. Lynn, S. V. Puram, R. Langer, *Journal of Controlled Release* **2005**, *107*, 449.
[29] D. M. Lynn, R. Langer, *Journal of the American Chemical Society* **2000**, *122*, 10761.
[30] G. T. Zugates, W. D. Peng, A. Zumbuehl, S. Jhunjhunwala, Y. H. Huang, R. Langer, J. A. Sawicki, D. G. Anderson, *Molecular Therapy* **2007**, *15*, 1306.
[31] D. G. Anderson, D. M. Lynn, R. Langer, *Angew. Chem. Int. Ed.* **2003**, *42*, 3151.
[32] K. C. Wood, J. Q. Boedicker, D. M. Lynn, P. T. Hammon, *Langmuir* **2005**, *21*, 1603.
[33] J. T. Zhang, N. J. Fredin, J. F. Janz, B. Sun, D. M. Lynn, *Langmuir* **2006**, *22*, 239.
[34] J. T. Zhang, N. J. Fredin, D. M. Lynn, *Journal of Polymer Science Part a-Polymer Chemistry* **2006**, *44*, 5161.
[35] J. Zhang, D. M. Lynn, *Macromolecules* **2006**, *39*, 8928.
[36] G. Klopman, H. Zhu, *Mini-Rev. Med. Chem. FIELD Full Journal Title:Mini-Reviews in Medicinal Chemistry* **2005**, *5*, 127.
[37] I. V. Tetko, J. Gasteiger, R. Todeschini, A. Mauri, D. Livingstone, P. Ertl, V. A. Palyulin, E. V. Radchenko, N. S. Zefirov, A. S. Makarenko, V. Y. Tanchuk, V. V. Prokopenko, *J. Comput.-Aided Mol. Des.* **2005**, *19*, 453.
[38] J. Livingstone David, *Curr Top Med Chem FIELD Full Journal Title:Current topics in medicinal chemistry* **2003**, *3*, 1171.
[39] *Vol.* http://www.vcclab.org, VCCLAB, Virtual Computational Chemistry Laboratory, **2005**.
[40] Z. Y. Zhong, Y. Song, J. F. J. Engbersen, M. C. Lok, W. E. Hennink, J. Feijen, *Journal of Controlled Release* **2005**, *109*, 317.
[41] B. Schoeler, G. Kumaraswamy, F. Caruso, *Macromolecules* **2002**, *35*, 889.
[42] J. Taskinen, J. Yliruusi, *Adv. Drug Delivery Rev.* **2003**, *55*, 1163.

# Chapter 3 : Layer – by – Layer Platform Technology for Small Molecule Delivery

This chapter has been reproduced in part from: R. C. Smith, M. Riollano, A. Leung, P. T. Hammond, *Angewandte Chemie-International Edition* **2009**, *48*, 8974 - 8978.

## Introduction

Small molecules are critical to every aspect of biological function, and comprise most medicines marketed to date.[1] Yet a large number of small organic molecules exhibit low aqueous solubility and > 40% of all drug failures in development are due to inadequate drug delivery.[2] As high-throughput methods continue to produce a myriad of chemical entities able to amend complex disease pathways, there is increased pressure to find effective and efficient ways to deliver these molecules in an appropriate manner. As science begins to understand the dynamic role a single molecule can have on critical, yet diverse, pathways throughout the body, we can no longer rely on systemic administration as the predominant means of therapeutic delivery. The cardiotoxicity of potent nonsteroidal anti-inflammatory drugs (NSAIDs), such as rofecoxib (Vioxx), are a prime example of the power and necessity of localized delivery.[3] Materials and methods capable of controlled, localized delivery will be essential for the implementation of these drugs in the future. As the use of small molecule probes provides more insight into biological function and therapeutic candidates the paucity of truly diverse delivery vehicles becomes a bottleneck in the application of potentially powerful and beneficial therapeutics. While methods to construct coatings for localized small molecule delivery exist, most rely on diffusion

based release and suffer from bolus dumping, short release timescales, harsh assembly conditions, complex manufacturing and/or limited therapeutic scope and incorporation. There exists a profound need to deliver a diverse set of neutral and hydrophobic small molecules with exact spatiotemporal control.

Layer-by-Layer (LbL) assembly, a directed assembly technique based on complementary chemical interactions, is a versatile technique for the creation of diverse, customized material systems with nanoscale control of composition.[4] These films are exceptional in their ability to incorporate a wide variety of materials, such as carbon nanotubes, functional polymers, viruses, cells, oligonucleotides, proteins, and inorganics, on virtually any surface regardless of geometry and surface chemistry.[5-8] The ability to produce nanoscale conformal films able to incorporate diverse set of materials for broad applications through mild aqueous manufacturing at room temperature is unique to LbL assembly. LbL films have been applied to almost every area of science and technology, including electronic, biological, agricultural, and chemical utilization.[6, 7, 9-11] This thin film system can easily enhance any existing technology or function as a standalone device. Still a fundamental limitation of LbL is the inability to delivery small molecules with the same characteristic control as macromolecular structures. Small molecule delivery is a vital deficit in the broad applicability of LbL constructs.

Rubner, Caruso, and others have worked to surmount this problem and address the demand for small molecule applications.[12-21] Rubner used direct absorption to incorporate ketoprofen, an anti-inflammatory drugs, and cytochalasin D, a mycotoxin, into nanoporous and microporous films composed of poly(allylamine hydrochloride) and

poly(acrylic acid).[12] Porosity was induced by acid and base treatments followed by crosslinking at 180°C for several hours to lock in porosity. The loading of small hydrophobic molecules was achieved through soaking in or wicking from a solution of drug dissolved in DMSO followed by rinsing in water for several hours to remove solvent and loosely bound drug. Nanoporous and microporous films were able to deliver active drug for 4 – 34 days with zero order or fickian diffusion release kinetics, respectively. While release duration and drug loading was controlled through bilayer number, release rate could not be modulated and drug loading did not exceed 600 ng. Though capable of sustained release of active therapeutics, the harsh fabrication methods limit the scope and utility of nanoporous and microporous films.

Other work has focused on particulate carriers for small molecules, namely dendrimers and micelles. Caruso first used dendrimers in layer-by-layer films.[15] These films were constructed of poly(styrenesulfonate) and a positively charged fourth generation poly(amidoamine) dendrimers. The dendrimers within the film acted as nanoreservoirs to sequester oppositely charged small molecules and release them over several hours. Hammond improved on this method by encapsulating dendrimer-drug complexes into LbL films for sustained release of uncharged hydrophobic small molecules.[19] Films were composed of poly(acrylic acid) and poly(propylene oxide)-poly(amidoamine) fourth generation dendrimers. Sustained release of triclosan, an antibiotic, was achieved for twenty days via fickian diffusion. Hammond also demonstrated the pH controlled release of triclosan from poly(ethylene oxide)-block-poly(ε-caprolactone) micelles.[16] While particulate carriers allow for drug incorporation and release, many are plagued by short release timescales and all are rate limited by

diffusion of molecules from the particle core. Thierry, et al. constructed LbL films composed of chitosan and hyaluronan prodrug of paclitaxel attached via a labile succinate ester linkage.[20] Controlled release of active drug was mediated by both linker hydrolysis and diffusion through the bulk matrix. However, the prodrug method is only applicable to small molecule that can form hydrolysable bonds with polyelctrolytes. In addition, drug loading was low due to a mere three mole percent degree of substitution for pacitaxel on the hyaluronan backbone.

LbL has been unable to address the demand for small molecule delivery with highly controlled release kinetics, and attempts have been plagued by diffusion-controlled rates, short release timescales, and often ill-defined release mechanisms. Diffusion kinetics prevent facile advanced engineering of release dynamics, and release is often modulated by increasing system complexity. For many drugs, burst release carries an increased risk of toxicity and short timescales limit general applicability. Direct absorption of molecules and use of carriers such as dendrimers, micelles, nanoparticles, and prodrugs have been unable to overcome these barriers.[12, 14-21]

Herein the first LbL system able to surmount the problems of diffusion, dumping, and limited timescale to attain previously unachievable release kinetics, while maintaining therapeutic activity is described. This approach used a charged cyclodextrin carrier capable of facile reversible complexation with the drug of choice in alternation with a degradable polyion. The key to this approach was the stable trapping of inclusion complexes in a hydrolytically degradable matrix. This technology was built on the fundamental noncovalent chemical interaction between neutral and/or hydrophobic molecules and cyclodextrins. Cyclodextrins are toroidally shaped oligosaccharides,

which present a hydrophobic interior and hydrophilic exterior.[22] This nature gives cyclodextrins the ability to host neutral and/or hydrophobic molecules by making inclusion compounds in aqueous environments. Cyclodextrin complexation is renowned as a simple method to increase drug solubility, bioavailability, stability, and resistance to degradative enzymes *in vivo* with no immunogenicity.[22-27] Monomeric cyclodextrins are versatile carriers of small molecule therapeutics, exemplified by their commercial presence and pharmaceutical use.[23, 27] Benkirane-Jessel et al first incorporated a drug into polyelectrolyte multilayers through inclusion complexes with monomeric cyclodextrins to render the film anti-inflammatory.[14] A synthesized anionic monomeric cyclodextrin was used as the charged carrier for piroxicam, a nonsteroidal anti-inflammatory drug (NSAID). Films were composed of poly(L-lysine) and poly(L-glutamic acid and up to three layers of cyclodextrin-drug complex. Drug release was monitored by suppression of TNF-α, an inflammatory cytokine, from stimulated monocytes. Suppression was monitored for up to twelve hours. However, the minimal incorporation of cyclodextrins, only one to three layers within a poly(L-lysine) and poly(L-glutamic acid) film does not give a clear indication of cyclodextrin utility, in polyelectrolyte multilayer assembly.

Both monomeric and polymeric cyclodextrins were investigated as carriers for small hydrophobic molecules. Monomeric cyclodextrins were unable to stably trap small molecules, resulting in rapid release. Polymeric cyclodextrins, which had never been incorporated in multilayer films, were necessary to capture the cyclodextrin-drug interaction in stable films able to undergo top down erosion. The ability of cyclodextrins to complex with myriad of drugs, proteins, and oligonucleotides, enable these films to be

engineered with versatility unavailable to many conventional drug delivery systems.[23, 26] Combined with the tunability of hydrolytically degradable films, these constructs provide the first opportunity to create truly custom coatings for small molecule applications.

## Materials and Methods

**Materials**: Captisol ®, sulfobutyl ether β-cyclodextrin ( $SBE_7$ – BCD), was purchased from CyDex Pharmaceuticals Inc (Lenexa, Kansas). Poly(carboxymethyl – beta cyclodextrin) had a degree of substitution between 2.8 – 4.1 % and was purchased from CTD Inc (Gainesville , FL). Diclofenac, naproxen, flurbiprofen, and ketoprofen were purchased from TCI America (Portland, Organ). $^3H$ – dexamethasone was purchased from American Radiolabeled Chemicals Inc (St. Louis, Missouri). Cyclooxygenase fluorescent inhibitor screening assay kit was purchased from Cayman Chemicals (Ann Arbor, Michigan). All other materials were purchased from Sigma Aldrich (St. Louis, Missouri) or by the sources indicated in chapter one.

**Cyclodextrin – Drug Complexation**: Complexes were formed by first determining crude drug solubility in the aqueous cyclodextrin solution. To accomplish this, varying concentrations of cyclodextrin were added to a fixed concentration of drug. The cyclodextrin concentration that solubilized the drug was used to make a drug concentration calibration curve for drug solution. Calibration ccurves were constructed by making serial dilutions of the stock concentration and recording fluorescence intensity versus concentration at the maximum wavelength of emission. The calibration curve was used to determine the complexation coefficient, strength of the complexation, from a phase solubility plot.[24, 28] The complexation coefficient ( $K_{1:1}$) or stability constant

was determined by making a 40 wt % cyclodextrin stock solution. The stock solution was then serially diluted. Each serial dilution was added to an excess amount of drug. Solutions were shaken, sonicated, or vortexed for 30 minutes at room temperature. The solutions were then filtered to remove undissolved drug. Drug solutions were analyzed for drug content. Then $S_t$, the concentration of solubilized drug, was plotted versus $[CD]_t$, the cyclodextration concentration. If 1:1 guest:host complexes are formed , which occur for most lipophilic molecules, the following equation can be used to determine $K_{1:1}$ where $S_o$ is the intrinsic aqueous solubility of the drug.[24] Intrinsic drug solubility were determined from the NIH ChemIDpus Advanced website (http://chem.sis.nlm.nih.gov/chemidplus/).

$$S_t = S_o + \frac{K_{1:1}S_o}{1 + K_{1:1}S_o}[CD]_t$$

If the plot of $S_t$ versus $[CD]_t$ is linear, the complexation constant can be calculated from the slope of and the intercept ($S_o$) as shown below.[24, 28]

$$K_{1:1} = \frac{slope}{S_o(1 - slope)}$$

The complexation coefficient was then used to determine the drug solubility for a given cyclodextrin concentration. Experiments were done in 0.1 M sodium acetate buffer at pH 5 and 6. The solubility at 20 mg/mL of cyclodextrin were found to be 17 mg/mL, 2.8 mg/mL, 0.538 mg/mL, 0.84 mg/mL for dexamethasone, diclofenac, flurbiprofen, and naproxen respectively.Dipping solutions were made my adding a 20 mg/mL cyclodextrin solution in 0.1 M sodium acetate buffer at pH 5 or 6 to the appropriate concentration of drug and vortexing for five to ten minutes.

**Polyelectrolyte Multilayer Assembly**: LBL films were constructed on 1.5 $cm^2$ glass, quartz, or Si substrates using an automated dipping system as previously described in chapter one. All substrates were plasma etched, and coated with ten bilayers of linear polyethylene imine and poly (styrene sulfonate). Hydrolytically degradable films were constructed with a degradable polycation and anionic cyclodextrin on ten bilayers of LPEI and PSS. The degradable polycations used in this experiment were Poly A/B1, Poly A2, and Poly A3. Monomeric cyclodextrin films, containing Captisol ®, were assembled in 0.1 M sodium acetate buffer at pH 5. Ionic strengths of 0.1, 02, and 0.5M were tested. The deposition time for Poly Xs and Captisol ® were 10 and 60 minutes respectively. Captisol and its drug complexes required an hour to deposit enough material to lead to charge reversal and film formation. Polymeric cyclodextrin films, containing poly(carboxymethyl-betacyclodextrin), were assembled in 0.1 M sodium acetate buffer at pH 6 with 10 minute deposition steps. Film growth was retarded at pH 5 even for a one hour dipping time. Assembly at pH 6 and 7 was more robust and occurred readily with 10 minute deposition times. Films were constructed at pH 6 to reduce degradation of poly(β-amino esters) over the time course of dipping. Poly(β-amino ester) solutions were changed every twelve hours. Following deposition, the films were dried thoroughly under a stream of dry nitrogen.

**Thin Film Characterization**: Growth curves were constructed by measuring the thickness of films constructed on Si at various bilayers. Film thickness was measured using a Gaertner Variable Angle Ellipsometer (6328 nm, 70° incident angle) and Gaertner Ellipsometer Measurement Program (GEMP) Version 1.2 software interface. Ns and Ks values with their respective standard deviations were measured for the bare

substrates prior to deposition. Those values were then used to determine the thickness of the base layers and subsequent bilayers. Degradation studies were performed with nonradiolabled 20 bilayer films. Films were immersed in 20 mL phosphate buffer solution (PBS) in a screw top glass vial and tightly sealed. At various times, films were removed, dried thoroughly under a stream of dry nitrogen, and thickness was measured using ellipsometry at five predetermined locations on the film surface. Following measurements, films were reimmersed in buffer solutions and resealed. All growth and degradation studies were performed in triplicate.

**Quantification of Drug Release**: Release profiles for films containing Captisol ® - dexamethasone complexes release were investigated by monitoring the release of $^{3}H$-dexamethasone (American Radiolabeled Chemicals, Inc.) in a similar manner as $^{14}C$-dextran sulfate described in chapter two. Briefly, for drug release experiments, 20 bilayer, radiolabeled films were constructed using radiolabeled dexamethasone. The radiolabled deposition solutions were prepared by combining $^{3}H$-dexamethasone (40 Ci/mmol, Mn = 318), unlabeled dexamethasone ($M_n$ = 318), and 100 mM acetate buffer to yield a total concentration of dexamethasone (unlabeled plus labeled) to 10 mg/mL (2 µCi/mL 3H). After fabrication, each twenty bilayer film was immersed in 10 mL phosphate buffer solution. A 1 mL sample was extracted at various time points and analyzed via scintillation counting. Fresh PBS was added to replace the extracted amount. Raw data (disintegrations per minute, DPM) were converted to micrograms (µg). Scintillation counting was performed on a Tri-carb liquid scintillation counter (Model U2200) and the amount of radiolabel in each sample vial was measured using

$^3H$ protocol. Release vials were tightly capped between sample extractions to prevent evaporation of the buffer solution.

Diclofenac, flurbiprofen, naproxen, and prodan release were monitored via fluorescence spectroscopy on a Fluorolog-3 spectrofluorometer. Cyclodextrin containing films were immersed in 10 mL of PBS buffer in a 50 mL falcon tube. At various time points, 3 mL of solution was removed and measured with fluorometry. Three milliliters of PBS were replaced in the falcon tube. The excitation for diclofenac, flurbiprofen, naproxen, and prodan were 289, 280, 280, and 385 nm, respectively. Emission spectra were collected between 300-500 for diclofenac, flurbiprofen, and naproxen. Emission spectra for prodan were collected between 400 – 600 nm. Fluorescence intensity was recorded at 365, 355, 362, and 425nm, respectively, for diclofenac, flurbiprofen, naproxen, and prodan. Film release for enzyme testing was performed in 1 mL of PBS contained in a microcentrifuge tube, and changed at the indicated time point

**Cyclooxygenase Enzyme Assay**: The cyclooxygenase fluorescent inhibitor screening assay was used to confirm drug activity after cyclodextrin complexation and release from hydrolytically degradable LbL films. The kit was purchased from Cayman Chemicals and used as directed. The assay capitalizes on the peroxidase activity of cyclooxygenase and the reaction between hydroperoxy endoperoxide ($PGG_2$) and 10 – acetyl – 3,7 – dihydroxyphenoxazine (ADHP), which produces resorufin, a highly fluorescent molecule. Resorufin can be easily quantified by exciting between 530 – 540nm and collecting emission between 585 – 595 nm. Experiments were performed on a black 96 well fluorescence plate. Each plate contained a diclofenac calibration curve, cyclodextrin controls, film eluent, 100 % initial activity controls, and background

controls. In a typical experiment, 150 uL of 100mM Tris – HCl, pH 8.0 buffer, 10 uL of heme in 1:25 DMSO:$H_2O$ solution, and 10 uL of ADHP was added to every well. Then 10 uL of human recombinant cyclooxygenase enzyme was added to all wells except the background wells, which received 10 uL of assay buffer. All control and eluent wells received 10uL of the appropriate sample. Activity and background wells received 10uL of PBS, the solvent used for film release and controls, instead. Lastly, 10 uL of arachodonic acid, which was prepared immediately beforehand, was added to every well. The plate was allowed to incubate for two minutes and the plate was read using an excitation wavelength of 535nm and emission wavelength of 590 nm. The activity of cyclodextrin-drug complexex versus free drug was assessed by using log order drug concentration. Free diclofenac was dissolved in DMSO:$H_2O$ solution due to limited water solubility. In this case the DMSO:$H_2O$ mixture was used as the solvent in the assay.

## Results and Discussion

### Monomeric Cyclodextrins as Carriers for Small Molecules

To ascertain if monomeric cyclodextrins could indeed be used as versatile carriers for sustained delivery of a variety of small hydrophobic molecules, a highly charged, commercially available and FDA approved cyclodextrin, Captisol ®, was used to construct hydrolytically degradable films. Figure 3.1 shows the film components.

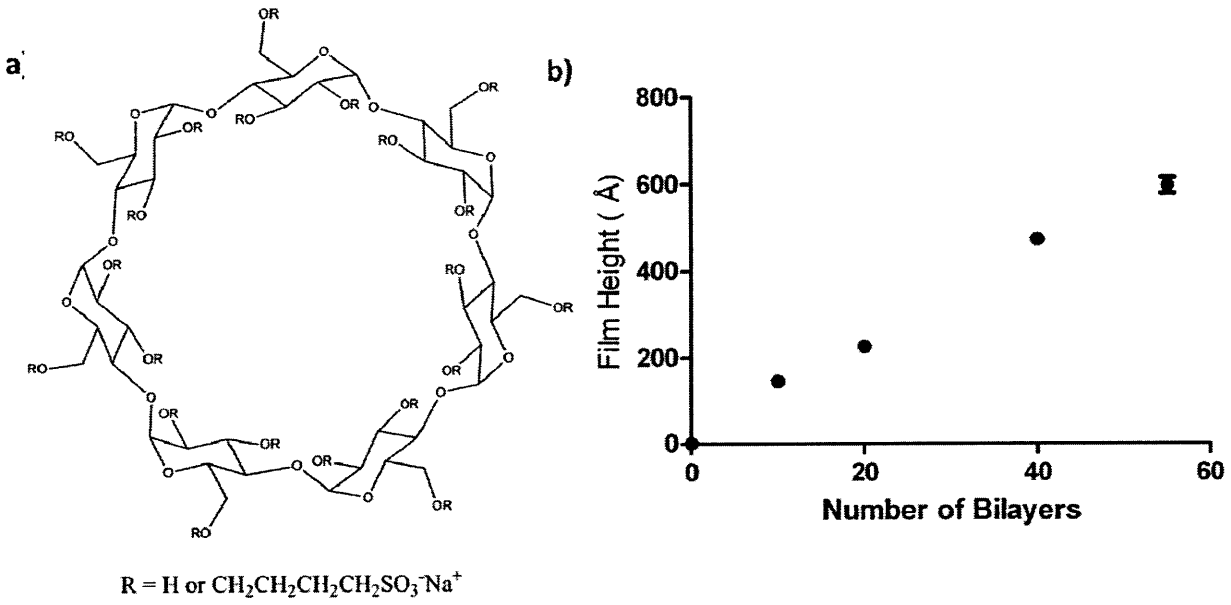


**Figure 3.1 Structure of Captisol ® and growth curve**

The image on the left shows the chemical structure of Captisol ®, which has seven sulfonate groups. The image on the right is the growth curve for PolyA2/Captisol®-dexamethasone films assembled in 0.1 M sodium acetate buffer.

Captisol ® is a sulfobutylether- betacyclodextrin with 7 sulfonate groups.[29-31] The growth curve of Captisol ® with Poly A2 assembled at pH 5 in 0.1 M sodium acetate buffer can also be seen in figure 3.1. Both ionic strength and deposition time were varied to determine the optimum conditions for assembly. Ionic strengths between 0.1 M to 0.2 M had no effect, but those assembled at 0.5 M were twice the thickness. High salt concentration results in greater charge shielding and loopier films. A deposition time of one hour was required to achieve the appropriate thermodynamics to form films, unlike most macromolecular polyelectrolytes. Films built and showed linear growth characteristics. Film growth was monitored for Captisol ® -dexamethasone complexes, and showed linear growth characteristics. Captisol – dexamethasone complexes were

investigated because of the size difference for uncomplexed and complexed cyclodextrin as well as the effect of complexation on the orientation of charged groups. Dexamethasone was chosen as the small molecule therapeutic because of its role as a powerful corticosteroid. Corticosteroids are used to treat a variety of inflammatory conditions, including joint pain, asthma, Crohn's disease, and sarcoidosis, and . are an important class of anti – inflammatory drugs.[32, 33] Control of inflammation mediated processes is vital to the success of medical implant.[34] Dexamethasone was also chosen because of its large complexation coefficient with Captisol ®. The complexation coefficient was found to be $K_{1:1}$ = 1821 $M^{-1}$; lipophilic molecules typically have a $K_{1:1}$ between 50 – 2000 $M^{-1}$. The solubility of dexamethasone in water went from 0.1 mg/mL to 20 mg/mL with cyclodextrin complexation. After film growth was confirmed, the release dynamics from twenty bilayer films were examined. Figure 3.2 shows the release curve for (Poly A2/ $SBE_7CD$-dexamethasone)$_{20}$ films. The release is very different than that observed for (Poly A2/ dextran sulfate)$_{20}$ films which had a $t_{1/2}$ of 48 hours. Captisol ® containing films completely released dexamethason in 12 hours, and have a half life very similar to LbL films that are unstable at physiological conditions.

To assess film stability, the degradation of (Poly A2/ $SBE_7CD$-dexamethasone)$_{20}$ films were monitored over time and can be seen in figure 3.3. The degradation correlates with drug release with over half of the film being lost within in 12 hours. Small molecules are known to form unstable or bulk eroding thin films, due to low charge density or diminished ability to form the necessary ionic crosslinks due to conformational constraints. Though cyclodextrins are not small molecules and can house portion of molecules, cyclodextrins are small in diameter. Cyclodextrins have a

toroidal shape with a maximum external diameter of 15.4 ± 0.4 Å and a minimum of 7.9 ± 0.1 Å.[23] Though captisol is a highly charged molecule with seven sulfonate groups, the charge is concentrated in a small area and does not have the same conformational freedom to form ionic crosslinks as macromolecular polyelectrolytes. Rapid drug release and film dissolution is mostly likely due to the inability to form sufficient ionic crosslinks required to maintain stable films in phosphate buffered saline.

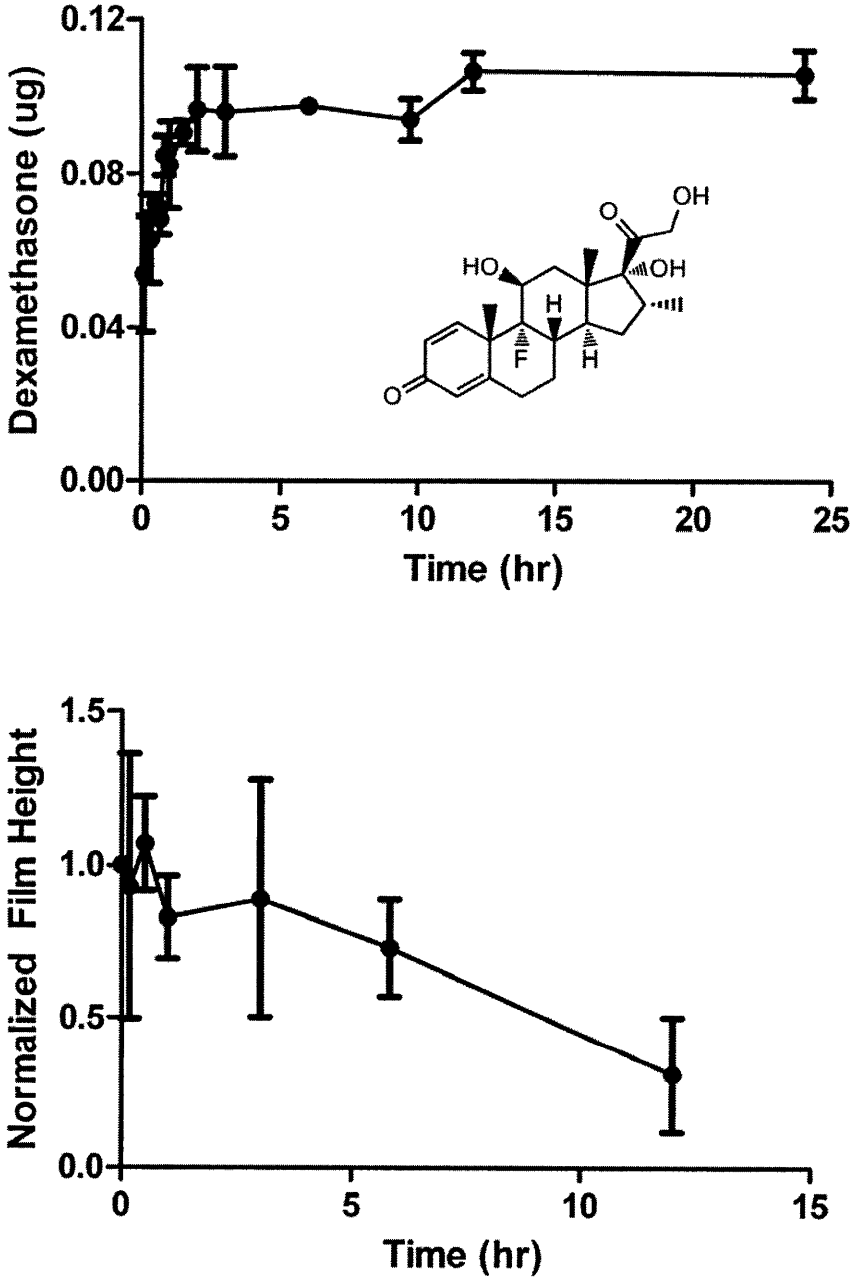


**Figure 3.2 Release and degradation for Captisol ® - dexamethasone films at 25°C**

The release and degradation curve for (Poly A2 / Captisol ®- dexamethasone)$_{20}$ films in PBS at 25°C. Results were normalized by total drug amount and film thickness before degradation respectively.

**Polymeric Cyclodextrins as Carrier for Small Molecule Drugs**

Monomeric cyclodextrins were unable to achieve controlled, sustained release of small molecules. To overcome the challenges with nonpolymeric carriers a commercially available polymeric cyclodextrin was used as a charge carrier. LbL films were composed of poly(β-amino esters) (PBAEs) as the degradable polycations and polycarboxymethyl-betacyclodextrin (PolyCD) complexed with a small molecule as the anionic supramolecular complex (figure 3.3).

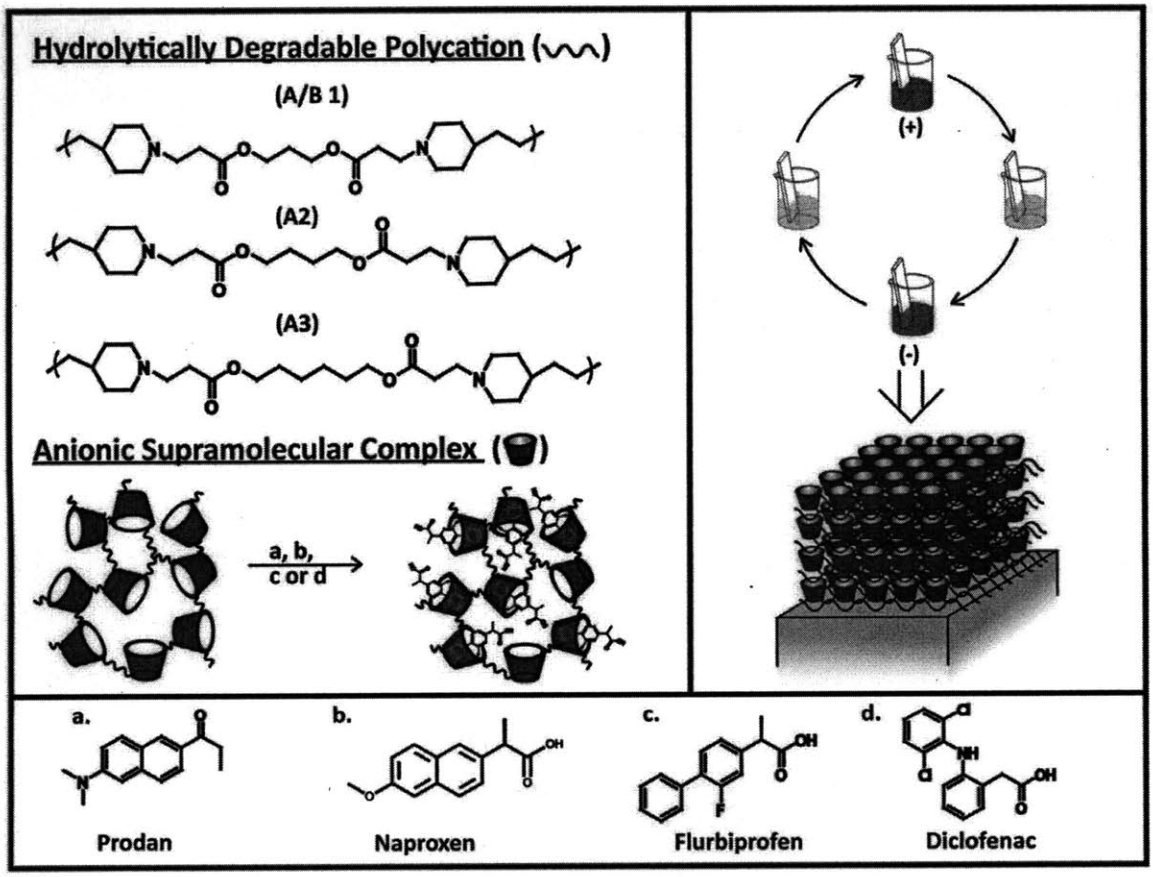


**Figure 3.3 Methodology for layer-by-layer films containing polymeric cyclodextrins**

Left shows film components. Three poly(β-amino esters) were investigated as degradable polycation. Poly(carboxymethylbetacyclodextrin) was used as the anionic supramolecular complex. Right shows electrostatic assembly; light blue is water. Bottom is molecules used in experimentation. Polymers were synthesized as previously described. [35]

In order to determine if hydrolytically degradable LbL films containing polymeric cyclodextrins would overcome the challenges associated with small molecule delivery, several key parameters were examined, including film growth, degradation, and release characteristics. To assess if films containing polymeric cyclodextrins could form stable films, film growth, and degradation were investigated. Film growth and degradation can be seen in Figure 3.5 for film containing PolyA2 and PolyCD. Polymeric cyclodextrin films were constructed in 0.1M sodium acetate buffer at pH 6. Films containing polymeric cyclodextrin did not require extra deposition time and ten minute deposition times were used. Films were found to be ultrathin, with an average bilayer thickness of 11 ± 2 Å (figure 3.4). These measurements are consistent with the dimensions of a beta-cyclodextrin. The largest and smallest dimensions are approximately 15.4 ± 0.4 Å and 7.9 ± 0.1 Å respectively.[23] Unlike monomeric cyclodextrins, these films exhibited linear degradation profiles characteristic of surface erosion in hydrolytically degradable LbL films, Figure 3.4.

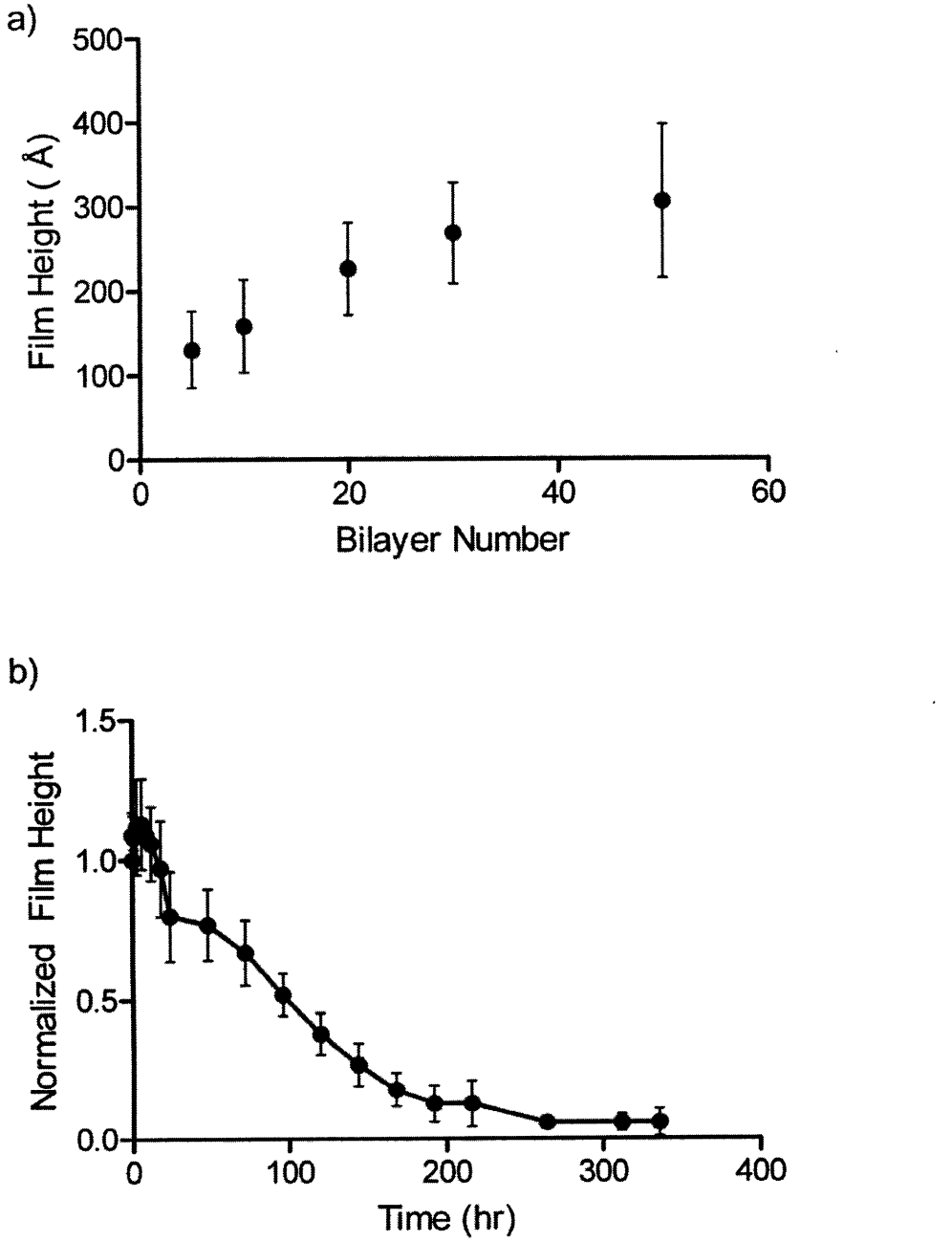


**Figure 3.4 Growth and degradation curve for (Poly A2 / PolyCD)$_{20}$ films at 25°C.**

A) The growth curve of (Poly A2/ PolyCD) in 0.1M sodium acetate buffer at pH 6 B) The degradation of (Poly A2/ PolyCD)$_{20}$ films at 25°C in phosphate buffered saline; graph is of normalized film height over time.

The release dynamics from these small molecule delivery constructs were investigated through complexation with a series of small molecule drugs: diclofenac, flurbiprofen, naproxen, and prodan. These molecules represent several types of nonsteroidal anti-inflammatory drugs (NSAID). NSAIDs are a major class of anti-inflammatory drugs and are commonly used to avoid the side effects of steroid.[36, 37] PolyCD has a much lower $K_{1:1}$ (800 $M^{-1}$) with dexamethasone than Captisol ®, so NSAIDs were selected due to their high $K_{1:1}$ (≥ 2000 $M^{-1}$) and ease of analysis. In addition, these molecules were chosen based on their relevance as potent anti-inflammatory drugs used for a range of medical applications and their aromatic nature, which enables them to be monitored via fluorescence spectroscopy. Prodan was also complexed and released as a small molecule fluorescent probe. Figure 3.5 shows the release of (Poly A2/PolyCD)$_{20}$ films containing diclofenac, flurbiprofen, or naproxen at 25°C. Drug loading varies from 0.8 – 2 ug of drug loading with naproxen and diclofenac being the lowest and highest loading respectively. Though loading was different, the release rate was the same suggesting that the release is governed by chemical degradation. It should be noted that drug loading is dependent on uniform surface coverage. If films assembled on thin rough LPEI/PSS base layers, cyclodextrin containing films do not assemble properly and drug loading is adversely affected.

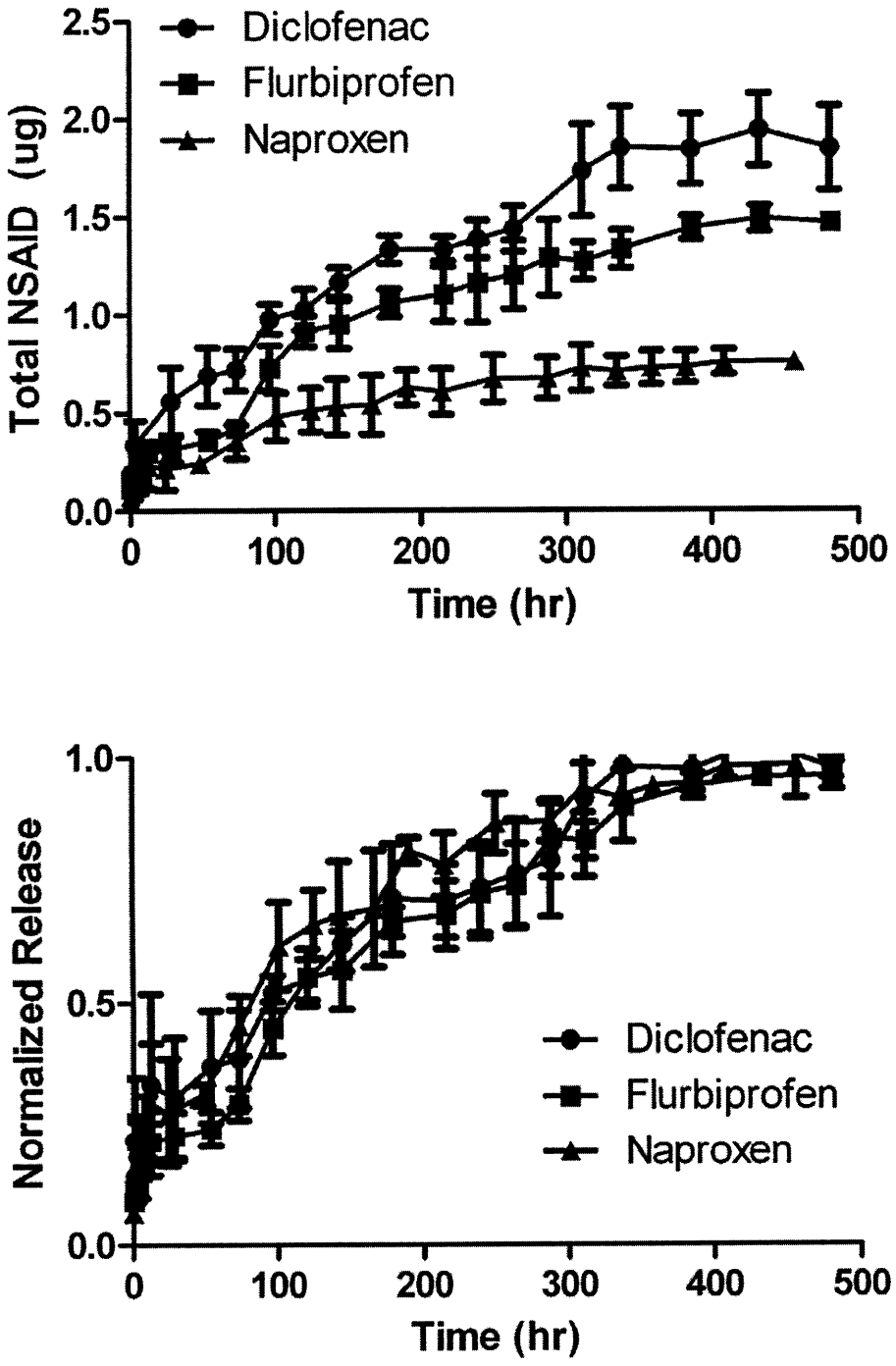


**Figure 3.5 Release of (Poly A2/ PolyCD-diclofenac)$_{20}$ films**

The release curves for (Poly A2/PolyCD)$_{20}$ films at 25°C in PBS. The top image illustrates the total amount of drug released. The bottom graph shows the normalized release.

**Surface Erosion in Films Containing Polymeric Cyclodextrins**

Since the interaction between cyclodextrins and drugs are noncovalent in nature, film degradation kinetics may not govern small molecule release. It is possible that while the cyclodextrin polymer is slowly released from the film via erosion of the PBAE, the small molecule partitions out of the cyclodextrin cavity from the film interior and diffuses into solution. Figure 2A depicts the possible mechanisms of release.

To determine the mechanism of release (Poly A2 /PolyCD-Prodan)$_{20}$ films were studied. Prodan is a fluorescent probe, whose emission spectra changes in response to the dipolarity of the solvent environment.[38] The cyclodextrin's interior creates a hydrophobic microenvironment in an aqueous solution. Therefore, if prodan diffuses out of the film, it will emit at a longer wavelength than if it is in the cyclodextrin pocket. Short timescales were monitored to capture the release characteristics of diffusion. At longer timescales and higher component concentrations, it is not possible to determine whether peaks are due to post release partitioning into or out of the cyclodextrin. Figure 3.6 shows that prodan is released while still in the cyclodextrin interior, indicating a surface erosion mechanism.

To test the efficacy of the surface erosion model, films constructed of different PBAEs were constructed. Previously, it was shown that increasing the hydrophobicity of poly(β-amino esters) up to a certain point led to an increase in release duration. In that study, poly A3 and poly A/B 1 were found to be one of the longest and shortest releasing films respectively. By employing these polymers, an obvious difference in release kinetics should be observed. Flurbiprofen, an NSAID, was chosen for this investigation because of its relevance as a commonly used anti-inflammatory agent for

osteoarthritis, rheumatoid arthritis, and ophthalmic applications. The release kinetics of films at 37°C can be seen in Figure 3.7.

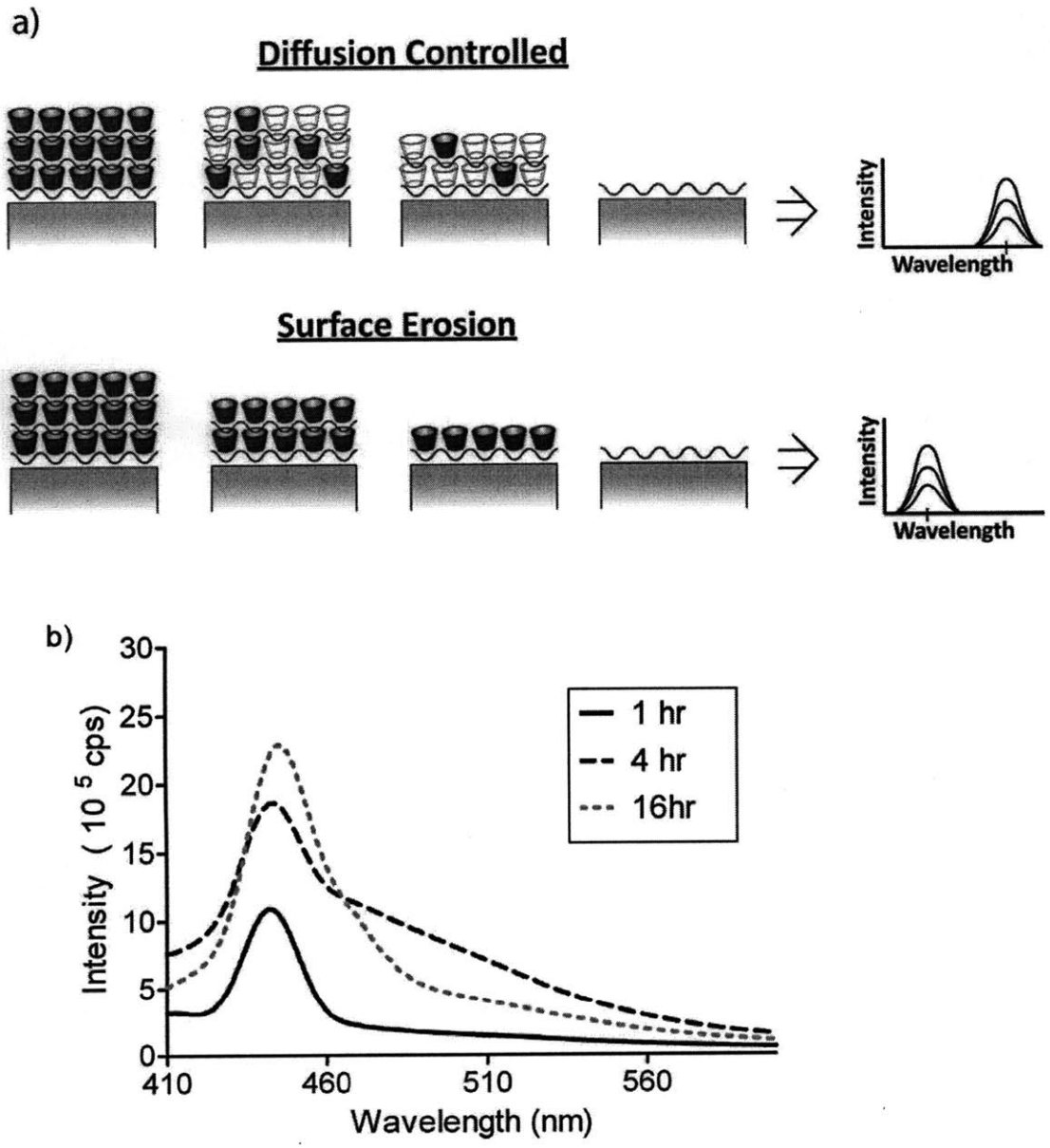


**Figure 3.6 Possible mechanisms of drug release**

Over time drug either diffuses out or is released via surface erosion from films. If prodan diffuses out into aqueous environment , it emits at 520nm when excited at 360nm. If prodan emits at 445nm, it is released within the cyclodextrin and is indicative of surface erosion. B) Release of (Poly (1)/PolyCD-Prodan)$_{20}$ films in PBS at 25°C.

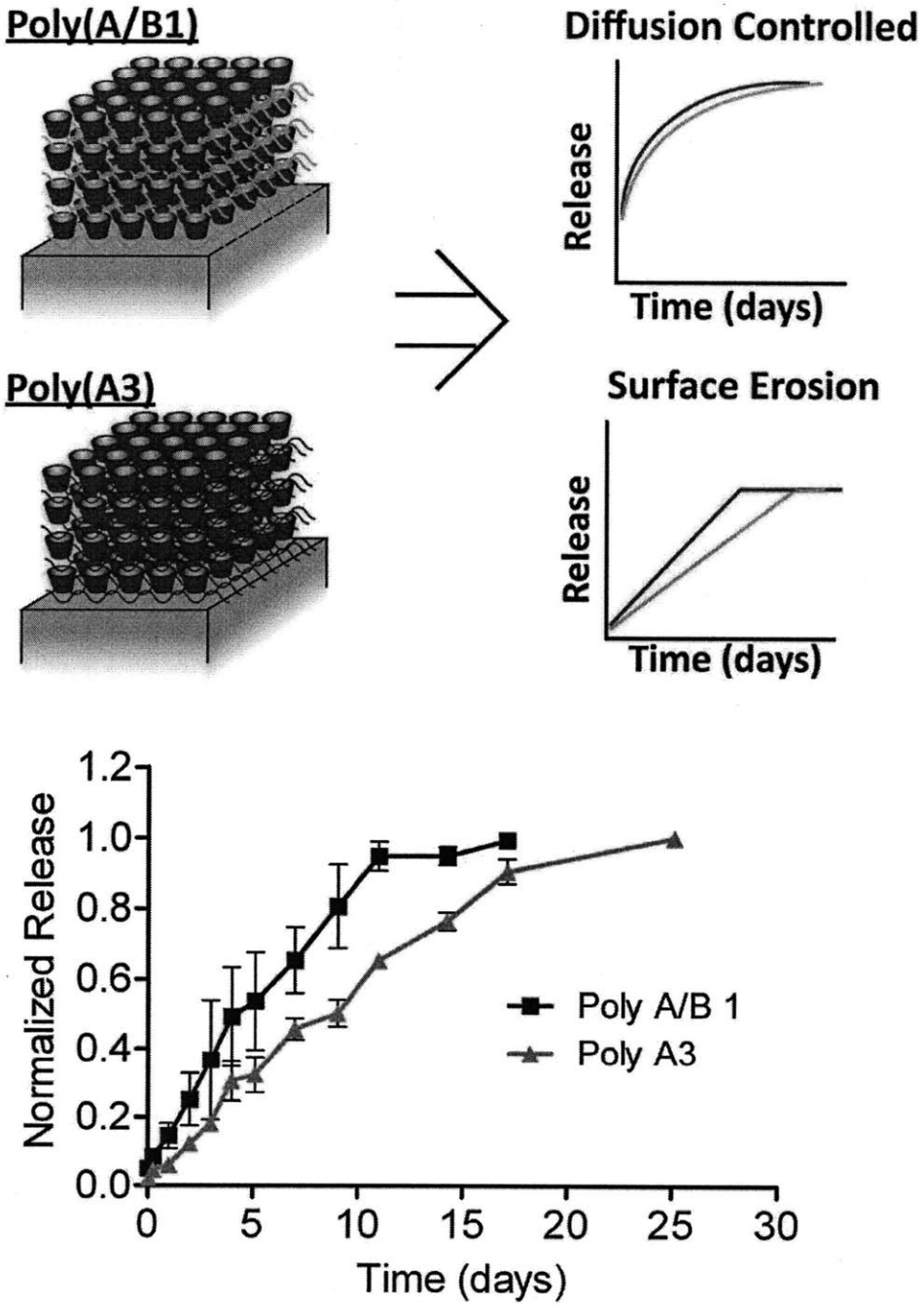


**Figure 3.7 Effect of polycation on release dynamics at 37°C**

A) Two possible release profiles for Poly (2) and Poly (3) B) Release of (Poly 2/PolyCD-Flurbiprofen)$_{20}$ and(Poly 3/PolyCD-Flurbiprofen)$_{20}$ at 37°C in PBS.

Both films released approximately 3 μg of flurbiprofen, but poly (3) released its cargo over 10 days, where as poly A3 completed release in about 17 days. The substantial difference between their release duration is due to difference in the compositions of the two PBAEs, and is consistent with a surface erosion mechanism based on hydrolytic degradation of the PBAE. The ability to finely control release of a small molecule with a linear profile in a sustained fashion is unprecedented in ultrathin films.

To ascertain the effect of the small molecule drug on release properties at physiologically relevant temperatures, films containing diclofenac and flurbiprofen were examined at 37°C. Diclofenac and flurbiprofen represent two different classes of NSAIDS and are structurally similarly only in the presence of a carboxylic acid and aromatic moieties. However, the key parameter for cyclodextrin complexation is the complexation coefficient. Diclofenac and flurbiprofen have coefficients ranging from 2000 to 4000 $M^{-1}$. It can be anticipated that molecules with stability constants that fall within that range will have similar release dynamics. The lowest complexation coefficient necessary to maintain the necessary release characteristic was not investigated, but is an important area of ongoing research. Figure 3.8 reveals no significant difference between the normalized film release profiles, though they each contain different hydrophobic drugs. Release behavior is thus independent of the complexation partner or drug for stability constants greater than 2000 $M^{-1}$, and can be tuned directly via choice of the PBAE.

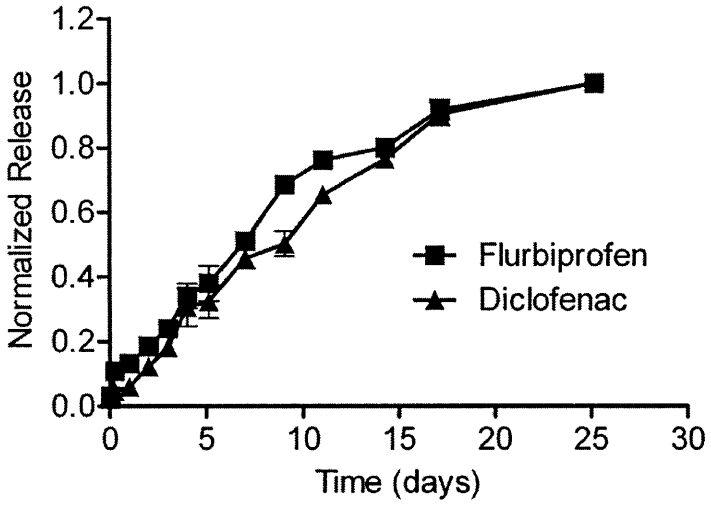


**Figure 3.8 Normalized release of (Poly A3/PolyCD-Flurbiprofen)$_{20}$ and (Poly A3/PolyCD-Diclofenac)$_{20}$ films at 37°C in PBS**

### Effect of Cyclodextrin Carrier on Drug Activity

To determine if PolyCD alters drug activity, the inhibition of cyclooxygenase (COX) by diclofenac was investigated. COX is the rate limiting enzyme in the production of prostaglandins, which are important in homeostasis and inflammatory pathways. [36] This enzyme is bifunctional with both cyclooxygenase and peroxidase activity. The cyclooxygenase component coverts arachidonic acid to a hydroperoxy endoperoxide ($PGG_2$) and the peroxidase reduces the endoperoxide to its alcohol form ($PGH_2$). The alcohol is the precursor for prostaglandins, thromboxanes and prostacyclins, cytokines critical to inflammation and other pathways.[37, 39, 40] To confirm that cyclodextrins and film incorporation did not adversely affect drug activity or availability, the ability of cyclodextrin – drug solution and film eluent to inhibit cyclooxygenase activity was investigated. The COX fluorescent inhibitor screening

assay from Cayman Chemicals was used. Figure 3.9 shows the reaction scheme for the assay.

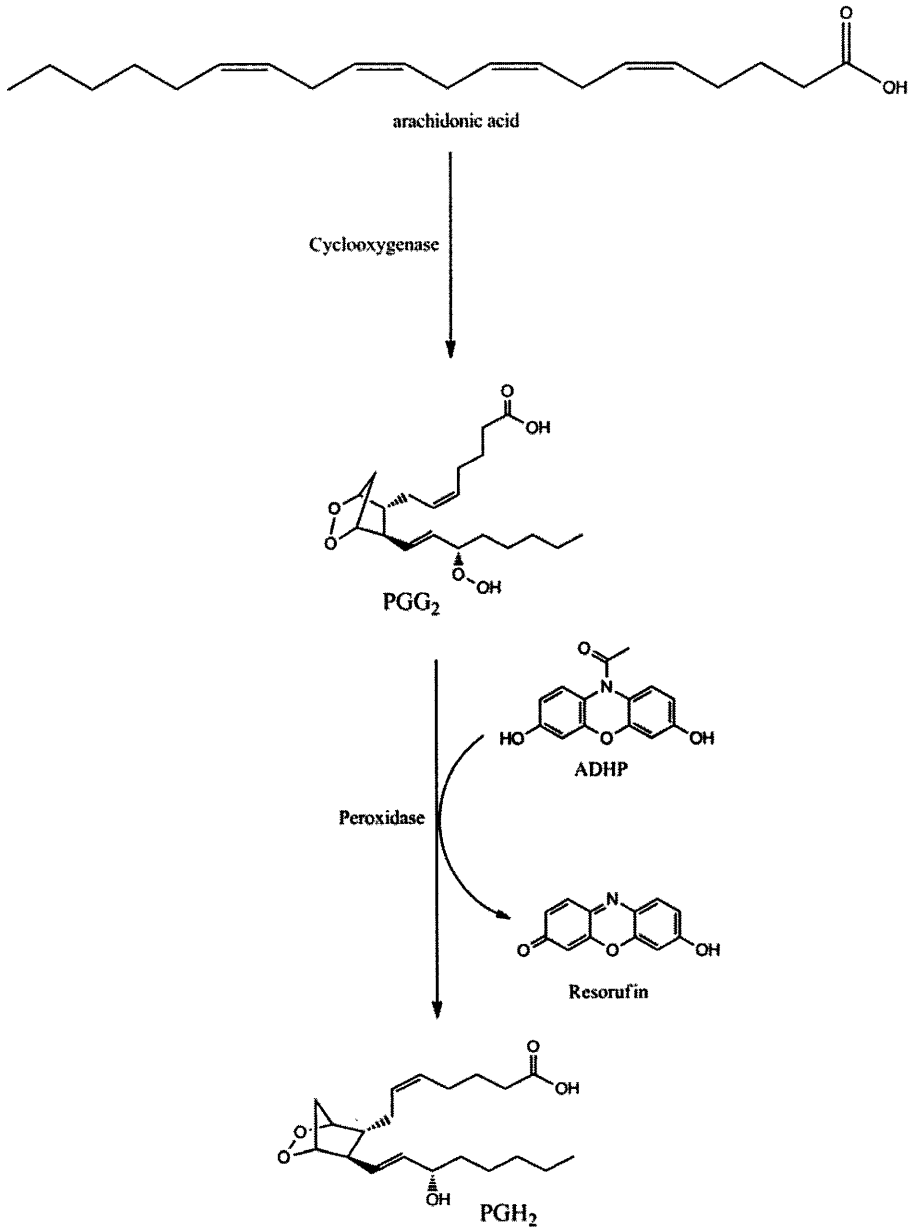


**Figure 3.9 Mechanism of cyclooxygenase inhibition assay.**

Resorufin, a highly fluorescent molecule, is produced as a result of the peroxidase reaction of the cyclooxygenase enzyme. If arachidonic acid is unable to be converted in $PGH_2$ due to drug

inhibition, resorufin will not be produced. The resorufin produced is proportional to cyclooxygenase enzyme activity and can be used to quantity the drug inhibition of the enzyme.

If the NSAID blocks the activity of human recombinant COX enzyme, the production of resorufin will be reduced and subsequently so will the fluorescence. However, if the sample is not effective the production of resorufin and the fluorescence will be higher. Figure 3.10 shows that there is only a slight difference in activity of cyclodextrin complexes at low concentrations. The released diclofenac is highly active over the time course of film release, leading to COX inhibition and suppressed resorufin production. This work thus demonstrates the release of active drug from slow-releasing ultrathin films of thickness less than a micron, which are capable of delivering therapeutic levels of drug.

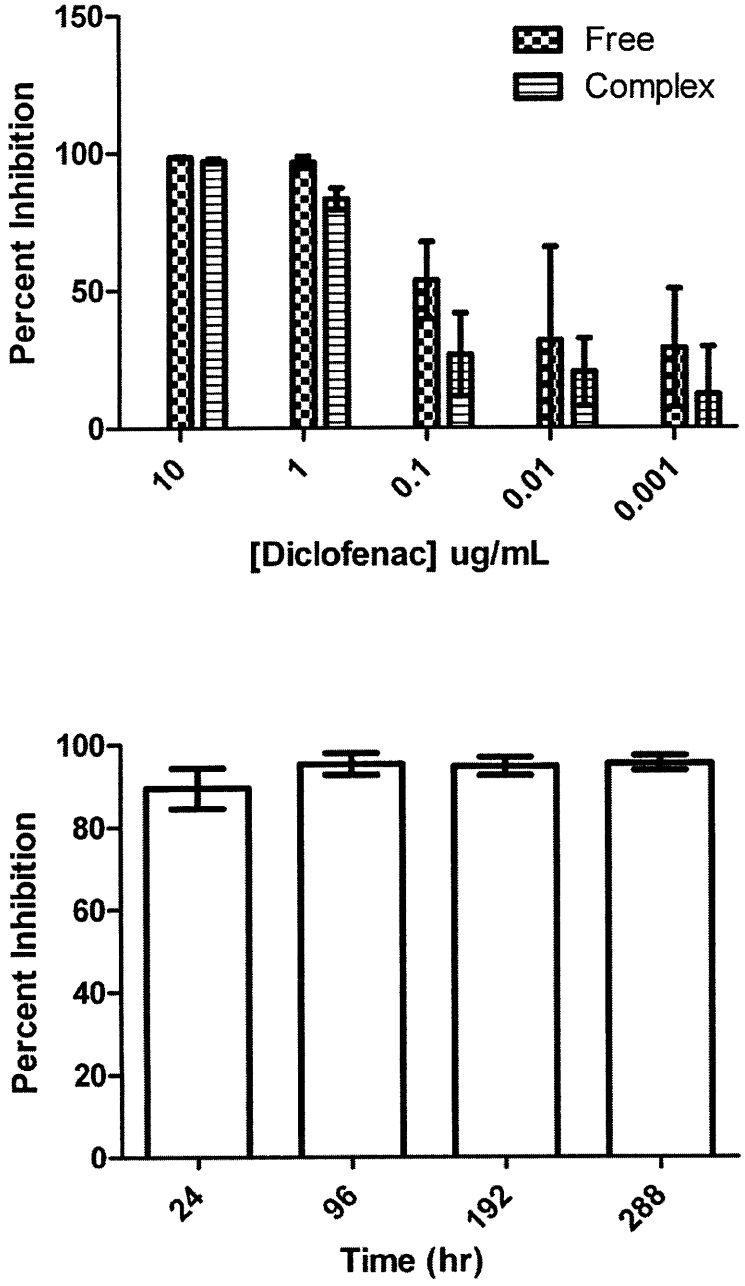


**Figure 3.10 Therapeutic activity for deposition solutions and film release.**

The top image compares the ability of free diclofenac versus polycd – diclofenac to inhibit COX activity. The bottom is a graph of the percent inhibition film eluent from (Poly A/B1 / PolyCD – diclofenac)$_{20}$. Films were released in PBS at 37°C.

Eighty five percent of all new chemical entities approved by the FDA between 1981 and 2002 were small molecules, many of which are not highly water soluble.[2] Here we report the first nanoscale coatings for small molecule delivery capable of hydrolytic top down film degradation, linear release profiles, and programmable release kinetics via facile aqueous manufacturing. Our approach is the first utilization of a charged polymeric carrier capable of facile reversible complexation with the drug of choice in alternation with a degradable polyion. Charged cyclodextrin polymers were essential for the trapping of cyclodextrin–drug complexes in stable, surface eroding films capable of drug release within the cyclodextrin carrier without altering activity. Monomeric cyclodextrins however resulted in rapid drug release and film dissolution. Release kinetics for polymeric cyclodextrin films were found to be independent of the therapeutic incorporated for drugs with high complexation coefficients and could be regulated through choice of degradable polycation. This technology opens the door to nanomedicine coatings for applications in personalized medicine, transdermal delivery, medical devices, nanoparticulate carriers, prosthetic implants, as well as small molecules for imaging, agriculture, and basic scientific research.

## References


[1] S. L. Schreiber, *Nature Chemical Biology* **2005**, *1*, 64.
[2] D. J. Newman, G. M. Cragg, K. M. Snader, *Journal of Natural Products* **2003**, *66*, 1022.
[3] J. A. Mitchell, T. D. Warner, *Nature Reviews Drug Discovery* **2006**, *5*, 75.
[4] G. Decher, *Science* **1997**, *277*, 1232.
[5] P. T. Hammond, *Advanced Materials* **2004**, *16*, 1271.
[6] K. Ariga, J. P. Hill, Q. M. Ji, *Physical Chemistry Chemical Physics* **2007**, *9*, 2319.
[7] D. M. Lynn, *Advanced Materials* **2007**, *19*, 4118.
[8] A. Quinn, G. K. Such, J. F. Quinn, F. Caruso, *Advanced Functional Materials* **2008**, *18*, 17.
[9] M. Grandcolas, A. Louvet, N. Keller, V. Keller, *Angewandte Chemie-International Edition* **2009**, *48*, 161.

[10] K. S. Schanze, A. H. Shelton, *Langmuir* **2009**, *25*, 13698.
[11] J. B. Schlenoff, *Langmuir* **2009**, *25*, 14007.
[12] M. C. Berg, L. Zhai, R. E. Cohen, M. F. Rubner, *Biomacromolecules* **2006**, *7*, 357.
[13] H. F. Chuang, R. C. Smith, P. T. Hammond, *Biomacromolecules* **2008**, *9*, 1660.
[14] N. B. Jessel, P. Schwinte, R. Donohue, P. Lavalle, F. Boulmedais, R. Darcy, B. Szalontai, J. C. Voegel, J. Ogier, *Advanced Functional Materials* **2004**, *14*, 963.
[15] A. J. Khopade, F. Caruso, *Nano Letters* **2002**, *2*, 415.
[16] B.-S. Kim, S. W. Park, P. T. Hammond, *ACS Nano* **2008**, *2*, 386.
[17] B.-S. Kim, R. e. C. Smith, Z. Poon, P. T. Hammond, *Langmuir* **2009**, *25*, 14086.
[18] T. G. Kim, H. Lee, Y. Jang, T. G. Park, *Biomacromolecules* **2009**, *10*, 1532.
[19] P. M. Nguyen, N. S. Zacharia, E. Verploegen, P. T. Hammond, *Chemistry of Materials* **2007**, *19*, 5524.
[20] B. Thierry, P. Kujawa, C. Tkaczyk, F. M. Winnik, L. Bilodeau, M. Tabrizian, *Journal of the American Chemical Society* **2005**, *127*, 1626.
[21] Y. Zhong, C. F. Whittington, D. T. Haynie, *Chemical Communications* **2007**, 1415.
[22] M. E. Brewster, T. Loftsson, *Advanced Drug Delivery Reviews* **2007**, *59*, 645.
[23] M. E. Davis, M. E. Brewster, *Nature Reviews Drug Discovery* **2004**, *3*, 1023.
[24] T. Loftsson, D. Hreinsdottir, M. Masson, *International Journal of Pharmaceutics* **2005**, *302*, 18.
[25] K. Uekama, F. Hirayama, T. Irie, *Chemical Reviews* **1998**, *98*, 2045.
[26] A. Vyas, S. Saraf, S. Saraf, *Journal of Inclusion Phenomena and Macrocyclic Chemistry* **2008**, *62*, 23.
[27] J. Szejtli, *Pure and Applied Chemistry* **2004**, *76*, 1825.
[28] R. Chadha, N. Kashid, A. Saini, *Journal of Scientific & Industrial Research* **2004**, *63*, 211.
[29] K. Okimoto, M. Miyake, N. Ohnishi, R. A. Rajewski, V. J. Stella, T. Irie, K. Uekama, *Pharmaceutical Research* **1998**, *15*, 1562.
[30] V. J. Stella, V. M. Rao, E. A. Zannou, *Journal of Inclusion Phenomena and Macrocyclic Chemistry* **2002**, *44*, 29.
[31] L. Szente, J. Szejtli, *Advanced Drug Delivery Reviews* **1999**, *36*, 17.
[32] T. Cole, *Biotechnology Annual Review* **2006**, *12*, 269.
[33] T. Rhen, J. A. Cidlowski, *N Engl J Med* **2005**, *353*, 1711.
[34] P. Wu, D. W. Grainger, *Biomaterials* **2006**, *27*, 2450.
[35] R. C. Smith, A. Leung, B. S. Kim, P. T. Hammond, *Chemistry of Materials* **2009**, *21*, 1108.
[36] T. D. Warner, F. Giuliano, I. Vojnovic, A. Bukasa, J. A. Mitchell, J. R. Vane, *Proceedings of the National Academy of Sciences of the United States of America* **1999**, *96*, 9966.
[37] R. J. Flower, *Nature Reviews Drug Discovery* **2003**, *2*, 179.
[38] N. J. Crane, R. C. Mayrhofer, T. A. Betts, G. A. Baker, *Journal of Chemical Education* **2002**, *79*, 1261.
[39] A. L. Blobaum, L. J. Marnett, *Journal of Medicinal Chemistry* **2007**, *50*, 1425.

[40] S. Kargman, E. Wong, G. M. Greig, J. P. Falgueyret, W. Cromlish, D. Ethier, J. A. Yergey, D. Riendeau, J. F. Evans, B. Kennedy, P. Tagari, D. A. Francis, G. P. ONeill, *Biochemical Pharmacolo*gy **1996**, *52*, 1113.

# Chapter 4 : In Vitro Characterization of Anti-inflammatory Films

## Introduction

Control of inflammation is vital to the success of biomedical implants. Adverse cell reactions at the device surface have caused lifesaving devices to fail, prompting their immediate removal and/or replacement.[1-3] Recent failures of implantable devices, such as coronary stents, have highlighted the importance of surface interactions and device design now focuses on the mitigation of inflammation and control of cell adhesion and proliferation. Methods capable of adding new and exquisite surface functionality without altering device functionality are critical to the future application of implantable devices, including biomaterial and tissue engineering constructs. Considerable efforts have focused on the functionalization of material surfaces for biological use.[4-9] The phenomenal architectural, compositional, and structural control of polyelectrolyte multilayers coupled with the ease of manufacturing and the ability to coat virtually any surface make these nanostructured materials a valuable tool in the regulation of cellular behavior.[10] Here, the first in vitro characterization of a layer-by-layer system able to control inflammation in situ over physiologically relevant timescales of days to weeks is described. In doing so, the first in vitro investigation of cell adhesion and proliferation on hydrolytically degradable multilayer films containing bioactive molecules is provided. Lastly, to validate hydrolytically degradable multilayer as a viable technology for the creation of ophthalmic combination devices, anti-inflammatory coatings were constructed on intraocular lenses.

All materials implanted in the body are subject to host responses. The response to medical devices starts at implantation, which results in tissue or organ injury.[1] Unfortunately most biomedical devices disrupt normal homeostasis and trigger adverse reactions which often lead to infection, inflammation, thrombosis, and/or fibrosis.[2] Typically, after injury, inflammatory, wound healing, foreign body, and/or fibrous encapsulation processes are initiated. The subsequent response to injury is critical as the magnitude and duration of adverse alterations dictate the host response and device outcome.[2] The response to injury occurs very early, within two to three weeks of the time of implantation, and is crucial to the success or failure of implantable devices.[1] It is known that the extent of inflammation is a major factor in the response to injury and affects the degree of foreign body reaction, fibrosis, and fibrous capsule development. In fact the biocompatibility of biomaterials, prostheses, and devices are often characterized by the intensity and/ or time duration of the inflammatory reaction.[1] There exists a profound need for surface coatings that prevent adverse inflammatory reactions while evoking desired tissue responses.

Layer-by-layer assembly, directed assembly through complementary interactions, has distinguished itself as a platform technology for the creation of dynamic thin films systems.[4, 11] Extensive work has focused on the creation of polyelectrolyte multilayer nanofilms with precise control of cellular interactions through delivery of bioactive molecules.[4, 12, 13] Numerous design and release modalities have been explored to produce efficacious systems. Most research has utilized natural biodegradable polymers, such as polypeptides and glycosaminoglycans, which degrade via enzymatic cleavage. In these systems, bioactive agents are embedded into the film and released

via diffusion or enzymatic breakdown. Voegel, Caruso, Picart, Hammond, and others have shown that growth factors, peptides, genetic materials, and small molecules could be used to direct cell proliferation, differentiation, and death.[4, 14-23] Additionally intracellular pathways could be activated and used to enhance cytokine expression. Benkirane-Jessel, et al showed that the anti-inflammatory drug, piroxicam, could be embedded into polypeptides films and used to control the inflammatory response of monocytes for twelve hours.[18] Schneider et al incorporated the anti-inflammatory drug, diclofenac, into glycosaminoglycan films and showed drug release over the course of ten hours.[20] Bioactive molecules have also been purposely embedded at the film surface to allow for control of inflammation through direct cell contact. Benkirane-Jessel et al showed that α-melanocyte-stimulating hormone could successfully regulate production of inflammatory cytokines from monocytes for twelve hours and influence cell morphology.[14]

Though polyelectrolyte multilayers, containing natural polymers, have proven to be effective regulators of cell behavior, most rely on diffusion and temporal control is hard to engineer. Hydrolytically degradable multilayers are a powerful class of LbL films and represent a key advance in the spatiotemporal controlled delivery of bioactive agents.[7, 11] These constructs composed of a poly(β-amino ester), as the degradable polycation, in alternation with a therapeutic have successfully delivered a variety of active agents with precise spatiotemporal control. Proteins, DNA, anticoagulants, antimicrobials, and small molecule therapeutics have been successfully incorporated and delivered from hydrolytically degradable films.[7, 24-28] Their facile degradability allows the nature of surface interactions to be modulated in a predictable fashion over

time. Moreover, superior control over release, surface compatibility, and mechanical properties can be easily achieved through polymer selection.[29, 30] Still cellular interactions, such as adhesion on and proliferation atop hydrolytically degradable films.

In chapter three, the ability of hydrolytically degradable polyelctrolyte multilayers containing polymeric cyclodextrins to act as a versatile carrier for small molecule therapeutics.[26] Programmable zero order release of anti-inflammatory agents, diclofenac and flurbiprofen, was achieved and activity against recombinant human cyclooxygenase enzyme was retained. Drug release was mediated through surface erosion and could be modulated from days to weeks through polymer selection. Here the interaction of cells with hydrolytically degradable polyelectrolyte multilayers containing an anti-inflammatory agent and its potential to modulate cell behavior was investigated. Cell adhesion and proliferation was investigated on layer-by-layer films composed of poly(β-amino esters) (PBAEs) as the degradable polycation and polycarboxymethylbetacyclodextrin (PolyCD) complexed with diclofenac as the polyanion and the film's ability to regulate inflammation was determined. Moreover, the ability of these constructs to serve as viable anti-inflammatory coatings for intraocular lenses was demonstrated.

## Materials and Methods

**Materials:** The human pulmonary epithelial cancer (A549) and human lens epithelial (HLE-B3) cell lines as well as Eagle's minimum essential medium (EMEM) were purchased from ATCC (Manassas, VA). Intraocular lenses were generously donated from the Aurolabs division of Aravind Eye Hospital (Madurai, Tamil Nadu, India). F-12K nutrient mixture, Kaighn's modification cell culture media, penicillin-

streptomycin solution (Pen Strep), fetal bovine serum, phosphate buffer saline, live/dead assay kit, and Hoechst 33342 dye were purchased from Invitrogen (Carlsbad, CA). Thiazolyl Blue Tetrazolium Bromide (MTT) and 10% neutral buffered formalin were purchased from Sigma Aldrich (St. Louis, MO) and Richard-Allen Scientific (Kalamazoo, MI), respectively. Diclofenac sodium salt and poly(carboxymethyl-betacyclodextrin) [PolyCD] were purchased from TCI America (Portland, OR) and CTD Inc (Gainesville, FL), respectively. Prostaglandin $E_2$ ELISA kit was purchased from Cayman Chemicals (Ann Arbor, MI). All other materials , such as linear polyethyleneimine (LPEI) and poly(styrene sulfonate) (PSS) were provided from previously detailed sources.

**In vitro cell culture:** Immortalized human pulmonary epithelial cancer (A549) and human lens epithelial (HLE-B3) cells were cultured in an incubator with a humidified atmosphere of 5% $CO_2$ at 37°C. The normal growth media for A549 cells was F-12K nutrient mixture, Kaighn's modification containing 10% fetal bovine serum, and 1% Pen Strep. The normal growth media for HLE-B3 cells was EMEM containing 20% fetal bovine serum and 1% Pen Strep. Previous research has shown that HLE-B3 grow best at high serum concentrations.[31] Media was changed twice weekly. Cellular growth was monitored under an Axiovert 200 inverted fluorescent microscope (Carl Zeiss) and cells were passaged at 80-90% confluence. For subculture, cells were harvested following 0.25% trypsin – 0.01% EDTA treatment at 37°C. The subcultivation ratio was 1:5 and 1:3 for A549 and HLE-B3 cells respectively.

**Cellular adhesion and proliferation on films:** Adhesion of A549 cells was investigated on glass and glass substrates coated with $(LPEI/PSS)_{10}$, $(LPEI/PSS)_{10}$-$(PolyA3/PolyCD)_{20}$, or $(LPEI/PSS)_{10}(PolyA3/PolyCD\text{-}Diclofenac)_{20}$ The samples were

named Glass, Base Layers, PolyCD, and Diclofenac, respectively. Substrates were placed in 6 well plates and seeded at 150,000 cell/ well (50,000 cells/ mL). Cells were cultured for five hours after seeding. After five hours, cell adhesion was investigated by examining metabolic activity, morphology, and viability using MTT analysis, staining, and imaging. For the MTT assay, cells were cultured in normal growth media for 2 hours and then 3 hours in normal growth media containing 10% MTT. After the three hour MTT incubation, substrates were transferred to a new six well plate and 1 mL of DMSO was used to dissolve crystals on a rotating shaker. Absorbance was measured in triplicate at 570 nm with a 690 nm correction using 100uL aliquots in a 96 well plate. Cells used for imaging were grown in normal media for four and a half hours and then phosphate buffer saline (PBS) solution containing ethidium homodimer, calcein AM, and Hoechst 3342 dye for 30 minutes. After staining, cells were washed with PBS and fixed in 10% neutral buffered formalin for ten minutes. Cells were imaged on an Axiovert 200 inverted fluorescent microscope (Carl Zeiss) microscope to determine morphology and viability. A549 proliferation on Glass, Base Layers, PolyCD, and Diclofenac was investigated in a similar manner as adhesion with the following exceptions. Proliferation was examined at 1, 3, and 7 days. For metabolic activity, cells were incubated with normal media containing 10% MTT three hours prior to analysis. For morphology and viability analysis, cells were incubated with stain for 30 minutes prior to fixation and imaging. All experiments were performed in triplicate.

**Polyelectrolyte multilayer assembly on intraocular lenses:** Films were built on glass substrates as previously described in chapter three. Films built on intraocular lenses were constructed in the same manner as glass substrates with the following

exceptions. Four different initial surface treatments were explored for intraocular lenses: 1) no plasma treatment 2) no plasma treatment with base layers 3) plasma treatment 4) plasma treatment with base layers. Plasma treatment refers to five minutes of plasma etching in air at ambient temperature and high RF level. Surface treatment is performed on substrates prior to film deposition to provide a uniformly charged substrate for optimal thin film growth and is typically done for silicon and glass substrates. Base Layers refer to ten bilayers of LPEI and PSS, which is often necessary to provide a uniform charged surface for film deposition. However, since the surface conditions necessary for optimal film formation were not known for intraocular lenses, four surface treatments were investigated. Anti-inflammatory films were composed of (Poly A3/ PolyCD – Diclofenac)$_{20}$. Intraocular lenses were attached to the deposition holder directly via a haptic or indirectly through a wire tied to a haptic. Drug release was performed in 1mL of PBS and monitored via fluorescence spectroscopy at various time points. At each time point, the IOL was removed from the microcentrifuge tube and placed in 1 mL of fresh PBS. All release experiments were performed in triplicate. To examine passive drug absorption from intraocular lenses, IOLs with plasma treatment and no treatment were soaked in polycd-diclofenac solution at dipping conditions for 10 minutes and 200 minutes. Films were then rinsed in water for 1 minute to remove loosely bound drug. Ten minutes is the amount of time the IOL would remain in drug solution during one bilayer deposition. Two hundred minutes is the total amount of time that the IOLs would be exposed to the polycd-diclofenac solution during film deposition. Drug release was performed in 1 mL of PBS and at each time point IOLs were placed in 1 mL of fresh PBS solution. All release experiments were done at 37 °C.

**Cellular adhesion and proliferation on intraocular lenses:** Adhesion and proliferation on intraocular lenses were investigated using HLE-B3 cells. The protocols used to investigate adhesion and proliferation on IOLs were the same as those used for glass substrates with the following exceptions. Uncoated IOLs and plasma treated $(LPEI/PSS)_{10}$(Poly A3/PolyCD-diclofenac)$_{20}$ IOLs were placed in a 48 well plate and seeded with 125,000 cells/well and 25,000 cells/ well in the presence of serum for adhesion and proliferation studies, respectively. Staining was not performed for intraocular lenses experiments due to high fluorescence background from the intraocular lens. Adhesion experiments were run for 8 hours with an MTT incubation time of four hours. Proliferation was analyzed at 6 hours, 24 hours, and 72 hours via Axiovert 200 inverted fluorescent microscope and at 3 days using MTT.

**Prostaglandin E2 assay:** Prostaglandin $E_2$ ($PGE_2$) was quantified for cells exposed to film eluent and cells grown on films using the prostaglandin $E_2$ EIA kit – monoclonal from Cayman Chemicals. For film eluent, A549 cells were seeded at confluence (20, 000 cells/well) in a 96 well plate. Cells were allowed to adhere for 24 hours and then stimulated with 1ng/mL of IL-1β for 24 hours. The cells were then washed twice with PBS and incubated with controls or film eluent in PBS for 1 hour. Then the cells were washed twice with PBS and 30 uM exogenous arachidonic acid in PBS was added to each well for 15 minutes. After 15 minutes, the PBS was collected for analysis and normal growth media containing 10% MTT was added to each well. After three hours, crystals were dissolved in 100 uL DMSO and absorbance was quantified at 570 nm with a 690 nm correction. Media samples were stored at -80°C until the $PGE_2$ ELISA was performed. For in situ experiments, 23mm x 25 mm glass or

$(LPEI/PSS)_{20}(Poly\ A3/PolyCD\text{-}diclofenac)_{20}$ coated glass substrates were placed in a six well plate and A549 cells were seeded on the constructs at confluence (500,000 cells/well). Then cells were stimulated with 1ng/mL IL-1β for 24 hours at day 2, 6, or 13 for 3, 7, or 14 day experiments respectively. Cells were washed with PBS and 30 uM exogenous arachidonic acid was added to each well for 15 minutes. After 15 minutes, the PBS was collected and stored at -80°C until analysis. Cells were incubated with normal media containing 10% MTT for three hours. The MTT assay was performed as described above for A549 adhesion and proliferation. For experiments lasting longer than three days, normal growth media was changed every 3 days. The ELISA assay is based on the competition between $PGE_2$ in the sample and $PGE_2$ tracer molecule for a limited amount of $PGE_2$ monoclonal antibody. Since the concentration of $PGE_2$ tracer is constant and the concentration of $PGE_2$ varies, the concentration of $PGE_2$ in the sample will be inversely proportional to the concentration of $PGE_2$ tracer bound to the antibody. Thus quantification of the amount of tracer leads to the concentration of $PGE_2$ in the sample.

## Results and Discussion

### A549 cell adherence on anti-inflammatory films

To ascertain if hydrolytically degradable films could be used to control inflammation in situ, the nature of interactions between the film and cells must be determined. Diclofenac films were composed of $(LPEI/PSS)_{10}(Poly\ A3/PolyCD\text{-}diclofenac)_{20}$ and were previously found to be ultrathin with a thickness of around 30 nm. Adhesion is the first point of direct physical communication between cells and biomaterials. Cell adhesion can be either beneficial, and a sign of biocompatibility, or unwanted depending on the application. The adhesive nature of multilayer films have

been shown to be highly dependent on stiffness, water content, and chemical composition, which are less well characterized for hydrolytically degradable films.[4] Additionally, hydrolytically degradable films steadily degrade in the presence of water and the ability of cells to stably adhere to this dynamic system is unknown.

The adhesive properties of hydrolytically degradable films were investigated by seeding human lung epithelial cancer cells (A549) on Glass, Base Layers, PolyCD, and Diclofenac in the presence and absence of serum. All coatings were constructed on glass substrates. Glass, Base Layers, PolyCD, and Diclofenac refer to clean glass, $(LPEI/PSS)_{10}$, $(LPEI/PSS)_{10}(PolyA3/PolyCD)_{20}$, and $(LPEI/PSS)_{10}(PolyA3/PolyCD\text{-}Diclofenac)_{20}$ respectively. Each system component was investigated so that the role of hydrolytically degradable films versus anti-inflammatory agent and supporting substrates could be ascertained. A549 cells are commonly used in the evaluation of nonsteroidal anti-inflammatory drugs (NSAIDs) because cyclooxgenase-2 (COX-2) production can be induced through stimulation with the inflammatory cytokine interleukin 1β (IL-1β).[32] COX-2 is responsible for the synthesis of pro-inflammatory compounds, such as prostaglandins. The presence of serum can mask the natural adhesive characteristics of a material. Proteins in the serum foul the material surface and provide a surface amenable to cell adhesion. After five hours, cell morphology, number, viability, and metabolic activity were determined and can be seen in figures 4.1, 4.2, and 4.3. Cells seeded on PolyCD and Diclofenac had similar appearances and were more rounded than Glass and Base Layers, which had similar appearances in the presence and absence of serum. Both PolyCD and Diclofenac had reduced live cell number and viabilities of ≤ 36 % and ≤ 28 % respectively with and without serum. Thus the

interaction between polymeric cyclodextrin containing films and cells are not serum dependent. Base Layers increased cell adhesion and had cell viabilities similar to glass in the presence and absence of serum. These trends were confirmed with MTT analysis. MTT measures the metabolic activity of cells. Under normal conditions, the metabolic activity linearly correlates to cell number. The reason for reduced adhesion on hydrolytically degradable films could be due to poly (β-amino ester) toxicity or its breakdown components. However, film eluent was found to be nontoxic. Cyclodextrins are composed of cyclic sugars and polymeric cyclodextrins are by definition polysaccharides. Cells are known to adhere poorly to some films containing polysaccharides due to their high water content.[4]

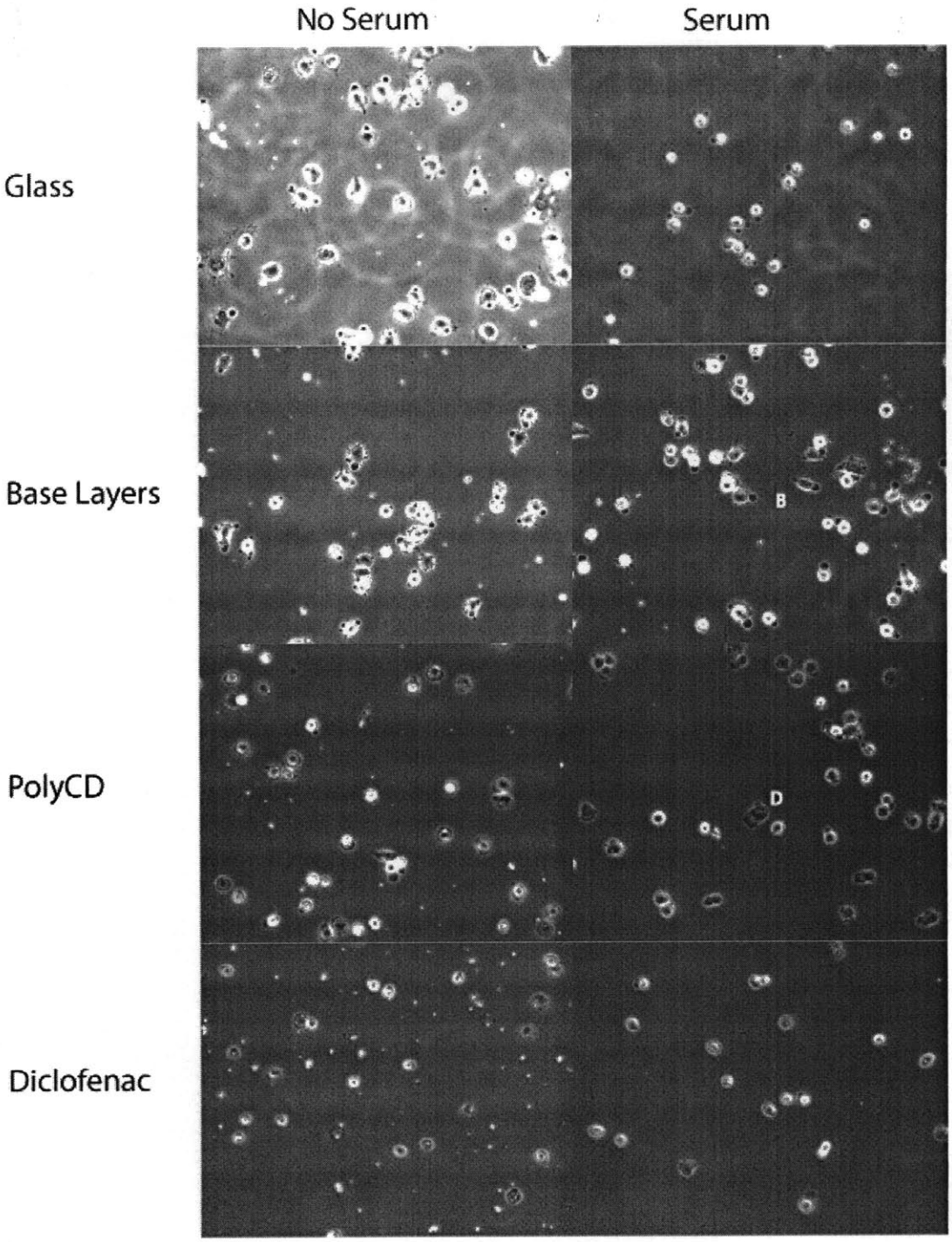


**Figure 4.1 A549 Cell adhesion pictures**

Microscope images of A549 cells after five hours of incubation on glass, $(LPEI/PSS)_{10}$ on glass [Base Layers], $(LPEI/PSS)_{10}(Poly\ A3/PolyCD)_{20}$ on glass [PolyCD], and $(LPEI/PSS)_{10}(Poly\ A3/PolyCD\text{-}Diclofenac)_{20}$ on glass [Diclofena] in the absence or presence of serum. Images were taken on a Carl Ziess Axiovert 200 inverted microscope.

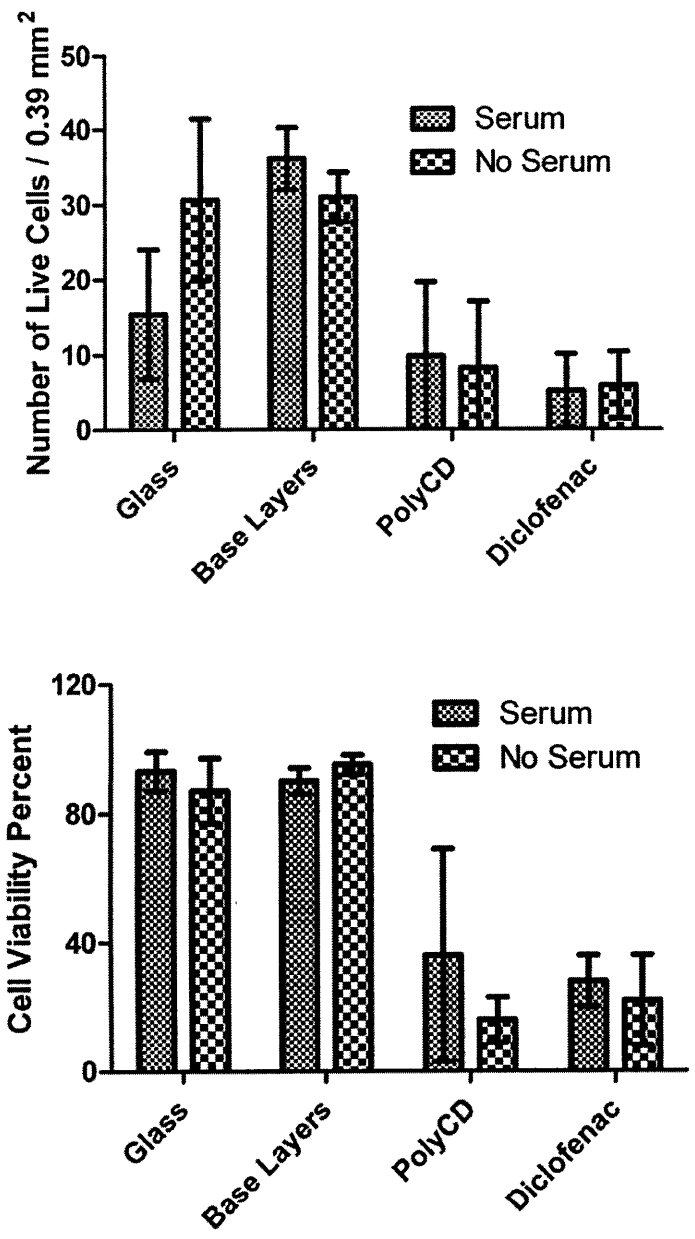


**Figure 4.2 Analysis of live cell number and cell viability during adhesion of A549 cells**

A549 cells were incubated on glass, $(LPEI/PSS)_{10}$ [base layers], $(LPEI/PSS)_{10}$(Poly A3/PolyCD)$_{20}$ [PolyCD], and $(LPEI/PSS)_{10}$(Poly A3/PolyCD-Diclofenac)$_{20}$ [Diclofenac] for five hours in the presence or absence of serum. Cells were stained with Hoechst 33342 and ethidium homodimer to allow for live and dead cells to be imaged with fluorescence microscopy and counted with ImageJ. The number of live cells, top, was calculated by subtraction total cells minus dead cells. Cell viability was determined by dividing live cells by the total number of cells.

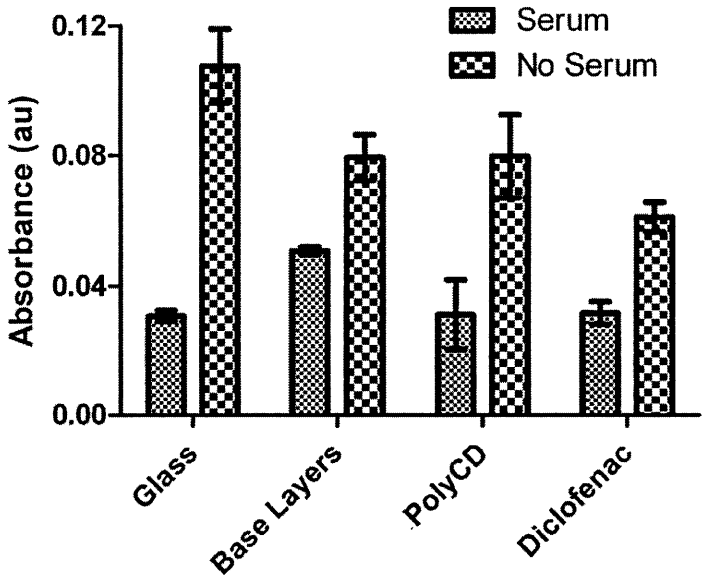


**Figure 4.3 Metabolic activity of A549 cells during adhesion**

A549 cells were incubated on glass, (LPEI/PSS)10 [Base Layers], (LPEI/PSS)10(Poly A3/PolyCD)20 [PolyCD], and (LPEI/PSS)10(Poly A3/PolyCD-Diclofenac)20 [Diclofenac] for five hours. The metabolic activity of cells was quantified and compared using thiazolyl blue tetrazolium bromide (MTT).

### A549 cell proliferation on anti-inflammatory films

Though cell adhesion was reduced on PolyCD and Diclofenac films, cells did attach to the surface and proliferative ability could be assessed. To assay inflammation in situ over time, the ability of cells to proliferate and form stable confluent layers had to be confirmed. Proliferation of cells on Glass, Base Layers, PolyCD, and Diclofenac were monitored via cell imaging, live/dead assay, and MTT. Growth was followed at one, three, and seven days after seeding, in the presence of serum. Cell images and quantitative analysis can be seen in figure 4.4 and 4.5 respectively.

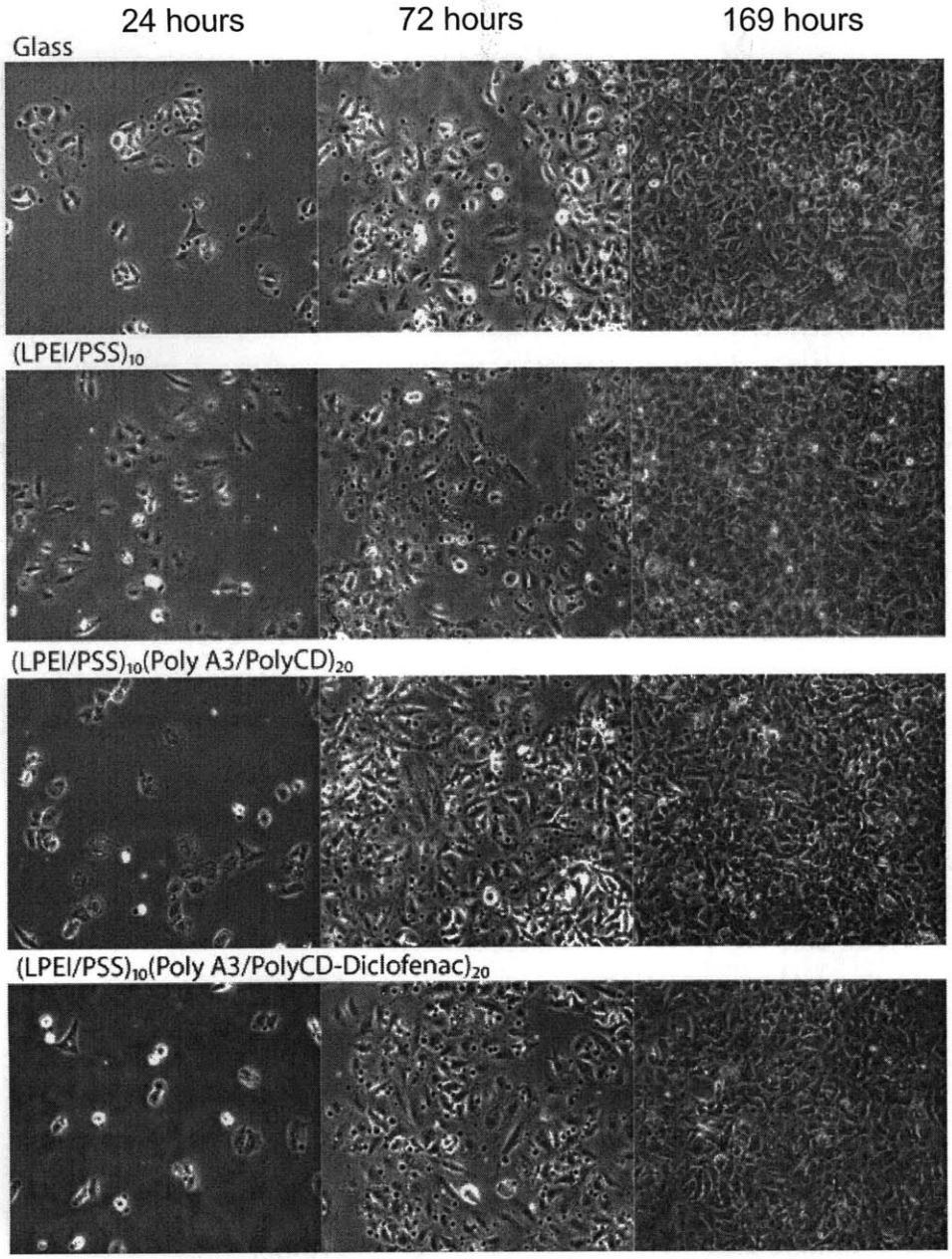


**Figure 4.4 A549 cell proliferation pictures**

Microscope images of A549 cells on glass or various thin film assemblies at different times. Images were taken at 24, 72, and 169 hours and are ordered from right and left. From top to bottom substrate complexity is increased starting with a clean glass substrate and ending with a functional anti-inflammatory film.

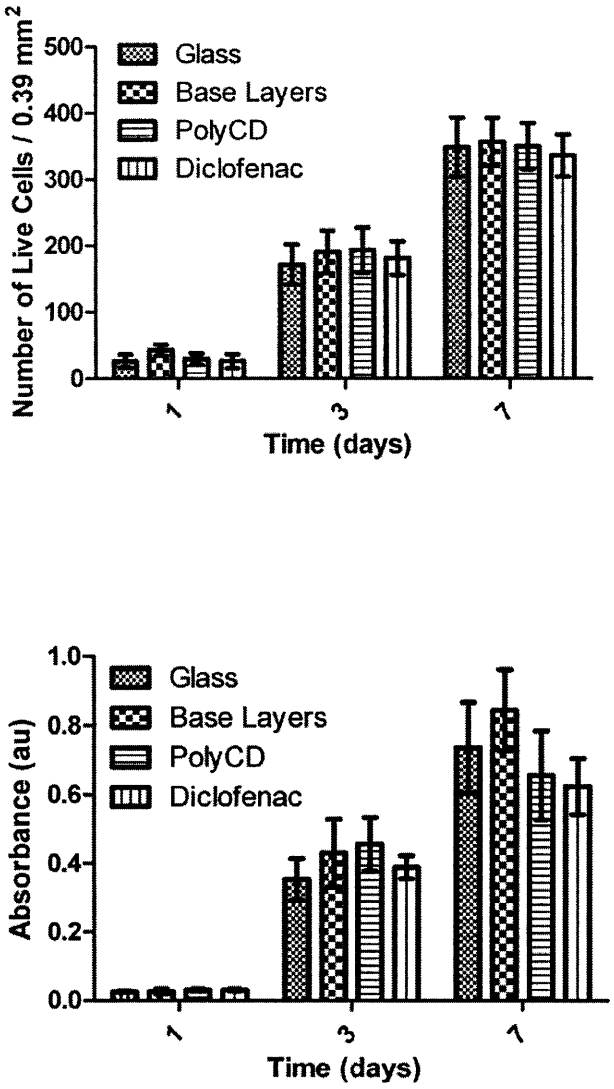


**Figure 4.5 Analysis of cell viability and metabolic activity during proliferation**

A549 cells were incubated on glass, $(LPEI/PSS)_{10}$ [Base Layers], $(LPEI/PSS)_{10}$(Poly A3/PolyCD)$_{20}$ [PolyCD], and $(LPEI/PSS)_{10}$(Poly A3/PolyCD-Diclofenac)$_{20}$ [Diclofenac] for 1,3, and 7 days. Cells were stained with Hoechst 33342 and ethidium homodimer to allow for live and dead cells to be imaged with fluorescence microscopy and counted with ImageJ. The number of live cells, top, was calculated by subtraction total cells minus dead cells. The metabolic activity of cells, bottom, were quantified and compared using thiazolyl blue tetrazolium bromide (MTT).

At 24 hours morphological differences between substrate with and without cyclodextrins existed. Substrates without cyclodextrins had fuller more elongated cells. However no significant difference was observed in live cell number and MTT analysis. At three days, cells were near confluence and no significant difference in cell appearance, number, and metabolic activity was observed. At seven days cells had been confluent for several days and cell behavior was within standard deviation of each other for all systems. Though cyclodextrin films were less adhesive, cells were able to recuperate after 24 hours and proliferate normally.

**Anti-inflammatory films regulate cellular inflammation**

Since the ability of cells to grow and adhere on hydrolytically degradable films was confirmed, the regulation of inflammation could be investigated. The nonsteroidal anti-inflammatory drug, diclofenac, was used as the anti-inflammatory agent. NSAIDs work by inhibiting the cyclooxygenase activity of cyclooxygenase enzyme (COX). COX is a bifunctional membrane bound enzyme with cyclooxygenase and peroxidase activity. The cyclooxygenase active site is found deep within a pocket that opens into a membrane. The peroxidase active site is on the upper surface of the enzyme. COX is found in the smooth endoplasmic reticulum and the nuclear envelope.[33, 34] For anti-inflammatory films to be effective, the inflammatory response of neighboring cells and those in direct physical contact should be suppressed. To assess the potential of films to regulate the behavior of neighboring cells, $(LPEI/PSS)_{10}$(Poly A/B1/PolyCD-diclofenac)$_{20}$ film eluent in PBS was collected at various time points and incubated with a confluent layer of A549 cells stimulated with IL-1β. Production of prostaglandin $E_2$, a pro-inflammatory cytokine produced by COX, was measured and can be seen in figure 4.6. Film eluent had the same activity as 30 uM solution of free diclofenac for all time

points assessed. A 20 mg/mL solution of the cyclodextrin carrier only slightly decreased COX activity. Diclofenac released from anti-inflammatory films can effectively control inflammation of neighboring cells.

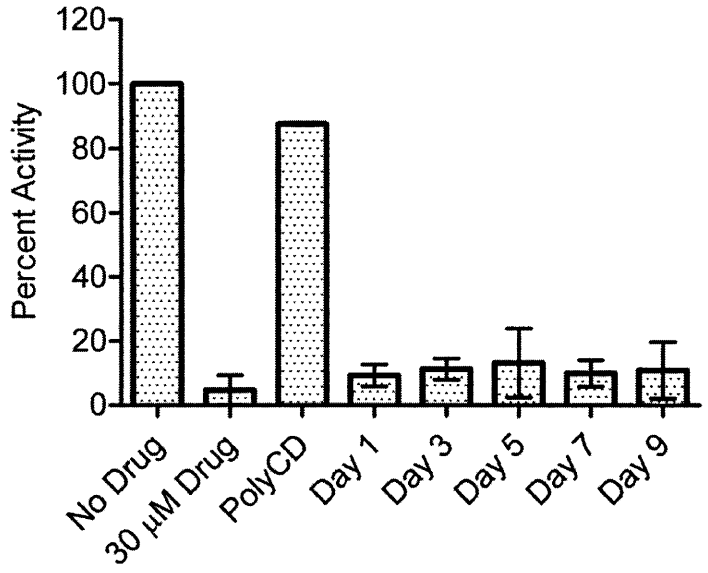


**Figure 4.6 $PGE_2$ with film eluent**

Percent activity of COX-2 in A549 cells after incubation with diclofenac, polyCD, film eluents, or media alone. from (Poly A/B1 /Poly (CMBCD)-Diclofenac)$_{20}$ on various days. Cell experiments were conducted using A549 cells. Briefly, cells were stimulated with IL-β for 24 hours and then incubated with samples for 1 hour. Cells were then washed twice and then incubated with arachidonic acid for 15 minutes. Supernatants were collected and prostaglandin $E_2$ quantified via ELISA.

To assess the ability of anti-inflammatory films to regulate the behavior of cells in direct physical contact, A549 cells were seeded on films at confluence. At two, six, and thirteen days cell were stimulated with IL-1β for 24 hours. After stimulation the cells were fed exogenous arachidonic acid and the concentration of prostaglandin $E_2$ was

measured. The comparison of anti-inflammatory films with glass can be seen in figure 4.7. Anti-inflammatory films were able to reduce $PGE_2$ production in situ by ≥ 76 ± 8 % percent for at least 14 days. To our knowledge, this is the longest documented control of inflammation from a polyelectrolyte multilayer film.

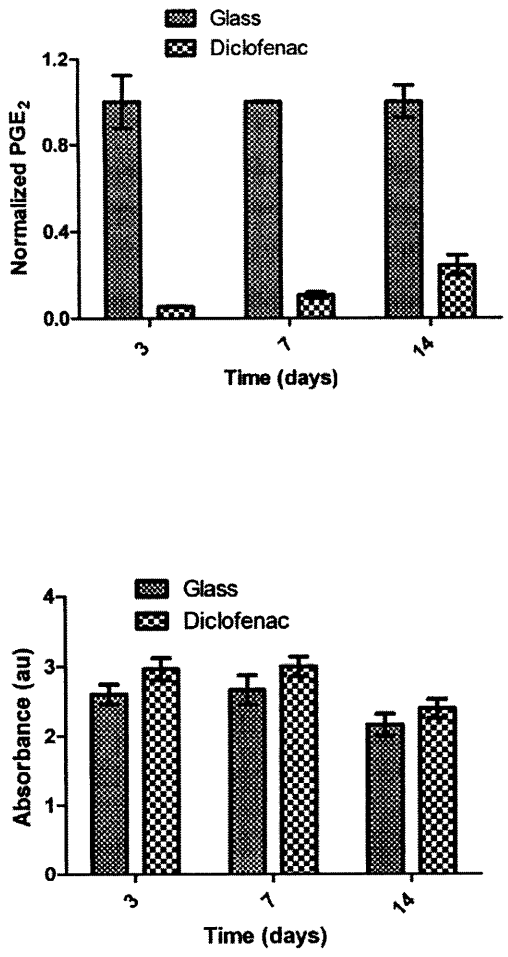


**Figure 4.7 $PGE_2$ assay in situ and MTT assay.**

A549 cells seeded at confluence on glass or glass coated with $(LPEI/PSS)_{10}$(Poly A3/PolyCD-diclofenac)$_{20}$. Cells were stimulated with IL-1β, feed exogenous arachidonic acid, and analyzed for $PGE_2$ production. MTT analysis was performed on cells after $PGE_2$ assay to confirm similar metabolic activity.

**Release dynamics from intraocular lenses**

Cataract surgery is one of the most common surgical procedures in the world. Cataract, the clouding of the eye's natural lens, is the leading cause of visual disability worldwide and is completely reversible through the surgical removal and replacement of the opaque lens with an artificial intraocular lens (IOL). Postoperative inflammation is a major side effect of cataract surgery and can results in patient discomfort, delayed recovery and suboptimal visual. If left untreated, inflammation can lead to complications, such as cystoid macular edema and posterior capsule opacification (PCO).[35-38] PCO, or secondary cataracts, is the most common postoperative complication of cataract surgery and is caused by changes in lens epithelial cells that cause them to migrate and proliferate across the lens.[39] These cells obstruct the passage of light causing opacities. Studies have shown that COX inhibition can effectively suppress lens epithelial cell changes that lead to PCO and prevent the retinal swelling that leads to cystoids macular edema.[40]

Diclofenac is FDA approved for minimizing inflammation following cataract surgery. After cataract surgery, diclofenac is administered four times daily via eye drops beginning 24 hours after surgery and continuing for at least the first two weeks of the postoperative period.[41] However, both the efficacy of topical drug delivery and patient compliance is low.[42] The local delivery of diclofenac from anti-inflammatory films would present an attractive replacement for eye drops due to the enhanced drug bioavailability. Since, anti-inflammatory films were found to effectively suppress inflammatory cytokine production over a two week time period, their utility as drug delivery coatings for intraocular lenses was investigated. A successful drug delivery

coating for IOLs must also maintain the lens' optical properties and not increase cell adhesion or proliferation.

To ascertain if these anti-inflammatory films could be used to create viable drug delivery coatings for intraocular lenses, the drug release, cell adhesion and proliferation, and macroscopic optical properties of coated IOLs were investigated. Since the necessary conditions to provide a uniform surface supportive of thin film growth on hydrophobic acrylic intraocular lenses is unknown, four different surface treatment methods were examined: 1) no plasma treatment 2) no plasma treatment with Base Layers 3) plasma treatment 4) plasma treatment with Base Layers. Plasma treatment refers to five minutes of plasma etching in air at ambient temperature and high RF level. The release curves can be seen in figure 4.8. All surface treatments resulted in burst release of diclofenac ranging from 0.5 – 2.5 ug/cm$^2$ which was 30 - 80 % of total drug loading.[43] Burst release is not consistent with release dynamics of Diclofenac films assembled on glass or silicon; the observed burst occur because IOLs are not inert substrates. Several papers have shown that IOLs can be used to absorb and release small molecule therapeutics by diffusion. The biggest burst was seen for plasma treated IOLs that did not have base layers. The lowest burst release was seen for untreated IOLs with no Base Layers. Treated and untreated films with Base Layers had similar burst release values. It was found that IOLs soaked in polycd-diclofenac deposition solution for 10 minutes, the time of one deposition, and 200 minutes, the total deposition time for the polyanion, absorbed and released 0.2-3 ug/cm$^2$ for twelve hours. If the burst amount is subtracted from the drug release amount, the curves are not significantly different from each other ($p = 0.3$) and do not deviate from linearity (run's test, p values

range from 0.1 – 0.6). Therefore discounting the burst, coatings on IOL have similar release characteristics as those on glass and are independent of surface treatment.

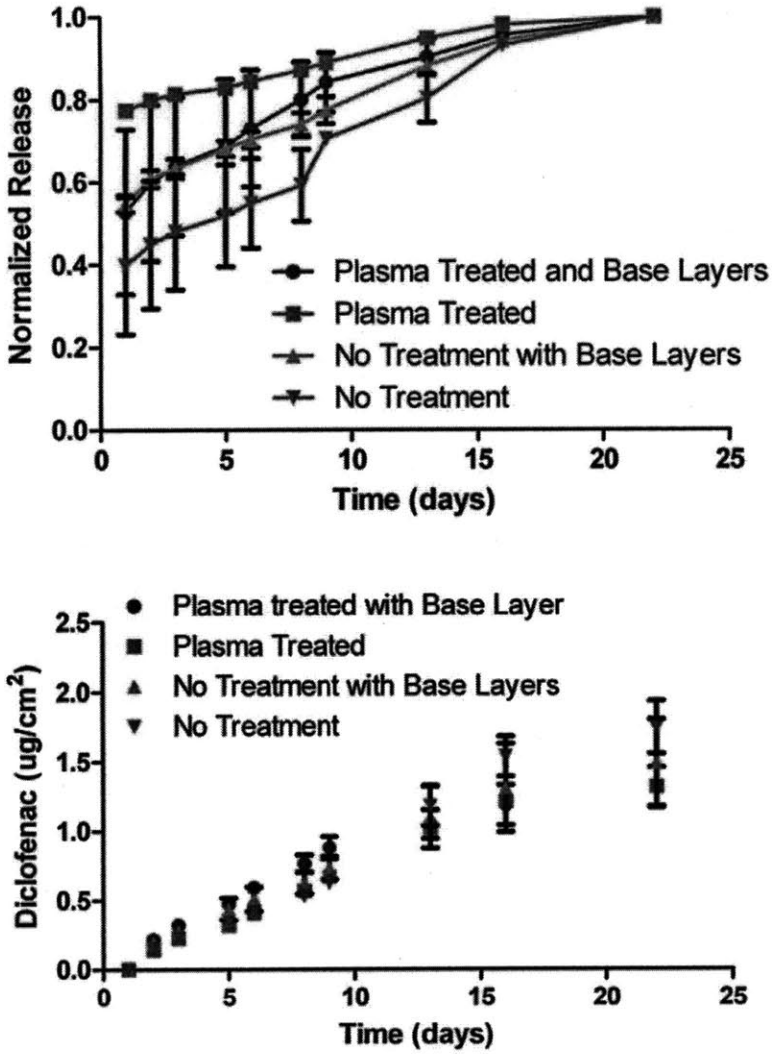


**Figure 4.8 Diclofenac release from intraocular lenses**

The top graph shows the normalized release of diclofenac from intraocular lenses with different surface treatments. Plasma treatment refers to five minutes of plasma etching at ambient conditions. Base layers refer to $(LPEI/PSS)_{10}$. The bottom graph is the release of diclofenac minus the initial burst that occurs within the first 24 hours.

The ability to form degradable delivery agents on top of permanent layers with altering release kinetics will enable the creation of dual functional film. Here $(LPEI/PSS)_{10}$ were used as the permanent surface, but films that impart permanent non-adhesive or antimicrobial properties could be used.

**HLE-B3 cell adhesion on coated intraocular lenses**

An ideal coating for IOLs must control inflammation without increasing cell adhesion or proliferation and maintain optical properties.[35] The proliferation of human lens epithelial cells on intraocular lenses causes opacities that result in visual disability; thus, cell adhesion and proliferation are important to device success. Extensive research has concentrated on the selection of IOL materials that do not support cell proliferation, thus coating should not increase the proliferative capacity of cells. The adhesion and proliferation of human lens epithelial cells on coated IOLs was investigated using cell imaging and MTT analysis. Human lens epithelial cells adhesion and proliferation are responsible for the formation of secondary cataracts and were used to more adequately the model *in vivo* scenario. Earlier studies used A549 cells because methods to explore inflammatory pathways are well established for A549 cells. The images and MTT results can be seen in figure 4.10 and 4.11 respectively. Cell stain and viability measurements were not used due to dye absorption by the IOL. Coated IOLs refer to Diclofenac films and do not increase cell adhesion or proliferation. In fact coated IOLs have a small negative effect on cell adhesion and proliferation. Images show that cells on the coated IOL are rounded after eight hours as compared to the elongated morphology of those on uncoated IOLs. By day three cell morphology and metabolic activity is similar between the groups. Coatings must also maintain the optical properties of the artificial intraocular lens. Figure 4.12 illustrates the optical properties of

coated IOLs. The stereo microscope image of the coated IOL on white background illustrates device clarity. The image on the right shows MIT inverted in the IOL. The bottom image shows the maintenance of magnification ability, as the “Te” of the word technology is magnified in the lens. However, microscopic properties should be examined with lens specific equipment, since the size and shape of lenses prevent analysis by routine laboratory techniques. Still, hydrolytically degradable films would only pose transient changes in optical properties because they provide temporary functionalization.

Intraocular Lenses

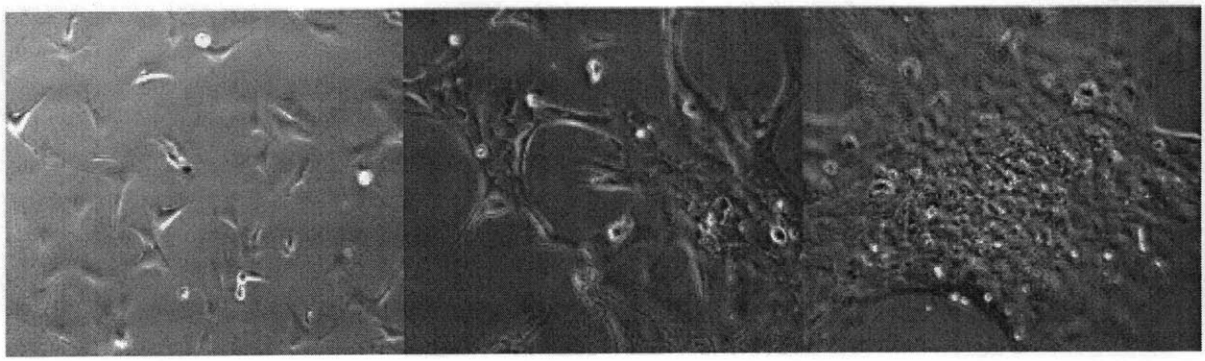

Plasma Treated and Coated Intraocular Lenses

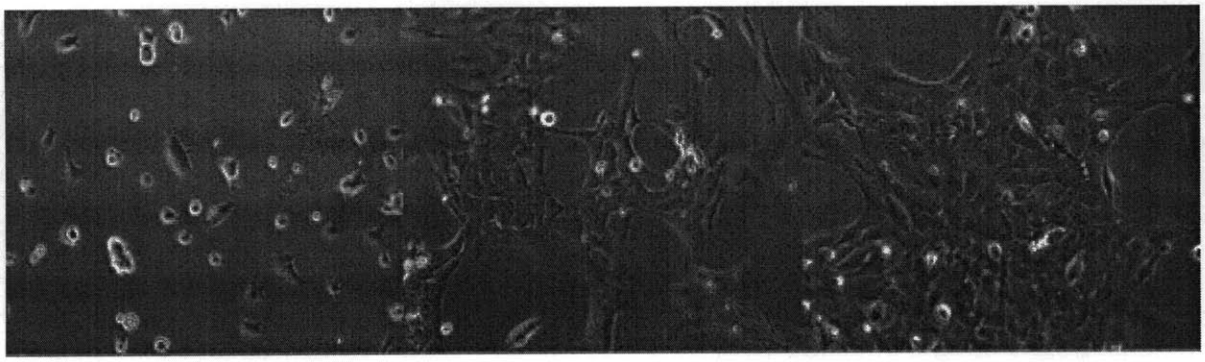

Coated Intraocular Lenses

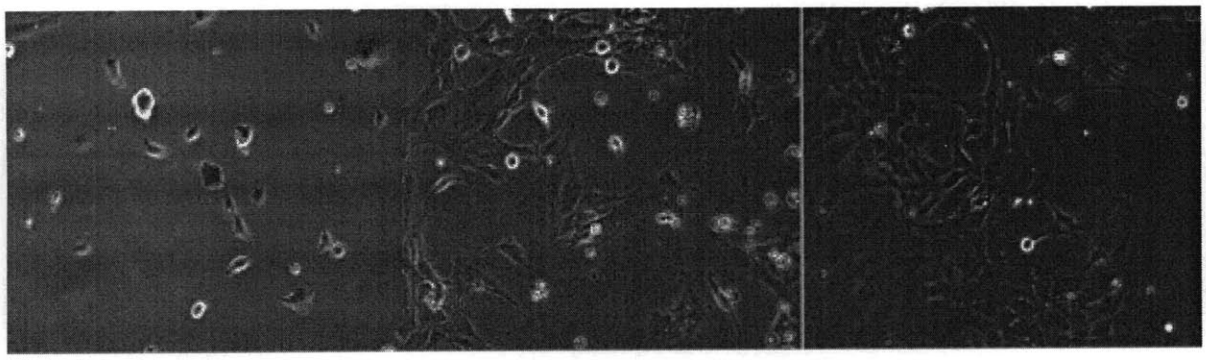

**Figure 4.9 HLE-B3 proliferation on intraocular lenses**

The growth of HLE-B3 cells on uncoated IOLs, coated IOLs, and plasma treated and coated IOLs. Coated refers to $(LPEI/PSS)_{10}$(Poly A3/ PolyCD-diclofenac)$_{20}$. Images were taken at 6, 24, and 72 hours from left to right.

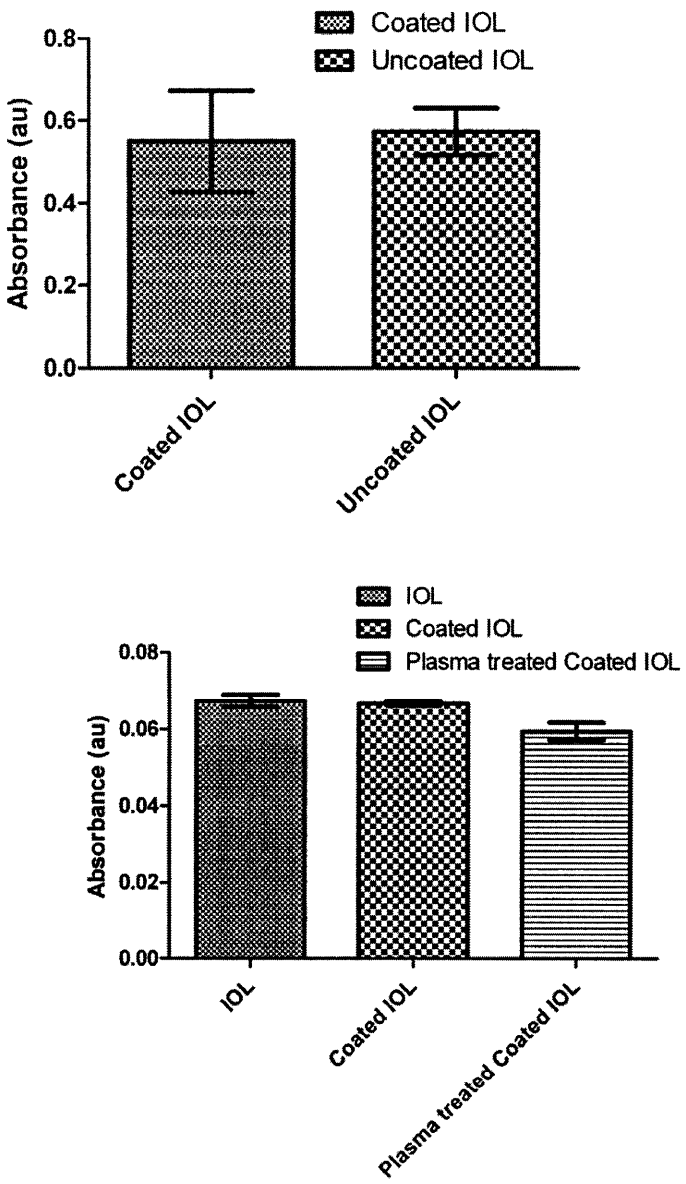


**Figure 4.10 HLE-B3 cell adhesion after eight hours and proliferation after three days on intraocular lenses**

Top: HLE-B3 cells were seeded on IOLs for eight hours and MTT was used to compare the cell number via metabolic activity. Uncoated IOLs and plasma treated IOLs with $(LPEI/PSS)_{10}$(Poly A3 / PolyCD-diclofenac)$_{20}$. Bottom:The metabolic activity of cells seeded on different IOLs was analyzed after three days. HLE-B3 cells were seeded on IOLs that were uncoated, coated, and plasma treated plus coated. Coated refers to $(LPEI/PSS)_{10}$(Poly A3/ Poly CD-diclofenac)$_{20}$. Plasma treatment refers to five minutes of plasma etching at ambient conditions.

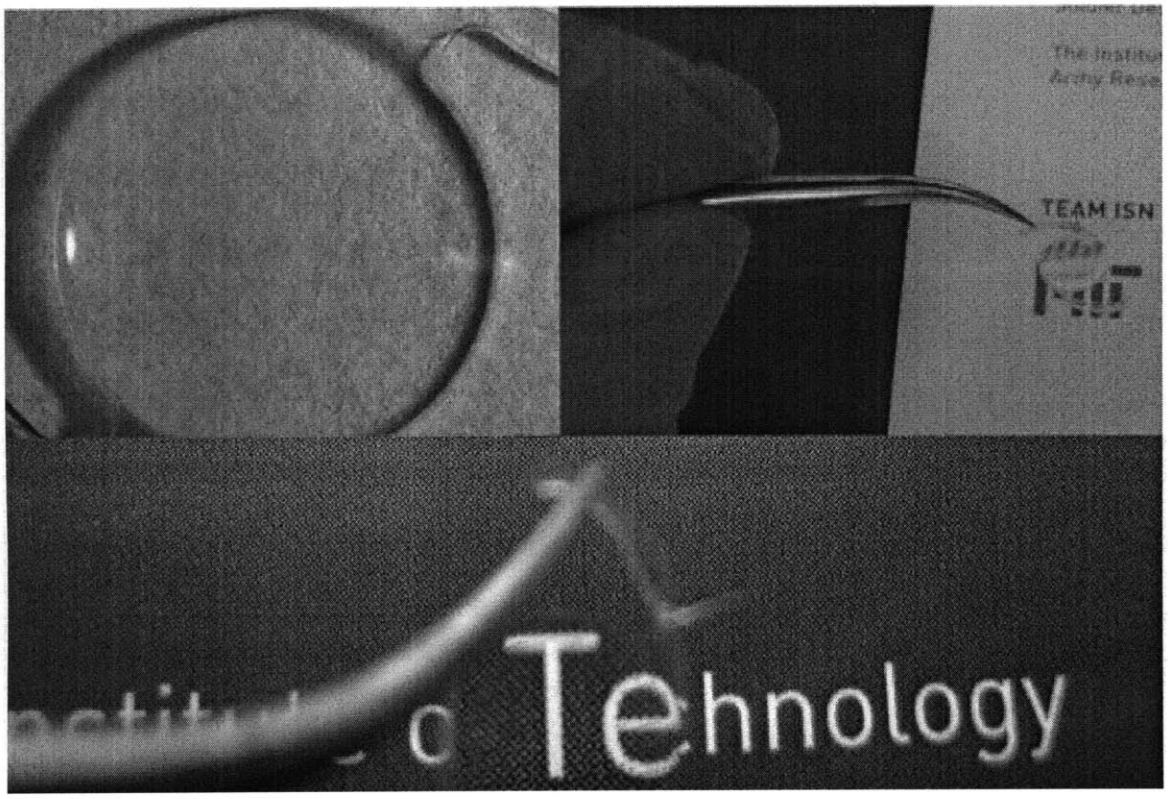


**Figure 4.11 Macroscopic IOL properties**

Intraocular lenses were plasma treated for five minutes and coated with $(LPEI/PSS)_{10}$(Poly A3/PolyCD-diclofenac)$_{20}$. The top left photograph was taken with a stereo microscope. The lens was placed on a white backgroung. The image on the top right shows the inversion of MIT in the lens. The bottom images shows the lens magnifying the "Te" of the word technology.

## Conclusion

Adverse host reactions have resulted in numerous implantable device failures annually. Some of the most deleterious effects are a result of acute and chronic inflammation.[1, 2] Control of inflammation remains a major barrier in the creation of effective implantable device. Surface properties govern the biological response of implants and key device design principles now center on the mitigation of inflammatory processes, control of cellular adhesion and proliferation, and prevention of infection in

addition to the intended device functionality. The ability of layer-by-layer films to widely vary chemical, physical, and mechanical properties during assembly or through mild and facile post treatment has enabled the advance engineering of nanostructured materials with fine control of cellular behavior. Much research has focused on drug carrying polyelectrolyte multilayers as modulators of cell behavior. While polelectrolyte multilayers have proven to be valuable tools in the regulation of cellular interactions, few papers demonstrate in situ control of inflammation and none over physiological relevant timescales with precise temporal control. Hydrolytically degradable multilayer films have demonstrated exquisite control of release duration for a variety of bioactive agents, including small molecules, through selection of the degradable polycation. In this work, the first investigation of cell adhesion and proliferation on hydrolytically degradable multilayer films was detailed. Degradable films containing polymeric cyclodextrins had reduced cell adhesion in the presence and absence of serum. However cells fully recovered after one day and cell proliferation was the same as blank substrate. In situ control of inflammation through the controlled release of a small molecule therapeutic was achieved for two weeks. To our knowledge, this is the longest documented regulation of inflammation from cells grown on polyelectrolyte multilayers. Anti-inflammatory release duration and amount were comparable to the standard of care for the treatment of postoperative ophthalmic inflammation after cataract surgery. To assess, the viability of these anti-inflammatory films in ophthalmic applications drug delivery coatings for intraocular lenses were fabricated. Sustained delivery of diclofenac from IOLs was demonstrated and the transparent coatings did not enhance cell adhesion or proliferation, making them ideal for cataract applications. The development

of an ultrathin film system able to modulate cellular behavior with exact spatiotemporal control represents a key advance for the future utility of implantable medical devices.

## References


[1] J. M. Anderson, A. Rodriguez, D. T. Chang, *Seminars in Immunology* **2008**, *20*, 86.

[2] P. Thevenot, W. J. Hu, L. P. Tang, *Current Topics in Medicinal Chemistry* **2008**, *8*, 270.

[3] P. Wu, D. W. Grainger, *Biomaterials* **2006**, *27*, 2450.

[4] T. Boudou, T. Crouzier, K. F. Ren, G. Blin, C. Picart, *Advanced Materials* **2010**, *22*, 441.

[5] G. Decher, *Science* **1997**, *277*, 1232.

[6] G. Decher, J. B. Schlenoff, Wiley-VCH, Weinheim, **2003**, p. 524.

[7] D. M. Lynn, *Soft Matter* **2006**, *2*, 269.

[8] J. F. Quinn, A. P. R. Johnston, G. K. Such, A. N. Zelikin, F. Caruso, *Chemical Society Reviews* **2007**, *36*, 707.

[9] D. L. Elbert, C. B. Herbert, J. A. Hubbell, *Langmuir* **1999**, *15*, 5355.

[10] Z. Y. Tang, Y. Wang, P. Podsiadlo, N. A. Kotov, *Advanced Materials* **2006**, *18*, 3203.

[11] P. T. Hammond, *Advanced Materials* **2004**, *16*, 1271.

[12] E. Leguen, A. Chassepot, G. Decher, P. Schaaf, J. C. Voegel, N. Jessel, *Biomolecular Engineering* **2007**, *24*, 33.

[13] A. Quinn, G. K. Such, J. F. Quinn, F. Caruso, *Advanced Functional Materials* **2008**, *18*, 17.

[14] N. Benkirane-Jessel, P. Schwinte, P. Falvey, R. Darcy, Y. Haikel, P. Schaaf, J. C. Voegel, J. Ogier, *Advanced Functional Materials* **2004**, *14*, 174.

[15] M. A. Borden, C. F. Caskey, E. Little, R. J. Gillies, K. W. Ferrara, *Langmuir* **2007**, *23*, 9401.

[16] A. Dierich, E. Le Guen, N. Messaddeq, J. F. Stoltz, P. Netter, P. Schaaf, J. C. Voegel, N. Benkirane-Jessel, *Advanced Materials* **2007**, *19*, 693.

[17] N. Jessel, M. Oulad-Abdeighani, F. Meyer, P. Lavalle, Y. Haikel, P. Schaaf, J. C. Voegel, *Proceedings of the National Academy of Sciences of the United States of America* **2006**, *103*, 8618.

[18] N. B. Jessel, P. Schwinte, R. Donohue, P. Lavalle, F. Boulmedais, R. Darcy, B. Szalontai, J. C. Voegel, J. Ogier, *Advanced Functional Materials* **2004**, *14*, 963.

[19] S. Muller, G. Koenig, A. Charpiot, C. Debry, J. C. Voegel, P. Lavalle, D. Vautier, *Advanced Functional Materials* **2008**, *18*, 1767.

[20] A. Schneider, C. Vodouhe, L. Richert, G. Francius, E. Le Guen, P. Schaaf, J. C. Voegel, B. Frisch, C. Picart, *Biomacromolecules* **2007**, *8*, 139.

[21] B. Thierry, P. Kujawa, C. Tkaczyk, F. M. Winnik, L. Bilodeau, M. Tabrizian, *Journal of the American Chemical Society* **2005**, *127*, 1626.

[22] J. C. Voegel, G. Decher, P. Schaaf, *Actualite Chimique* **2003**, 30.

[23] A. M. Yu, Z. J. Liang, F. Caruso, *Chemistry of Materials* **2005**, *17*, 171.

[24] H. F. Chuang, R. C. Smith, P. T. Hammond, *Biomacromolecules* **2008**, *9*, 1660.

[25] A. Shukla, K. E. Fleming, H. F. Chuang, T. M. Chau, C. R. Loose, G. N. Stephanopoulos, P. T. Hammond, *Biomaterials* **2010**, *31*, 2348.
[26] R. C. Smith, M. Riollano, A. Leung, P. T. Hammond, *Angewandte Chemie-International Edition* **2009**, *48*, 8974.
[27] K. C. Wood, J. Q. Boedicker, D. M. Lynn, P. T. Hammon, *Langmuir* **2005**, *21*, 1603.
[28] M. Macdonald, N. M. Rodriguez, R. Smith, P. T. Hammond, *J Control Release* **2008**, *131*, 228.
[29] R. C. Smith, A. Leung, B. S. Kim, P. T. Hammond, *Chemistry of Materials* **2009**, *21*, 1108.
[30] D. G. Anderson, C. A. Tweedie, N. Hossain, S. M. Navarro, D. M. Brey, K. J. Van Vliet, R. Langer, J. A. Burdick, *Advanced Materials* **2006**, *18*, 2614.
[31] N. Ibaraki, K. Ohara, *Investigative Ophthalmology & Visual Science* **1993**, *34*, 887.
[32] T. D. Warner, F. Giuliano, I. Vojnovic, A. Bukasa, J. A. Mitchell, J. R. Vane, *Proceedings of the National Academy of Sciences of the United States of America* **1999**, *96*, 9966.
[33] R. N. Dubois, S. B. Abramson, L. Crofford, R. A. Gupta, L. S. Simon, L. B. A. Van De Putte, P. E. Lipsky, *Faseb Journal* **1998**, *12*, 1063.
[34] D. S. Goodsell, *Stem Cells* **2000**, *18*, 227.
[35] C. Parsons, D. S. Jones, S. P. Gorman, *Expert Review of Medical Devices* **2005**, *2*, 161.
[36] I. M. Wormstone, *Experimental Eye Research* **2002**, *74*, 337.
[37] H. L. Chandler, C. A. Barden, P. Lu, D. F. Kusewitt, C. M. H. Colitz, *Molecular Vision* **2007**, *13*, 677.
[38] N. Awasthi, S. Q. Guo, B. J. Wagner, *Archives of Ophthalmology* **2009**, *127*, 555.
[39] H. Matsushima, H. Iwamoto, K. Mukai, Y. Katsuki, M. Nagata, T. Senoo, *Expert Review of Medical Devices* **2008**, *5*, 197.
[40] F. Giuliano, T. D. Warner, *British Journal of Pharmacology* **1999**, *126*, 1824.
[41] J. Colin, *Drugs* **2007**, *67*, 1291.
[42] D. Ghate, H. F. Edelhauser, *Expert Opin, Drug Deliv.* **2006**, *3*, 275.
[43] G. Kleinmann, D. J. Apple, J. Chew, B. Hunter, S. Stevens, S. Larson, N. Mamalis, R. J. Olson, *J Cataract Refract Surg* **2006**, *32*, 1717.

# Chapter 5 : Multi-agent Delivery of Small Molecule Therapeutics from Multilayer Films

This work was done in collaboration with Anita Shukla

## Introduction

Infection and inflammation are two of the most common postoperative complications faced by patients worldwide.[1-4] Nowhere is this more pronounced than in the field of implantable biomaterials and devices, where postoperative side effects account for millions of morbidities and mortalities annually.[2] Significant work has aimed to forestall these degenerative and debilitating complications by creating technologies that mitigate adverse inflammatory processes while preventing infections. However infectious and inflammatory processes are clinically distinct pathways that require unique interventions to effectively address each condition and few systems have the necessary functionality to treat both. As a result, current gold standards rely heavily on the systemic administration of small molecule pharmaceuticals.[1, 2, 4] There is a paucity of drug delivery systems with the ability to control the release of antibiotic and anti-inflammatory agents with distinct programmed release. Hydrolytically degradable multilayer films, capable of both sequential and concurrent drug delivery, offer a unique opportunity to create multi-functional thin films with the ability to address both inflammatory and infectious pathways.[5-9] Here we describe the first multilayer thin film system able to address the demands of both infection and inflammation using FDA approved pharmaceutics.

Infection starts when bacterial adhesion and colonization of implants occur before tissue integration.[1, 2] The absence of tissue integration enables the formation of bacteria films (biofilms), which are resistant to both immune responses and systemic antibiotics and are the leading cause of device associated infections.[2, 10] Strategies aimed to mitigate infection focus on prevention of biofilm formation through immediate bacterial eradication post implantation. Research has shown that the prevention of bacterial adhesion during the first six hours post-implantation is critical to device success.[2] Ideal antibiotic regimen should provide high doses hours after implantation to prevent bacterial adhesion followed by a small taper of drug above the minimum inhibitory concentration (MIC) to clear remaining bacteria. Systemic antibiotic therapy is traditionally used to prevent and treat implant associated infection. However, reduced therapeutic efficacy has been observed with systemic administration and thousands of implants are removed annually due to uncontrolled infection.[2, 10] To prevent device associated infection, research has focused on local control of infection through modification of device surfaces with microbicidal thin film systems.

Layer-by-layer (LbL) films have emerged as a promising source of microbicidal coatings. Rubner, Voegel, and others have extensively investigated polyelectrolyte multilayers films as barriers to infection through release of active agents, alterations of physicochemical surface properties, or permanent modification of device surfaces with microbicidal components.[7, 11-16] Voegel demonstrated the ability of liposome-silver ion conjugates to inhibit the activity of E. coli through release of the antibacterial silver ions from poly (L-lysine) and hyaluronic acid films.[13] Rubner has explored the use of dual functional anti-microbial films that were both contact and release killing.[12] This system

employed polyelectrolyte multilayer films containing silver ions and a surface cap of nanoparticles with immobilized bactericides. Films were able to prevent the growth of bacteria even after the silver ions had been completely released from the film. Others have utilized films containing dendrimer and micelle- antibiotic assemblies, and antimicrobial peptides as methods to control infection to effectively inhibiting bacterial activity.[7, 11, 14, 17] Still, these methods rely on contact killing mechanisms, release of non-FDA approved antimicrobial materials, and/or cannot be easily tuned with regard to drug dosage or release rate. High doses of FDA approved antibiotic at the implant site remain the most direct and proven method of infection control. Shukla, et al utilized hydrolytically degradable multilayers to construct coatings able to deliver vancomycin, a potent FDA approved antibiotic, with flexible dosages and timescales. These films successfully prevented biofilm formation through eradication of bacteria in solution and on the device surface.[17]

Inflammation is a key factor in the host response to device implantation. The extent and duration of inflammation is a marker for both biocompatibility and device success.[3, 4] The control of adverse inflammatory pathways is paramount to the success of implantable devices and is an active area of research. While some efforts have focused on the creation of immune camouflaged, non-fouling, and non-adhesive surfaces, a great deal of emphasis has been placed on the release of bioactive molecules.[16] Versatility, compositional control, and ease of manufacturing has brought layer-by-layer to the forefront of these efforts. Benkirane-Jessel, et al showed that piroxicam, an anti-inflammatory drug, could be released from polypeptides films and used to regulate the production of inflammatory cytokines.[18] Similarly, Picart

highlighted the ability of glycosaminoglycan films to incorporate and release diclofenac, an anti-inflammatory drug, through hydrophobic interactions.[19] Anti-inflammatory peptides have also been embedded at the surface of multilayer films to control inflammation through direct cell contact. Benkirane-Jessel et al showed that α-melanocyte-stimulating hormone could successfully regulate cell morphology and the production of inflammatory cytokines.[20] In chapter four, the first multilayer thin film system able to control inflammation *in vitro* on physiologically relevant timescales was described.

Research, to date, has focused on the creation of drug delivery coatings tailored to address the unique demands of infection or inflammation. As a result, excellent LbL systems able to mitigate some postoperative complications of device implantation have been created. However, ultrathin multilayer films with broad therapeutic scope able to surmount the multitude of complications arising from both infection and inflammation do not exist. In this chapter, two layer-by-layer systems were combined to form the first LbL coating able to regulate the two most common complications of device implantation using FDA approved pharmaceutics. These dual functional films were composed of the antibacterial system designed by Shukla, et al and the anti-inflammatory system previously described in chapter four; films contained vancomycin and diclofenac to control infection and inflammation respectively. The power and broad applicability of these multi-functional films were highlighted by creation of combination devices, drug coatings on functional implants, and regulation of infection and inflammation in vitro. Therapeutic release could be easily tuned via assembly conditions to address a variety of clinical scenarios, including infection and inflammation post cataract surgery.

## Materials and Methods

**Materials:** Intraocular lenses were generously donated by the Aurolabs division of Aravind Eye Hospital (Madurai, Tamil Nadu, India). Sutures and commercial bandages were purchased from Massachusetts Institute of Technology Department of Comparative Medicine and RiteAid respectively. Poly(carboxymethyl – beta cyclodextrin) had a degree of substitution of 2.8 % and was purchased from CTD Inc (Gainesville , FL). Diclofenac was purchased from TCI America (Portland, Organ). Poly (sodium 4styrenesulfonate) (SPS, $M_n$ = 70,000), vancomycin hydrochloride, alginic acid sodium salt ($M_n$ = 120–190 kDa), HPLC grade solvents, and sodium acetate buffer (3 m, tissue culture grade) were purchased from Sigma Aldrich (St. Louis, MO). Silicon (test grade, *n* type) and glass substrates were obtained from Silicon Quest International (Santa Clara, CA) and VWR Scientific (Edison NJ), respectively. Linear polyethyleneimine (LPEI, $M_n$ = 25,000) and dextran sulfate sodium salt ($M_n$ = 500 kDa) were purchased from Polysciences, Inc (Warrington, PA). Chondroitin sulfate sodium salt was purchased from TCI International (Tokyo, Japan; $M_n$ estimated using water GPC to be approximately 85 kDa). Poly(*β*-amino ester), Poly A3, was synthesized as previously described. Deionized water (18.2 MΩ, Milli-Q Ultrapure Water System, Millipore) was used for washing steps during film construction and substrate preparation. Dulbecco's phosphate buffered saline (PBS, 10×) was purchased from Invitrogen (Carlsbad, CA). Cyclooxygenase fluorescent inhibitor screening assay kit was purchased from Cayman Chemicals (Ann Arbor, Michigan). *S. aureus* 25923 was purchased from ATCC (Manassas, VA). Cation-adjusted Mueller Hinton Broth (CaMHB) and Bacto agar were obtained from BD Biosciences (San Jose, CA). All agents were used as provided without further purification.

**Polyelectrolyte Multilayer Assembly:** Dip LbL films were constructed on 1.5 $cm^2$ silicon or glass substrates as previously described using a Carl Ziess HSM series programmable slide stainer.[7, 8, 17, 21] The silicon or glass substrates were plasma etched using a Harrick PDC-32G plasma cleaner on high RF power for 1 or 5 minutes, respectively, to generate a uniform, negatively charged surface prior to deposition. Immediately after etching, substrates were placed in linear polyethylenimine solution, the first deposition solution, to prevent contamination by materials in the air. All substrates were coated with ten bilayers of linear polyethylene imine and poly (styrene sulfonate) to ensure uniform adhesion of degradable layers to the surface. All polyelectrolyte solutions for degradable films were prepared at a concentration of 2 mg/mL, except polycarboxymethyl-betacyclodextrin (PolyCD) and polycarboxymethyl-betacyclodextrin-diclofenac solutions (PolyCD-diclofenac), which were composed of 20 mg/mL polycarboxymethylbetacyclodextrin and 1.4 mg/mL diclofenac for diclofenac containing assemblies.

Hydrolytically degradable multilayer films containing the antibiotic vancomycin (AB) were constructed in 0.1 M sodium acetate buffer at pH 5.1 using a tetralayer repeat architecture. The architecture of the film is denoted as: (poly A3/polyanion/vancomycin/polyanion)$_n$, where $n$ represents the number of deposited tetralayer repeats. After loading onto the robotic arm, the first deposition step was a 10 min submersion is Poly A3, followed by three deionized water rinse steps (10, 20, and 30 s each). For films containing dextran sulfate buffered pH 5.1 solution was used for all water rinse steps.The substrate was then submerged in the polyanion of choice for the particular architecture being constructed for 7.5 min, followed by three deionized

water rinse steps (10, 20, and 30 s each). After this, the substrate was submerged in a 10 min deposition step of vancomycin hydrochloride. This was followed by two deionized water rinse steps (20 and 30 s each). Following these three deposition steps, the second step sequence of polyanion dipping and rinsing was repeated. Together these four deposition steps complete one tetralayer of the film. For the purposes of this work, $n = 60$ was used for all architecture except films constructed on the intraocular lens which used n = 80. Three different polyanions were examined to form the following architectures: (Poly A3/Alginic acid/vancomycin/Alginic acid)$_{60}$, (Poly A3/Chondroitin sulfate/vancomycin/Chondroitin sulfate)$_{60}$, and (Poly A3/Dextran sulfate/vancomycin/Dextran sulfate)$_{60}$ .

Hydrolytically degradable anti-inflammatory films (AI) were constructed with a degradable polycation, Poly A3, and anionic polymeric cyclodextrin-drug conjugate, poly(carboxymethyl-betacyclodextrin)-diclofenac as previously described.[21-23] Anti-inflammatory films, containing poly(carboxymethyl-betacyclodextrin)-diclofenac conjugates, were assembled in 0.1 M sodium acetate buffer at pH 6. Anti-inflammatory films have a bilayer architecture and films were constructing by dipping into polycation solutions for 10 minutes and then washing with agitation for 10, 20, and 30 seconds in three different pH 6 water baths to remove all physically absorbed polymer. This process was repeated with the polyanion solution to form a bilayer. Poly(β-amino ester) solutions were changed every twelve hours. Twenty bilayers were formed and anti-inflammatory films are denoted as (Poly A3/ PolyCD-diclofenac)$_{20}$. Following deposition, the films were dried thoroughly under a stream of dry nitrogen.

Spray LbL films were constructed in a similar fashion as dip LbL assemblies, except misting was used instead of soaking in solution as previously described.[24] Misting times were 2 seconds for the polycations and polyanions. Instead of having three wash steps after each layer, a 5 second water mist was used. Chrondroitin sulfate was the only polyanion used in the spray LbL system.

Combination or joint films, films containing antibiotic and anti-inflammatory agents, had the following architectures: 1) $(LPEI/PSS)_{10}$(Poly A3/PolyCD-diclofenac)$_{20}$(Poly A3/Polyanion/Vancomycin/Polyanion)$_{60}$ 2) $(LPEI/PSS)_{10}$(Poly A3/Polyanion/Vancomycin/Polyanion)$_{60}$(Poly A3/PolyCD-diclofenac)$_{20}$ and 3) $(LPEI/PSS)_{10}$(Poly A3/Polyanion/Vancomycin/Polyanion)$_{80}$(Poly A3/PolyCD-diclofenac)$_{20}$. Joint films were constructed by building one film on top of the other using the protocols described above. For example (Poly A3/PolyCD-diclofenac)$_{20}$(Poly A3/Polyanion/Vancomycin/Polyanion)$_{60}$ films were constructed by building anti-inflammatory films as described and then building the degradable portion of the antibiotic film (i.e no LPEI/PSS layers) directly on top of the anti-inflammatory film. Combination films were assembled on hydrophobic acrylic intraocular lenses, bandage, and Vicryl degradable sutures. These materials were treated just like silicon and glass substrates. Bandage and sutures were plasma etched for one minute and spray LbL was used to construct $(LPEI/PSS)_{10}$(Poly A3/Chondroitin sulfate/Vancomycin/Chondroitin sulfate)$_{60}$(Poly A3/PolyCD-diclofenac)$_{20}$ films. Intraocular lenses were plasma etched for five minutes and dip LbL was used to construct $(LPEI/PSS)_{10}$(Poly A3/Dextran sulfate/Vancomycin/Dextran sulfate)$_{60}$ (Poly A3/PolyCD-diclofenac)$_{20}$ films.

**Quantification of Dual Drug Release:** Upon construction, films were dried under nitrogen and laid flat in a vial containing 500 µL of PBS at pH 7.4, completely submerging the film. These films were then incubated at 37 °C. At predetermined time points, the films were removed from the vial and placed into a fresh 500 µL aliquot of PBS. All release samples were stored at −20 °C until analysis. The amount of vancomycin and diclofenac release from films was analyzed by Agilent 1100 series high pressure liquid chromatography (HPLC) equipped with absorbance and fluorescence detectors. A Discovery ® C18 column and Discovery® C18 Supelguard™ Guard Cartridge with 5µm particle size were used for analysis. For vancomycin analysis, 500 uL sample injections were run with 70:30 phosphate buffer solution:methanol mobile phase at a flow rate of 1 mL/min. Samples were run for ten minutes and vancomycin eluted at six minutes. For diclofenac analysis, 100uL sample injections were run with 70:30 phosphate buffer solution:acetonitrile mobile phase at a flow rate of 1 mL/min. Samples were run for twenty minutes and vancomycin eluted at thirteen minutes. The fluorescence detector was set on excitation and emission wavelength of 280 nm and 355 nm respectively. Diclofenac and vancomycin calibration curves were constructed to determine the concentration of drug in the film eluent.

**Determination of System Interactions:** To determine if interdiffusion or exchange occurred during the assembly of combination films, single component films, containing diclofenac or vancomycin were placed in deposition buffers and solutions. For exchange experiments, antibiotic films were placed in polycd-diclofenac deposition solution, pH 5.1 deposition buffer solution, and pH 6 deposition buffer solution. Then films were rinsed with deionized water for one minute. The amount of vancomycin in

solution was analyzed with HPLC as described. Anti-inflammatory films were placed in vancomycin deposition solution, pH 5.1 deposition buffer, and pH 6 deposition buffer. The amount of diclofenac was quantified using HPLC anaylsis as described above. Interdiffusion experiments were conducted by placing antibiotic and anti-inflammatory films in diclofenac or vancomycin deposition solution respectively for ten minutes. PolyCD films, $(\text{Poly A3/PolyCD})_{20}$, were also placed in vancomycin deposition solution for ten minutes. Films were then rinsed in deionized water for one minute. The films contents were completely released in PBS at 37°C and the concentration of vancomycin or diclofenac was determined as described.

To determine the interaction of polycd with vancomycin changes in the optical and chromatographic properties were analyzed. To test for changes in absorbance, 60 ug/mL vancomycin deposition solution were mixed with 0, 4, 8, 12, 16, and 20 mM polycd deposition solution. These samples were run on a Varian UV-vis spectrophotometer. Spectra were obtained from 200 – 800 nm. Chromatographic analysis was performed by running the same solutions on the HPLC with the vancomycin analysis protocol. An absorbance detector was used to detect absorbance of peaks with a retention time of four minutes at 280 nm. Changes in peak intensity and retention time were noted. To examine diclofenac-vancomycin interactions, solubility changes in vancomycin solution were investigated. Vancomycin at 2 ug/mL and 2 mg/mL in pH 5.1 and pH 6 deposition buffer were used to dissolved a large excess of diclofenac ( 5-10 mg/mL). Diclofenac solubility in pH 5.1 and pH 6 deposition buffer are 20 ug/mL and 200 ug/mL respectively. After vortexing for five minutes, solutions were syringe filtered and run on the HPLC. Diclofenac analysis method was used. The

fluorescence peak intensity of vancomycin and diclofenac were compared at four and thirteen minutes, respectively, and compared to the controls that contained no vancomycin.

**Bacterial Assays:** The antibacterial activity of combination films was investigated using S. aureus 25923. This particular strain was selected based on the recommendations of the Clinical and Laboratory Standards Institute.[25] Antibacterial activity was examined using a Kirby Bauer analysis and a modified macrodilution assay, similar to a technique reported by the Clinical and Laboratory Standards Institute.[25] For the macrodilution assay combination films were soaked in 0.5 mL of PBS for duration long enough to release the entire contents of the film; film release was monitored using HPLC as described earlier. A serial dilution of release solution as well as a control solution of vancomycin dissolved in PBS (after passing solutions through 0.2 mm sterile filters) with CaMHB was performed, to make a total of 8 dilutions of the vancomycin solutions in a 96-well polystyrene tissue culture plate.

S. aureus in its exponential growth phase (3–4 h following inoculation) was added to each of these dilutions at a final concentration of $10^5$ CFU/mL. The bacteria concentration was assessed with optical density measurements at 600 nm using an HP Agilent UV–Vis Spectrophotometer. Negative controls used PBS with vancomycin and serial dilution in CaMHB with no final bacterial challenge. Positive controls were made similarly with bacterial challenge. All measurements were made in triplicate. The 96-well plates containing the test samples, negative, and positive controls were incubated at 37 °C with gentle agitation for 16–18 h. Following this, a Biotek PowerWave XPS plate reader was used to monitor the optical density of the wells at 600 nm, corresponding

directly to the cell density. A normalized bacteria density was computed for all test samples with the appropriate negative and positive controls using the following equation:

$$Normalized\ Bacteria\ Density = \frac{(OD_{600,sample\ avg} - OD_{600,negative\ control\ avg}}{OD_{600,positive\ control\ avg} - OD_{600,negative\ control\ avg}}$$

Kirby–Bauer bacterial inhibition was also assessed using an agar plate assay following the protocol described by the Clinical and Laboratory Standards Institute [40]. Agar plates were made from CaMHB and Bacto agar. S. aureus in the exponential growth phase at a concentration of 108 CFU/mL was evenly applied over the agar surface. Devices coated with combination films were placed face down on top of the bacteria coated agar. Negative controls of clean substrates with no film coating were also placed on the agar. Positive controls were 30 ug vancomycin tablets and were placed on the agar. These plates were incubated for 16–18 h at 37°C. All films were examined for reduction in bacterial growth as compared to the positive and negative controls.

**Cyclooxygenase Inhibition Assay:** The cyclooxygenase fluorescent inhibitor screening assay was used to confirm drug activity after cyclodextrin complexation and release from hydrolytically degradable LbL films as previously described. The kit was purchased from Cayman Chemicals and used as directed. Briefly, the assay capitalizes on the peroxidase activity of cyclooxygenase and the reaction between hydroperoxy endoperoxide ($PGG_2$) and 10 – acetyl – 3,7 – dihydroxyphenoxazine (ADHP), which produces resorufin, a highly fluorescent molecule. Resorufin can be easily quantified by exciting between 530 – 540nm and collecting emission between 585 – 595 nm. The

activity of polycd, polycd-diclofenca, and vancomycin was assessed along with release samples.

## Results and Discussion

### Characterization of Release Dynamics

Combination films were composed of two previously described hydrolytically degradable layer-by-layer systems able to address infection or inflammation. The antibiotic component of this system was selected due to high loading and flexible release of vancomycin, a potent FDA approved broad spectrum antibiotic.[17] Ideal release kinetics for antibiotics include initial burst with a small taper of antibiotic above the minimum inhibitory concentration. Antibiotic films were shown to release 20-100 ug of vancomycin over 8 – 60 hours depending on the polyanion used in assembly. Vancomycin is used for the treatment of serious gram positive bacteria infections. It is highly effective against Staph Aureus, one of the most common device associated infectious agents, and is routinely used in clinical settings.[2] These hydrolytically degradable antibiotic multilayer films were composed of Poly A3, a cationic poly(β-amino ester), biologival polyanion, and vancomycin in a tetralayer fashion. The polyanion used in assembly were alginic acid, a natural polysaccharide, chondroitin sulfate, a glycosaminoglycan found in the extracellular matrix, and dextran sulfate, a natural polysaccharide. Tetralayers are used when both the degradable polymer and the therapeutic are the same charge. An oppositely charged spacer molecule is incorporated between the degradable polymer and the therapeutic with the same charge therapeutic. An exploded view of the tetralayer architecture used for antibiotic film assembly with the chemical structure of film components can be seen in figure 5.1

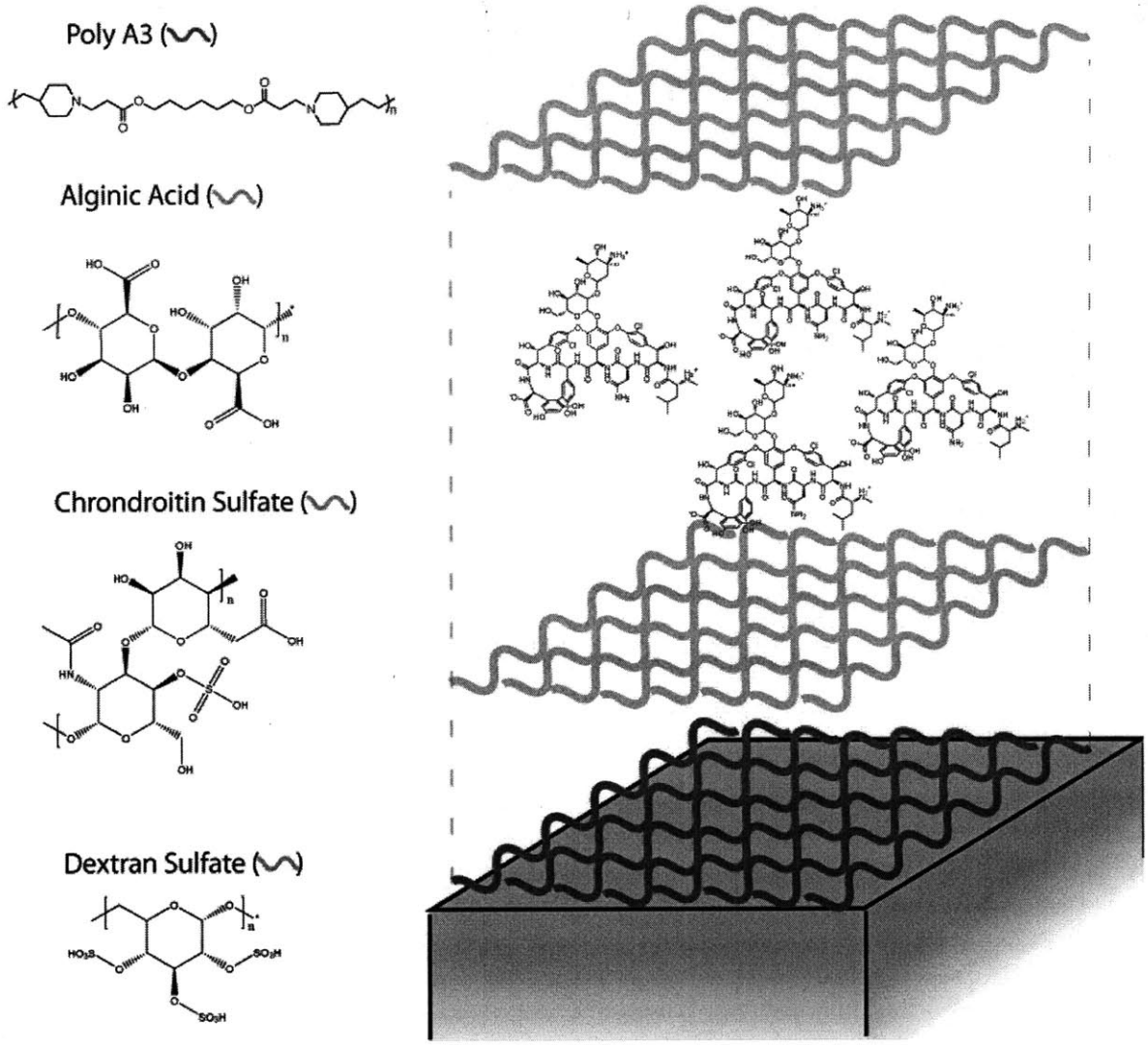


**Figure 5.1 Exploded view of repeat unit used in the construction of antibiotic films with chemical structures.**

The schematic is an exploded view of the tetralayer repeat unit of antibiotic films and the chemical structures of the film components. The antibiotic portion of combination films were constructed with a tetralayer repeat unit and had the following architecture: (Poly A3/Polyanion/Vancomycin/Polyanion)$_n$ where n equals 60 or 80. The polyanion used in assembly were alginic acid, chondroitin sulfate, and dextran sulfate and are represented by the orange (light) line. Poly A3 was used as the degradable poly(β-amino ester) and is represented by the blue (dark) lines. The structure of vancomycin is shown in the schematic.

The anti-inflammatory component was described in chapter four and utilized for its *in vitro* efficacy and programmable release kinetics.[8] Diclofenac, a potent nonsteroidal anti-inflammatory drug, was chosen as the anti-inflammatory agent due to its use in a range of clinical scenarios including orthopedic and ophthalmologic applications. The hydrolytically degradable anti-inflammatory multilayer films were composed of Poly A3 and polycarboxymethyl-betacyclodextrin-diclofenac conjugates (polycd-diclofenac) as the polyanion. Multi-agent films were constructed with two architectures, antibiotic containing films (AB) layered on top and underneath anti-inflammatory films (AI) to form AI/AB and AB/AI films respectively. A schematic of the film architecture utilized can be seen in figure 5.2. The antibiotic component are abbreviated, AB, where AB is $(PolyA3/polyanion/vancomycin/polyanion)_{60}$. Unless otherwise noted the polyanion used in assembly is chondroitin sulfate. Anti-inflammatory films are abbreviated, AI, where AI is $(Poly\ A3/PolyCD\text{-}diclofenac)_{20}$. Antibiotic and anti-inflammatory films were combined to allow for the simultaneous control of inflammatory and infectious pathways. However concurrent drug delivery and thus simultaneous control of pathological processes is only possible if AI and AB films interact when layered together.

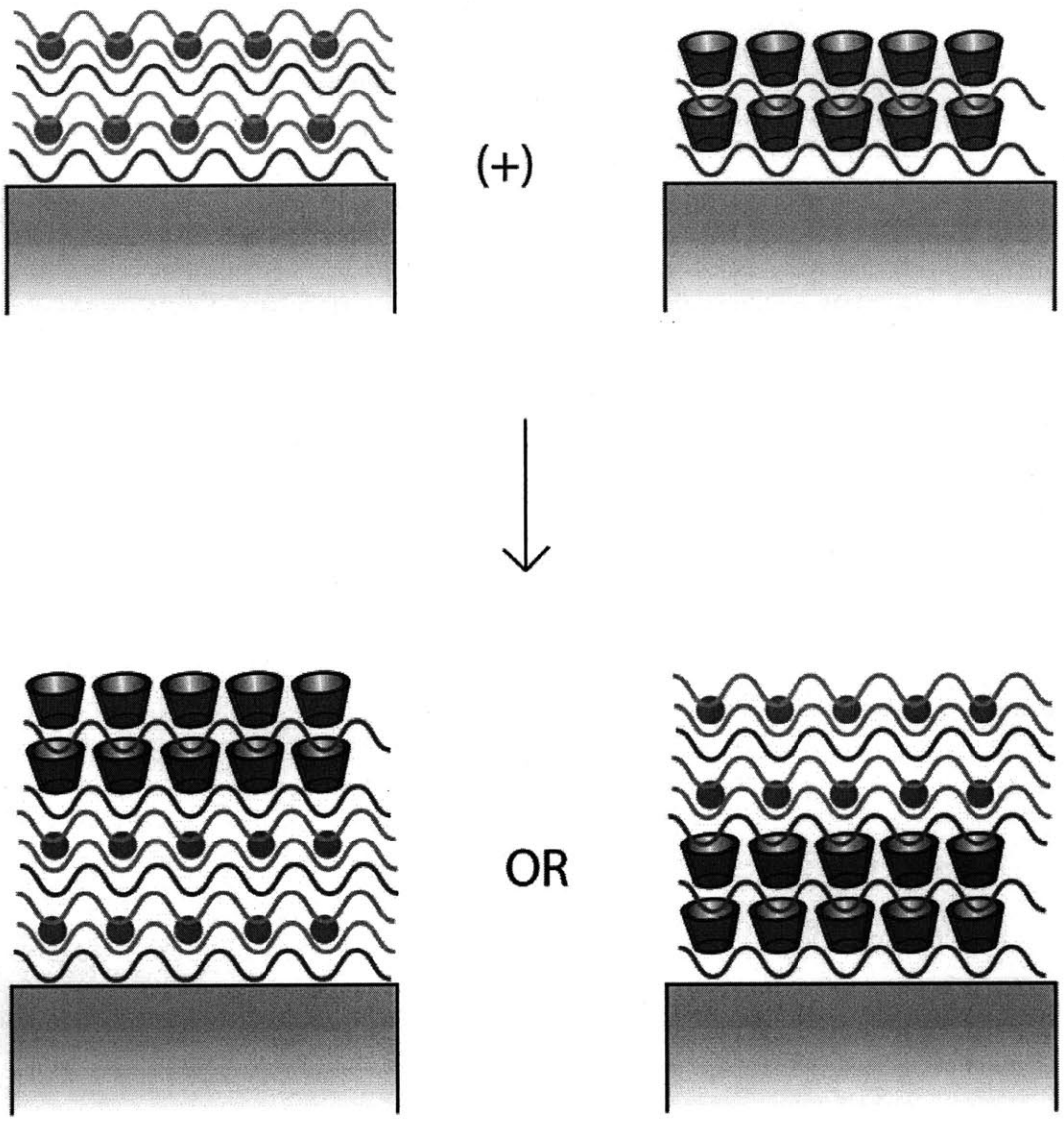


**Figure 5.2 Architecture of multi-agent films**

Schematic of the combination film architectures. In the schematic, blue (dark) lines represents poly(β-amino ester), orange (light) lines represents alginic acid, chrondroitin sulfate, or dextran sulfate, and the green balls represent vancomycin. The red cups represent polycd-diclofenac conjugates. Single component antibiotic films can be seen in the top left and single component anti-inflammatory films can be seen on the top right. Antibiotic and anti-inflammatory films were combined in two ways: 1) anti-inflammatory film layered on top on antibiotic film, seen on the bottom left and 2) antibiotic film layered on top of anti-inflammatory film, seen on the bottom right.

When LbL delivery systems with different components and architectures are combined, release dynamics are dictated by the presence or absence of interactions between the systems. Interactions can occur as one system is being built on the other system, and include interdiffusion, exchange, and pH effects amongst others.[16] Interdiffusion is the diffusion of materials into the film system and is commonly observed in LbL assembly. Exchange is the replacement of a film component by a component in the deposition solution. Exchange has been extensively documented in LbL films and is driven by thermodynamics to form more stable complexes; pH, salt concentration, and energy of complexation influence the exchange process.[16] The effects of pH are well known in polyelectrolyte multilayer films and can cause film dissolution as well as morphological and mechanical changes. In hydrolytically degradable films, systems that do not interact will definitely have release kinetics independent of each other. However systems that interact will have release properties dictated by the nature of the interactions. Sequential delivery is obtained for systems without interactions and release mediated by surface erosion for both components. To effectively address infection and inflammation co-delivery is required. Co-release is achieved when systems interact or release is mediated through diffusion. To determine if combination films could be used for concurrent release of therapeutics, joint antibiotic and anti-inflammatory films with chondroitin sulfate as the polyanion were constructed; the release profiles can be seen in figure 5.3

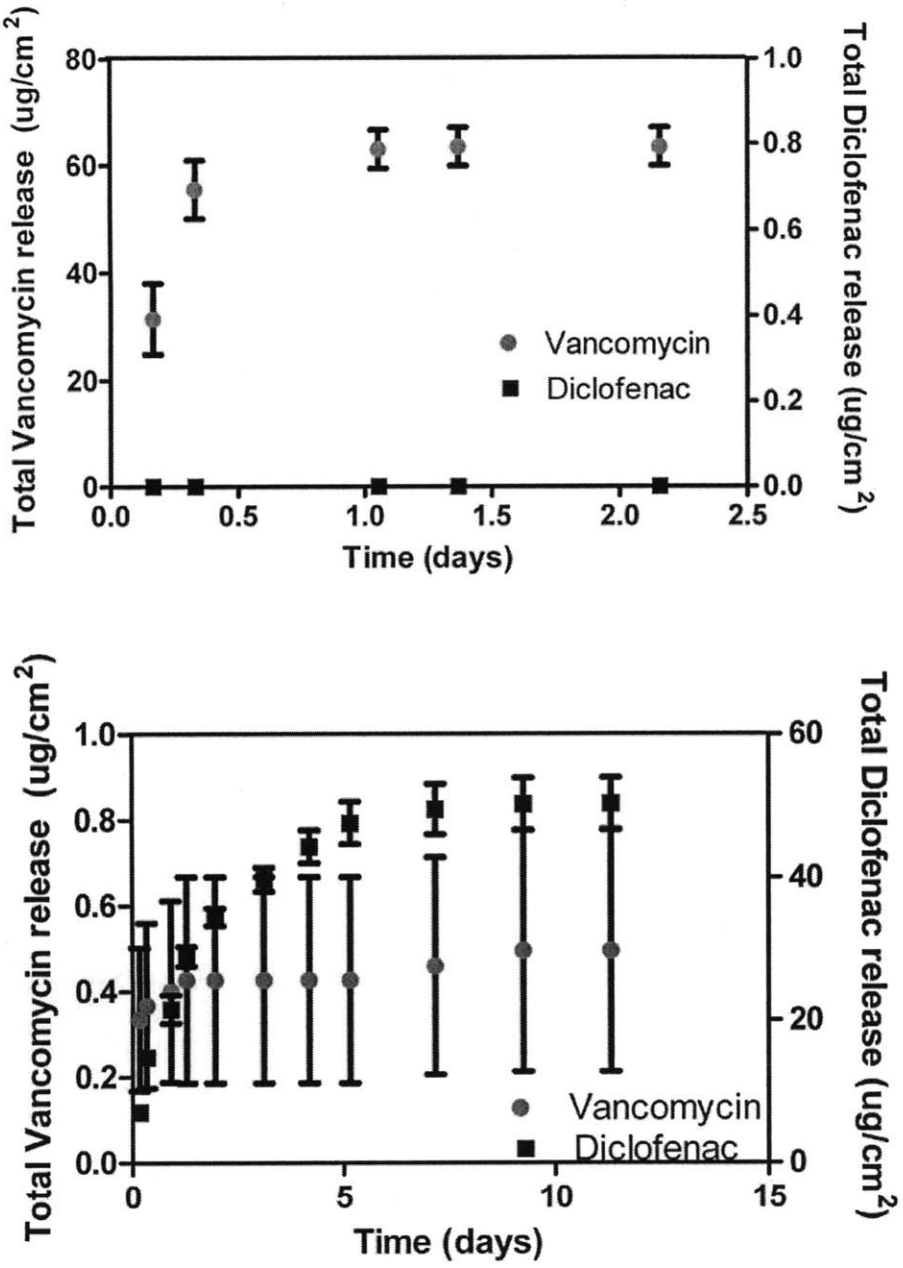


**Figure 5.3 Release of combination films containing chondroitin sulfate as the polyanion.**

The top graph depicts the total amount of vancomycin and diclofenac released from (Poly A3/ PolyCD-diclofenac)$_{20}$(Poly A3/Chondroitin sulfate/Vancomycin/Chondroitin sulfate)$_{60}$ films. No diclofenac was present in this construct. The bottom graph shows the release of (Poly A3/Chondroitin sulfate/Vancomycin/Chondroitin sulfate)$_{60}$(Poly A3/ PolyCD-diclofenac)$_{20}$ films. Release experiments were carried out at 37°C in PBS.

Antibiotic films containing chondroitin sulfate typically release 107 ± 0.2 ug over 2.1 days, while anti-inflammatory films typically release 5 ± 1 ug of diclofenac over 17 days. Drug release for AB/AI and AI/AB films were different than the single component films. AI/AB films released 63 ± 3 ug of vancomycin for 1.4 days, but contained no diclofenac. AB/AI films released 0.5 ug ± 0.3 ug of vancomycin over nine days and 50 ± 4 ug of diclofenac for nine days. In AB/AI architecture the total amount of diclofenac increased by 900% but release duration was reduced by more than a week. Vancomycin release duration increased by seven days but the total drug amount decreased by 99%. In AI/AB films the total amount of vancomycin is decreased 41% and no diclofenac was present within the films. In both systems, most of the vancomycin release occured over the first day. This is ideal because the first six hours post implantation is the decisive period for prevention of infection and the formation of biofilms.[2] Longer release of antibiotic is often discouraged due to the possible formation of multi-drug resistant bacteria. In addition, while the MIC of vancomycin for Staph. aureus is between 0.5 - 1 ug/mL, certain implant sites have low aqueous volumes, such as the anterior and posterior ocular chamber with 60 uL and 250 uL respectively, where vancomycin release would be above the MIC for several days.[26] The release profiles of AI/AB and AB/AI films indicate that the anti-inflammatory and antibiotic systems interact and enable concurrent release. The interactions between anti-inflammatory and antibiotic systems dictate key release dynamics including dosage and release duration. In order to construct superior drug delivery coatings, the nature of these interactions must be elucidated.

**System Interactions Dictate Release**

To uncover interactions between antibiotic and anti-inflammatory thin film systems, an established antibiotic or anti-inflammatory film was placed in a deposition solution used to assemble the anti-inflammatory or antibiotic systems respectively. Interdiffusion, exchange, and pH effects were investigated. Interdiffusion, the ability of components to diffuse and absorb within the film bulk, is a common phenomenon in multilayer assemblies.[16] To ascertain if interdiffusion occurs when the antibiotic and anti-inflammatory systems are combined, single component films were placed in a deposition solutions for 10 minutes (the deposition time necessary for layer deposition), washed to remove nonspecifically bound drug, and the amount of the drug absorbed within the film quantified. The experimental design and amount absorbed can be seen in figure 5.4. Antibiotic films were assembled from materials dissolved in 0.1 M sodium acetate buffer at pH 5. All deposition solutions for antibiotic films were at these conditions. Similarly, anti-inflammatory films were assembled from materials dissolved in 0.1 M sodium acetate buffer at pH 6. All deposition solutions for anti-inflammatory films were at these conditions. Buffer solution refers to 0.1 M sodium acetate at pH 5 or pH 6.

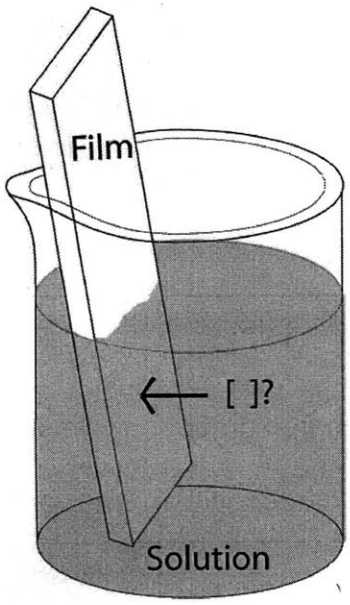


| Film | Deposition Solution | Vancomycin (ug) | Diclofenac (ug) |
|---|---|---|---|
| Diclofenac | Vancomycin | 5 ± 3 | - |
| PolyCD | Vancomycin | 13 ± 6 | - |
| Vancomycin | PolyCD-Diclofenac | - | 28 ± 10 |

**Figure 5.4 Interdiffusion of species into antibiotic or anti-inflammatory films**

The schematic is an illustration of the experimental design of interdiffusion studies. The ability of deposition components to absorb into single component films was examined. Vancomycin deposition solution contained 2 mg/mL of vancomycin in 0.1 M sodium acetate pH 5 buffer. PolyCD - diclofenac and polycd deposition solutions contained 1.4 mg/mL diclofenac and/or 20mg/mL polycd dissolved in 0.1 M sodium acetate pH 6 buffer respectively. Antibiotic, anti-inflammatory, or PolyCD films were placed in a deposition solution. The amount of drug, absorbed was measured via HPLC. The table shows the amount of drug absorbed. Diclofenac refers to films composed on polycd-diclofenac.

The antibiotic film was placed in polycd-diclofenac deposition solution and found to absorb 28 ± 10 ug of diclofenac. This most likely explains the large increase in diclofenac when anti-inflammatory films are assembled on top of antibiotic films. Anti-inflammatory films with and without diclofenac were placed in vancomycin deposition solution. Vancomycin was absorbed within anti-inflammatory films at 5 ± 3 ug and 13 ± 6 ug for films with and without diclofenac respectively. The increase of vancomycin in

films without diclofenac suggests that vancomycin and polycd interact via secondary interactions in a way that is inhibited by the complexation of diclofenac with polycd. To explore the influence of time on interdiffusion the amount of vancomycin absorbed in PolyCD was examined after three and 24 hours. There was no significant difference the amount of vancomycin absorbed in ten minutes, three hours, and 24 hours.

Exchange experiments were performed by placing the single component films in deposition solutions for ten minutes, which is the standard layer deposition time, and then rinsing with water to remove nonspecifically bound material. The amount of drug released from the single component films into the deposition solution was measured. Antibiotic films were placed in pH 5, pH 6, polycd, and polycd-diclofenac solutions at deposition conditions. The amount of vancomycin released in the different solutions along with a schematic of the exchange experiment can be seen in figure 5.5

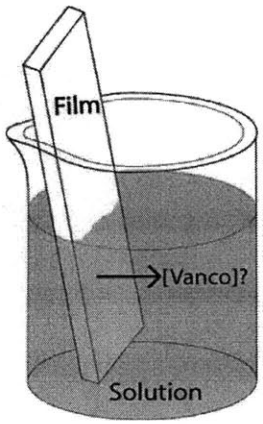


| Deposition Solution | Vancomycin (ug) |
|---|---|
| pH 5 | 0 |
| pH 6 | 11 ± 3 |
| PolyCD | 8 ± 1 |
| PolyCD-Diclofenac | 4 ± 1 |

**Figure 5.5 Exchange in antibiotic films**

The schematic is an illustration of the experimental design of exchange studies with antibiotic films. Antibiotic films were placed in 0.1 M sodium acetate pH 5 and pH 6 buffers and polycd, polycd-diclofenac deposition solutions, which were made with 0.1 M sodium acetate pH 6 buffer. The amount of vancomycin released from the film was measured via HPLC. The table shows the amount of vancomycin released.

Since antibiotic and anti-inflammatory components are assembled at different pHs, the effect of changing the pH alone was observed by placing films in the 0.1 M sodium acetate pH 5 and pH 6 buffers used to form deposition solutions. Antibiotic films are assembled at pH 5 in 0.1 M sodium acetate buffer whereas anti-inflammatory films were constructed at pH 6 in 0.1 M sodium acetate buffer. Vancomycin has one net positive charge at pH 5, two positive charges and one negative charge, and an isoelectric point at pH 7.2. Thus at pH 6 vancomycin is closer to its isoelectric point. Antibiotic films were stable at pH 5, but 11 ± 3 ug of vancomycin, which corresponds to 10% of total loading, was released at pH 6. In polycd and polycd-diclofenac deposition solutions 8 ± 1 ug and 4 ± 1 ug of vancomycin were released respectively; this corresponds to 8% and 4% of total loading respectively. The amount of vancomycin released was greatest in plain pH 6 buffer and least in polycd-diclofenac deposition solution. If it is assumed that 4 ± 1 ug is lost at each deposition step in polycd-diclofenac solution, 86 ± 14 ug would be removed from the antibiotic film. This is close to the 106 ug that is actually lost. Drug loss in the Poly A3 deposition solution and the pH 6 buffered wash solutions more than accounts for the small discrepancy. The release of vancomycin in pH 6 buffer might be due to the low charge density of vancomycin and changes in its ionization.

A similar experiment was performed with anti-inflammatory films and the results plus experimental design can be seen in figure 5.6. Anti-inflammatory films were placed in 0.1 M sodium acetate pH 5 and pH 6 buffers as well as vancomycin deposition solution. The amount of diclofenac in solution was measured. Anti – inflammatory films were stable in pH 5 and pH 6 buffers. Since diclofenac is complexed with a polymeric

anionic carrier, small changes in pH should not drastically disrupt film assembly. Interestingly, the vancomycin solution soak resulted in a loss of 4.1 ± 0.7ug of diclofenac, which was the total amount of diclofenac in the film. This suggests a driving force for diclofenac release into vancomycin solution and explains the absence of diclofenac in assemblies with the anti-inflammatory system on the bottom.

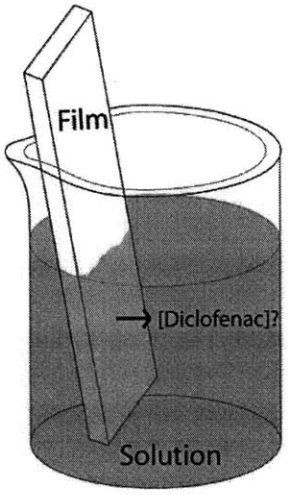


| Deposition Solution | Diclofenac (ug) |
|---|---|
| pH 5 | 0 |
| pH 6 | 0 |
| Vancomycin | 4 ± 1 |

**Figure 5.6 Exchange in anti-inflammatory films**

The schematic is an illustration of the experimental design of exchange studies with anti-inflammatory films. Anti-inflammatory films were placed in pH 5, pH 6, vancomycin deposition solutions. The amount of diclofenac released from the film was measured via HPLC. The table shows the amount of diclofenac released. In the table pH 5 and pH 6 refer to 0.1 M sodium acetate buffers at pH 5 and pH 6 respectively. Vancomycin deposition solution contains 2 mg/mL vancomycin dissolved in the pH 5 buffer.

By examining interdiffusion, exchange, and pH stability, it's possible to get a picture of the combination system dynamics. Antibiotic films are destabilized in 0.1 M sodium acetate pH 6 buffer and large amounts of vancomycin and chondroitin sulfate

are lost from the film, while large amounts of polycd-diclofenac are absorbed. This is consistent with film height measurements that indicate 75 % of the original antibiotic film thickness is lost with anti-inflammatory film construction on top of antibiotic films. It is possible that the negatively charged polycd-diclofenac is absorbed to maintain charge neutrality or the interaction between polycd and vancomycin acts as a driving force for polycd-diclofenac incorporation. However, polyCD and polycd-diclofenac reduce the destabilizing effect of pH 6 on antibiotic films implying a favorable complexation. On the other hand vancomycin deposition solution causes the rapid elution of diclofenac from anti-inflammatory films. Taken together, these results suggest an interaction between vancomycin-polycd and vancomycin-diclofenac. To validate the existence of these interactions, vancomycin-polycd and vancomycin-diclofenac interactions were recapitulated, outside of the thin film system, in solution.

The interaction between chemical compounds is often investigated through optical and chromatographic techniques.[27] Cyclodextrins are specifically known to alter the absorbance and fluorescence of complexed molecules.[28] In addition, cyclodextrins are known to change the retention time of complexed molecules. To confirm the interaction between vancomycin and polycd, the change in abosorbance and retention time of vancomycin at varying cyclodextrin concentrations was examined and can be seen in figure 5.7.

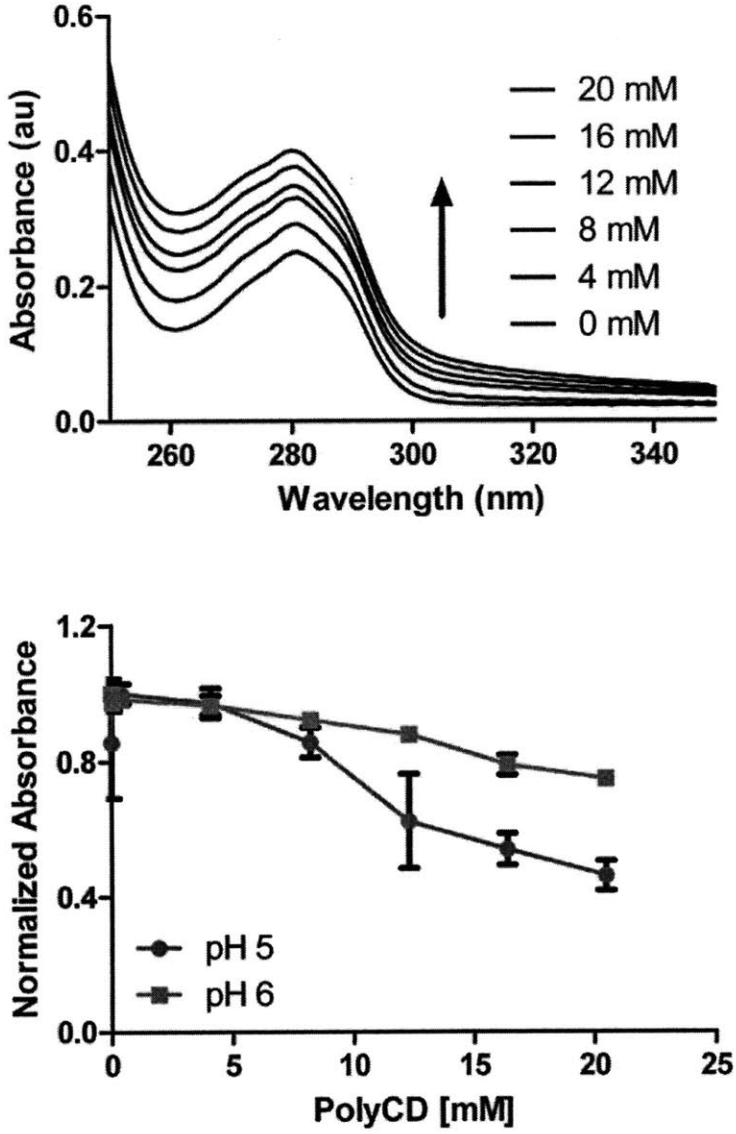


**Figure 5.7 Interaction of vancomycin and polycd**

The interaction between vancomycin and polycd is illustrated by showing the change in absorbance of vancomycin. The top image is the UV spectra of 60 ug/mL of vancomycin mixed with 0, 4, 8, 12, 16, and 20 mM polycd solution at pH 6. The bottom graph shows the change in normalized HPLC absorbance peak height of vancomycin with increasing concentrations of polycd at pH 5 and 6 solution. Absorbance changes are a function of changes in retention time. Absorbance was normalized by dividing the absorbance of all samples by the absorbance of solutions containing 60 ug/mL vancomycin and no polycd.

Figure 5.7 shows that the intensity of a constant concentration of vancomycin increases with cyclodextrin. The bottom figure shows the decrease in vancomycin absorbance peak height at retention time of four minutes due to formation of another peak and change in retention time. The effect was observed at pH 5 and pH 6. The interaction was more pronounced at pH 5, but still existed to some extent at pH 6. Therefore when an anti-inflammatory film is placed in vancomycin deposition solution, it can be expected that vancomycin-polycd interaction might lead to absorption of vancomycin within the film. Previous research has shown interaction between vancomycin and cyclodextrins.[29, 30] Studies focused on using beta and gamma cyclodextrins as carriers for vancomycin for drug delivery applications. However, the nature of the interaction between vancomycin and the cyclodextrin were not elucidated. To determine if the interaction between polycd and vancomycin was purely electrostatic, salt was added to solutions containing vancomycin – polycd complexes. If the interactions are purely electrostatic, increasing the salt concentration should shield ions and disrupt ionic interactions between vancomycin and polycd. Sodium acetate concentration was increased from 0.1 M to 3 M and no change in vancomycin – polycd complexation as monitored via HPLC was observed.

Vancomycin deposition solution completely stripped diclofenac from anti-inflammatory films. Diclofenac has low water solubility in 0.1 M sodium acetate pH 5 buffer and interacts strongly with the cyclodextrins. Vancomycin must be able to disrupt cyclodextrin-diclofenac interacts and enhance the solubility of diclofenac. To confirm this interaction, vancomycin solution at different concentrations and pHs were mixed

with a large excess of diclofenac. The solution was filtered and the amount of diclofenac in solution was determined. Table 5.1 shows the result.

| Solution pH | Vancomycin (ug/mL) | Normalized Absorbance |
|---|---|---|
| 5 | 2 | 1.8 ± 0.1 |
| 5 | 2000 | 13.1 ± 3.1 |
| 6 | 2 | 1 ± 0.004 |
| 6 | 2000 | 1.2 ± 0.2 |

**Table 5.1 Solubility of diclofenac in vancomycin solution**

The normalized HPLC peak absorbance of diclofenac in vancomycin solution. Vancomycin solutions were mixed with a large excess of diclofenac. The filtered solution was run on HPLC to determine the relative amount of diclofenac in vancomycin solution compared to deposition buffer.

Vancomycin at deposition conditions, 2mg/mL in 0.1M sodium acetate pH 5, had a 13 times higher equilibrium diclofenac concentrations than deposition buffer alone. Vancomycin deposition solution, thus, greatly enhances diclofenac solubility. Smaller concentrations of vancomycin also increased solubility, slightly. Vancomycin at pH 6 had a much smaller effect up to only 1.8 times, however diclofenac is naturally more soluble at pH 6. The interaction of vancomycin and diclofenac at concentrations were diclofenac is soluble could not isolated. Vancomycin is commonly used as a chiral selector in chromatography and known to interact strongly with small organic molecules.

**Control of System Interactions**

Control of system interactions will allow for the advanced engineering of release profiles. Two key phenomena must be controlled, the destabilization of antibiotic films in pH 6 buffer and the solubilization of diclofenac by vancomycin. Anti-inflammatory films were previously shown to not assembly as well at pH 5; thus anti-inflammatory films could not be assembled at pH 5. However, the release dynamics of vancomycin films are known to vary based on polyanion choice, due to secondary interactions. In fact, dextran sulfate was shown to interact so strongly with vancomycin that it significantly alters the retention time of vancomycin by several minutes in HPLC analysis.[17] The interaction between vancomycin and the various polyanions used in thin film assembly may act to stabilize the antibiotic film in pH 6 buffer. The release of AB/AI and AI/AB films with alginic acid and dextran sulfate as the polyanion was investigated. The release curves can be seen in figure 5.8 and figure 5.9.

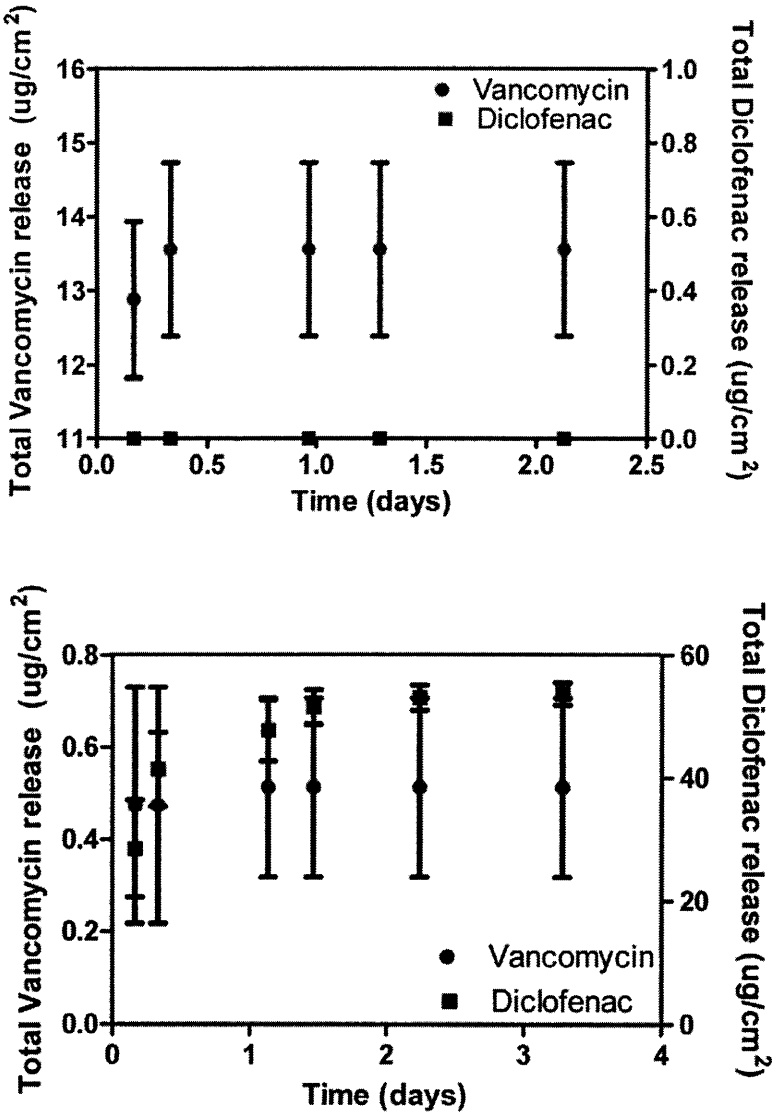


**Figure 5.8 Release of anti-inflammatory and antibiotic films with alginic acid as the polyanion**

The top graph depicts the total amount of vancomycin and diclofenac released from (Poly A3/ PolyCD-diclofenac)$_{20}$(Poly A3/Alginic acid/Vancomycin/Alginic acid)$_{60}$ films. Note the range for total vancomycin is from 11 - 16 ug/cm$^2$. The bottom graph shows the release of (Poly A3/Alginic acid/Vancomycin/Alginic acid)$_{60}$(Poly A3/ PolyCD-diclofenac)$_{20}$ films. Release experiments were carried out at 37°C in PBS.

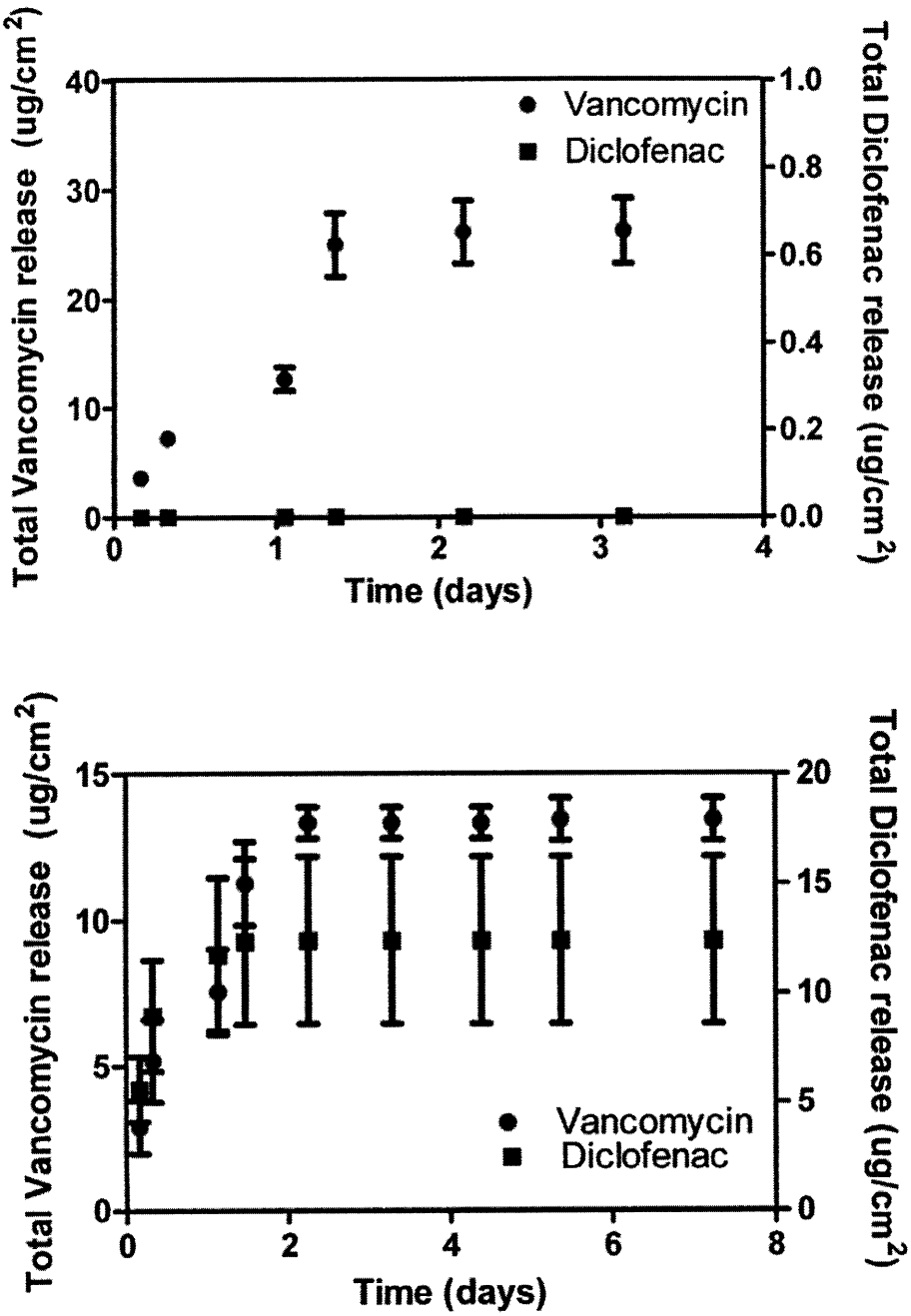


**Figure 5.9 Release of anti-inflammatory and antibiotic films with dextran sulfate as the polyanion**

The top graph depicts the total amount of vancomycin and diclofenac released from (Poly A3/ PolyCD-diclofenac)$_{20}$(Poly A3/Dextran sulfate/Vancomycin/Dextran sulfate)$_{60}$ films. The bottom graph shows the release of (Poly A3/Dextran sulfate/Vancomycin/Dextran sulfate)$_{60}$(Poly A3/ PolyCD-diclofenac)$_{20}$ films. Release experiments were carried out at 37°C in PBS.

Antibiotic films containing alginic acid typically release 90 ± 0.3 ug over eight hours, while dextran sulfate based films release 22 ug over 2.5 days. AB/Al films containing alginic acid had very similar release characteristics as films containing chondroitin sulfate. Vancomycin release occurred over one day and 0.5 ± 0.2 ug was released. Combination films containing dextran sulfate released more than half of its normal amount of dextran sulfate over five days, longer than the usual 2.5 days. Dextran sulfate containing films were thus more stable in pH 6 buffer. For this system diclofenac release was shortened to two days but the dosage was increased to 12 ug. Nevertheless diclofenac solubilization was not affected by polyanion choice as expected. A summary of the effect of counter polyanion can be seen in table 5.2

| Film | Polyanion | Vancomycin (ug) | Time (days) | Diclofenac (ug) | Time (days) |
|---|---|---|---|---|---|
| AB | Alginate | 90 ± 0.3 | 0.3 | - | - |
| AB | Chondroitin | 107 ± 0.2 | 2.1 | - | - |
| AB | Dextran | 22 ± 2.2 | 2.2 | - | - |
| Al | - | - | - | 5 ± 1 | 20 |
| Al/AB | Alginate | 14 ± 1 | 0.3 | 0 | - |
| Al/AB | Chondroitin | 63 ± 3 | 1.4 | 0 | - |
| Al/AB | Dextran | 26 ± 3 | 3 | 0 | - |
| AB/Al | Alginate | 0.5 ± 0.2 | 1 | 54 ± 2 | 7 |
| AB/Al | Chondroitin | 0.5 ± 0.3 | 9 | 50 ± 4 | 9 |
| AB/Al | Dextran | 13 ± 0.7 | 5 | 12 ± 4 | 2 |

**Table 5.2 Comparison of the release dynamics of combination films with different polyanions as well as single component films**

The table offers a comprehensive comparison of the release duration and dosage of (Poly A3/Alginic acid /Vancomycin/Alginic acid)$_{60}$, (Poly A3/chondroitin sulfate/Vancomycin/chondroitin sulfate)$_{60}$, (Poly A3/dextran sulfate/Vancomycin/dextran sulfate)$_{60}$, (Poly A3/ PolyCD-diclofenac)$_{20}$, (Poly A3/ PolyCD-diclofenac)$_{20}$ (Poly A3/alginic acid/Vancomycin/alginic acid)$_{60}$, (Poly A3/ PolyCD-diclofenac)$_{20}$ (Poly A3/chondroitin sulfate/Vancomycin/chondroitin sulfate)$_{60}$, (Poly A3/ PolyCD-diclofenac)$_{20}$ (Poly A3/dextran sulfate/Vancomycin/dextran sulfate)$_{60}$, (Poly A3/alginic acid/Vancomycin/alginic acid)$_{60}$(Poly A3/ PolyCD-diclofenac)$_{20}$, (Poly A3/chondroitin sulfate/Vancomycin/chondroitin sulfate)$_{60}$(Poly A3/ PolyCD-diclofenac)$_{20}$, and (Poly A3/dextran sulfate/Vancomycin/dextran sulfate)$_{60}$(Poly A3/ PolyCD-diclofenac)$_{20}$ films at 37°C. Alginate, chondroitin, and dextran stand for alginic acid, chondroitin sulfate, and dextran sulfate respectively.

To prevent vancomycin from solubilizing diclofenac, the ability of vancomycin to interact with diclofenac must be limited. Since interactions occur with soaking in deposition solution, using a non-soak based deposition method may prevent the interaction. Spray LbL uses misting instead of dipping to create polyelectrolyte multilayers films.[31-33] Spray LbL has been observed to change film structure and release dynamics. For example, the release duration of antibiotic films containing chondroitin sulfate as the polyanion went from 50 to 8 hours using dip and spray LbL respectively.[17] Spray LbL was used to construct combination films and the release can be seen in figure 5.10.

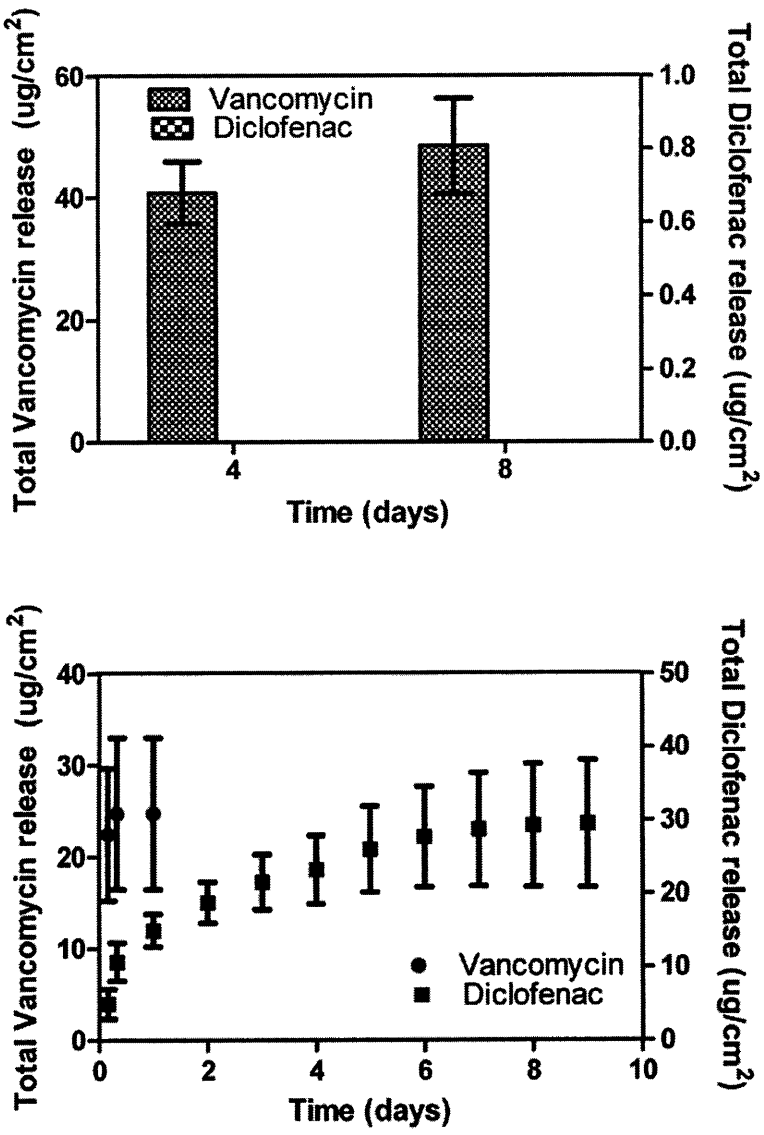


**Figure 5.10 Release dynamics of combination films with chondroitin as the polyanion fabricated with spray LbL.**

The top graph depicts the total amount of vancomycin and diclofenac released from (Poly A3/ PolyCD-diclofenac)$_{20}$(Poly A3/Chondroitin sulfate/Vancomycin/Chondroitin sulfate)$_{60}$ films. No diclofenac was in this system.The bottom graph shows the release of (Poly A3/Chondroitin sulfate/Vancomycin/Chondroitin sulfate)$_{60}$(Poly A3/ PolyCD-diclofenac)$_{20}$ films. Release experiments were carried out at 37°C in PBS. Films were fabricated using spray layer-by-layer assembly.

Spray LbL was unable to prevent the interaction between vancomycin and diclofenac. No diclofenac remained in the AI/AB films. However, spray LbL did prevent the destabilization of antibiotic films at pH 6. AB/AI films released 25 ± 8 ug of vancomycin over eight hours and 30 ± 9 ug of dicofenac over 9 days. Both spray LbL and polyanion choice were able to prevent destabilization of antibiotic films and create LbL films that had the same architecture but different release profiles.

Through the use of secondary interactions via polyanion choice and spray LbL, two ideal dual delivery systems were created. AB/AI films composed with dextran sulfate allowed for sustained release of vancomycin above the MIC for several days, and short efficacious release of diclofenac. This system is ideal for situations where anti-inflammatory drugs are primarily used as painkillers and long term suppression of proinflammatory cytokines has adverse side effects. The spray LbL system allowed for the creation of films with a large burst of antibiotic for eight hours and long term release of anti-inflammatory drug. This system is ideal for situations were antibiotics are needed during the decisive six hour period to eradicate infections, but long term release may contribute to multi-resistant bacteria formation. In addition, the long term release of anti-inflammatory drugs would allow for adverse inflammatory reactions to be addressed over physiologically relevant timescales.

**Combination Devices**

To highlight the utility and versatility of combination films, a variety of common medical products were coated. Scanning electron microscopy (SEM) images of an intraocular lens, bandage, and degradable sutures before and after coating can be seen in figure 5.11. The intraocular lenses were coated with AB/AI films using dip assembly

with dextran sulfate as the polyanion. The bandage and sutures were coated using spray LbL with AB/AI films with chondroitin sulfate as the polyanion. Intraocular lenses are used to replace the natural opaque lens in cataract surgery. Infection and inflammation are the most common side effects in cataract surgery. The SEM shows a smooth coating in the intraocular lens, which originally had a smooth surface. The only evidence of the coating is a crack in the film. Bandages are used to cover abrasions and wounds while protecting them from pathogens in the environment. The film coats the bandage fibers and covers some of the open spaces. Sutures are commonly used in surgical procedures, and fibers were completely coated by the film.

To confirm that combination devices are active against infection and inflammation, the *in vitro* activity was determined. Kirby Bauer assay and macrodilution bacterial assays were performed. The results of the Kirby Bauer assay for the bandage and macrodilution assay for the intraocular lens can be seen in figure 5.12.

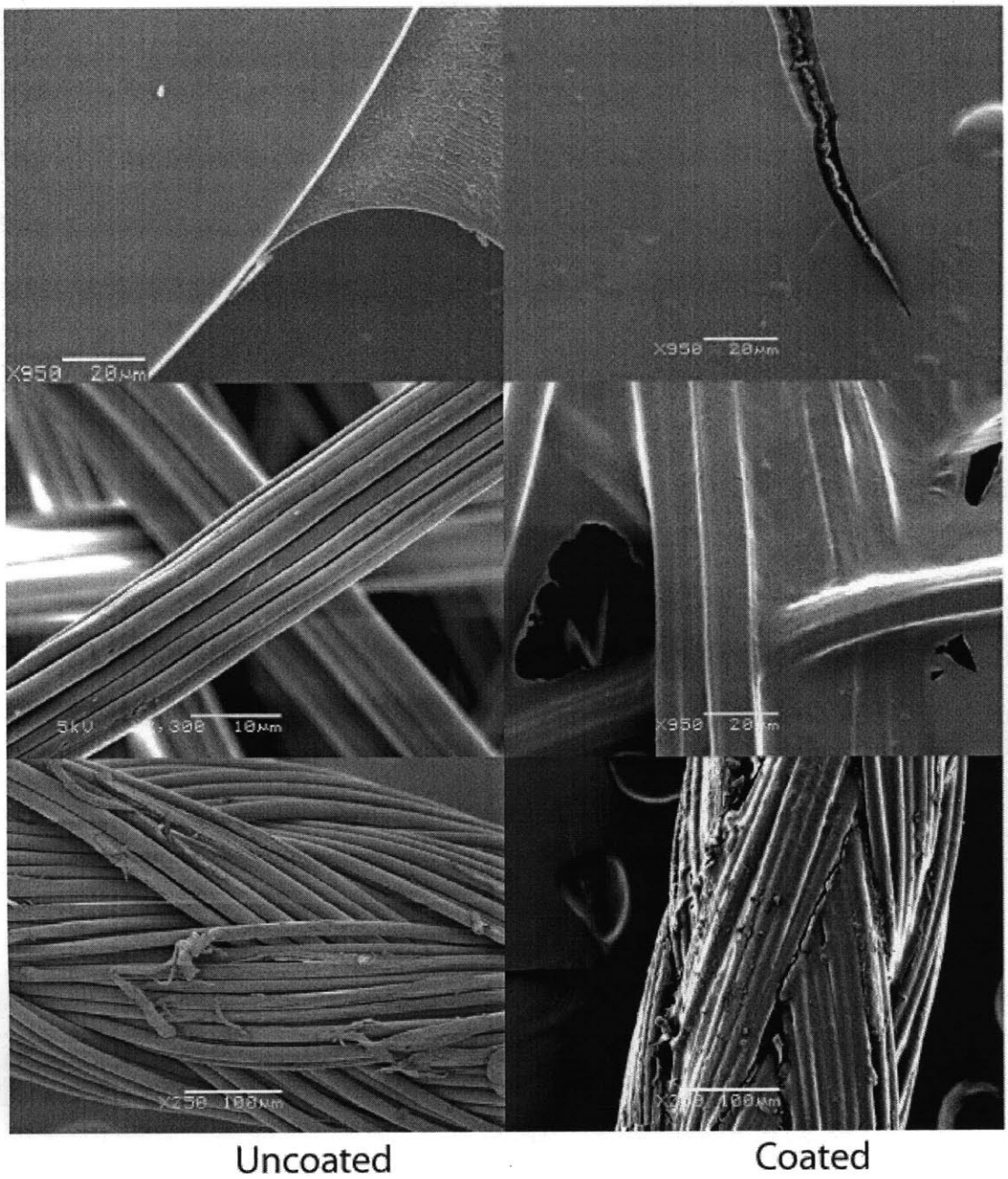


**Figure 5.11 Scanning electron microscope images of medical devices before and after coating with combination films**

Intraocular lenses, bandage, and Vicryl sutures were imaged using scanning electron microscopy before and after coating with combination films. Intraocular lenses were coated with (Poly A3/Dextran sulfate/Vancomycin/Dextran sulfate)$_{80}$(Poly A3/ PolyCD-diclofenac)$_{20}$ by dip LBL. Bandage and sutures were coated with (Poly A3/Chondroitin sulfate/Vancomycin/Chondroitin sulfate)$_{60}$(Poly A3/ PolyCD-diclofenac)$_{20}$ .

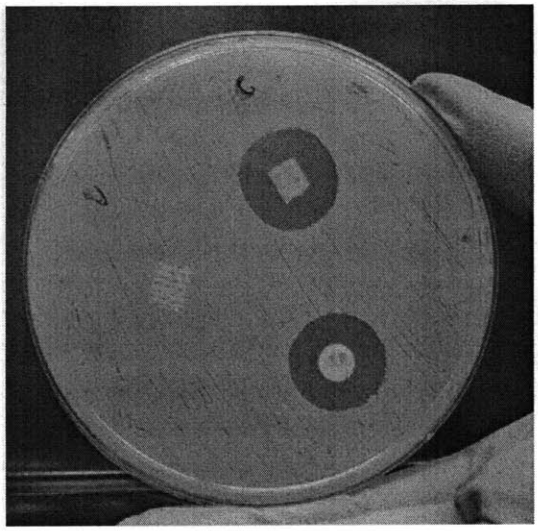

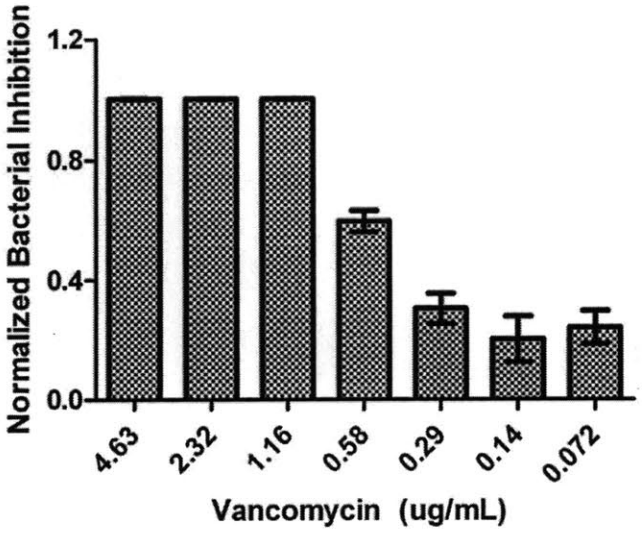


**Figure 5.12 Baterial assays on coated devices**

Kirby Bauer and macrodilution bacterial assays were performed on bandage and intraocular lenses, respectively. The top image shows the qualitative results of the Kirby Bauer assay. The top piece of bandage is coated and the piece of bandage on the left is uncoated. The disk is a 30 ug tablet of vancomycin. The bandage was coated with Poly A3/Chondroitin sulfate/Vancomycin/Chondroitin sulfate)$_{60}$(Poly A3/ PolyCD-diclofenac)$_{20}$ using spray LbL The bottom graph is the result of the macrodilution assay on the total amount of vancomycin released from intraocular lenses. The intraocular lens was coated with Poly A3/Dextran sulfate/Vancomycin/Dextran sulfate)$_{80}$(Poly A3/ PolyCD-diclofenac)$_{20}$ and fabricated using dip LbL.

The bandage resulted in a zone of inhibition similar to the 30 ug vancomycin control. Intraocular lenses inhibited bacterial growth and released vancomycin had a MIC between 0.5-1 ug of vancomycin, the same as vancomycin standard. Release media from intraocular lenses was also examined for activity against cyclooxygenase enzyme (COX), which is responsible for the production of inflammatory cytokines. Film eluent was able to suppress COX activity over the time course of release and can be seen in figure 5. 13.

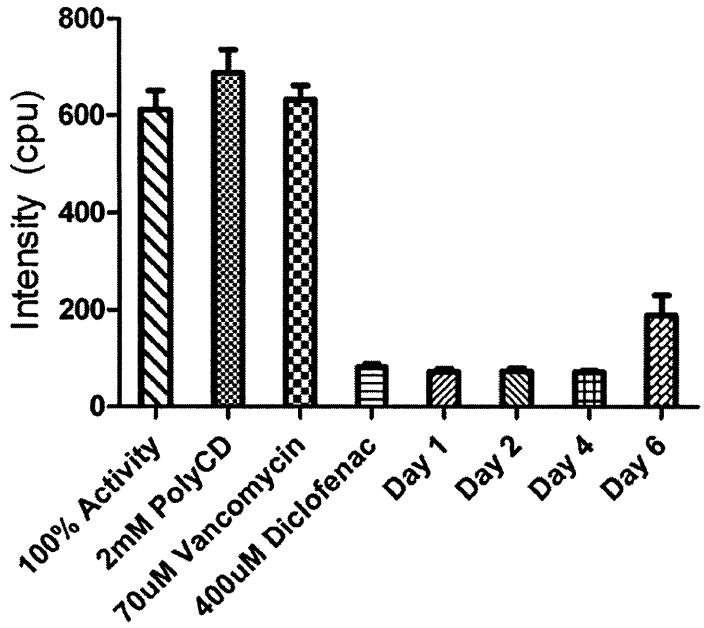


**Figure 5.13 Activity of combination films against cyclooxygenase enzyme**

The activity of cyclooxygenase enzyme incubated with polycd solution, vancomycin solution, diclofenac solution, and film eluent. Films were composed of (Poly A3/Dextran sulfate/Vancomycin/Dextran sulfate)$_{80}$(Poly A3/ PolyCD-diclofenac)$_{20}$ and released in PBS at 37°C.

## Conclusion

Infection and inflammation have plagued the success of medical procedures and device implantation for generations. Though sophisticated pharmaceuticals have been created to prevent and treat these conditions, they have been unable to eradicate complications. Moreover, the systemic administration of therapeutics is often associated with adverse side effects and/or toxicity. There is a need for systems able to control both infection and inflammation at the pathological site. The modification of device surfaces with drug loaded thin films is a promising technology for local inflammatory and infection control. The ability to coat virtually any surface regardless of geometry and surface chemistry has brought layer-by-layer to the forefront of these endeavors. Here, the first layer-by-layer (LbL) system able to counteract both infection and inflammation is described. The system utilized both dip and spray LbL to construct hydrolytically degradable multilayer films composed of an antibiotic and anti-inflammatory agent. Both release and dosage could be widely varied through the selection of film components and assembly methods. A novel interaction between vancomycin hydrochloride and diclofenac was discovered and the interaction between vancomycin and a polymeric cyclodextrin was demonstrated. Spray LbL and secondary chemical interaction were used to enhance drug release and overcome undesired interactions observed during dip LbL. The versatility of combination films was illustrated through the coating of ubiquitous healthcare products. Combination antibiotic and anti-inflammatory films sufficiently coated device surfaces and effectively prevented bacterial growth while suppressing the production of inflammatory cytokines. The creation of a drug delivery coating capable of sustained release of an antibiotic and anti-inflammatory therapeutic is a powerful tool in

the fight against device associate morbidity and mortality and represent a key advance in the utilization of layer-by-layer for biomedical applications.

## References


[1] M. Zilberman, J. J. Elsner, *J. Controlled Release* **2008**, *130*, 202.
[2] E. M. Hetrick, M. H. Schoenfisch, *Chem. Soc. Rev.* **2006**, *35*, 780.
[3] J. M. Anderson, A. Rodriguez, D. T. Chang, *Seminars in Immunology* **2008**, *20*, 86.
[4] P. Thevenot, W. J. Hu, L. P. Tang, *Current Topics in Medicinal Chemistry* **2008**, *8*, 270.
[5] D. M. Lynn, *Soft Matter* **2006**, *2*, 269.
[6] K. C. Wood, H. F. Chuang, R. D. Batten, D. M. Lynn, P. T. Hammond, *Proceedings of the National Academy of Sciences of the United States of America* **2006**, *103*, 10207.
[7] A. Shukla, K. E. Fleming, H. F. Chuang, T. M. Chau, C. R. Loose, G. N. Stephanopoulos, P. T. Hammond, *Biomaterials* **2010**, *31*, 2348.
[8] R. C. Smith, M. Riollano, A. Leung, P. T. Hammond, *Angewandte Chemie-International Edition* **2009**, *48*, 8974.
[9] B. S. Kim, R. C. Smith, Z. Poon, P. T. Hammond, *Langmuir* **2009**.
[10] H. J. Busscher, R. J. Ploeg, d. M. H. C. van, *Biomaterials* **2009**, *30*, 4247.
[11] B.-S. Kim, S. W. Park, P. T. Hammond, *ACS Nano* **2008**, *2*, 386.
[12] Z. Li, D. Lee, X. Sheng, R. E. Cohen, M. F. Rubner, *Langmuir* **2006**, *22*, 9820.
[13] M. Malcher, D. Volodkin, B. Heurtault, P. Andre, P. Schaaf, H. Mohwald, J. C. Voegel, A. Sokolowski, V. Ball, F. Boulmedais, B. Frisch, *Langmuir* **2008**, *24*, 10209.
[14] P. M. Nguyen, N. S. Zacharia, E. Verploegen, P. T. Hammond, *Chemistry of Materials* **2007**, *19*, 5524.
[15] S. Y. Wong, Q. Li, J. Veselinovic, B. S. Kim, A. M. Klibanov, P. T. Hammond, *Biomaterials*, *31*, 4079.
[16] T. Boudou, T. Crouzier, K. F. Ren, G. Blin, C. Picart, *Advanced Materials* **2010**, *22*, 441.
[17] A. Shukla, P. T. Hammond, *Unpublished work* **2010**.
[18] N. B. Jessel, P. Schwinte, R. Donohue, P. Lavalle, F. Boulmedais, R. Darcy, B. Szalontai, J. C. Voegel, J. Ogier, *Advanced Functional Materials* **2004**, *14*, 963.
[19] A. Schneider, C. Vodouhe, L. Richert, G. Francius, E. Le Guen, P. Schaaf, J. C. Voegel, B. Frisch, C. Picart, *Biomacromolecules* **2007**, *8*, 139.
[20] N. Benkirane-Jessel, P. Schwinte, P. Falvey, R. Darcy, Y. Haikel, P. Schaaf, J. C. Voegel, J. Ogier, *Advanced Functional Materials* **2004**, *14*, 174.
[21] R. C. Smith, A. Leung, B. S. Kim, P. T. Hammond, *Chemistry of Materials* **2009**, *21*, 1108.
[22] D. G. Anderson, D. M. Lynn, R. Langer, *Angew. Chem. Int. Ed.* **2003**, *42*, 3151.

[23] E. Vazquez, D. M. Dewitt, P. T. Hammond, D. M. Lynn, *Journal of the American Chemical Society* **2002**, *124*, 13992.
[24] K. C. Krogman, N. S. Zacharia, S. Schroeder, P. T. Hammond, *Langmuir* **2007**, *23*, 3137.
[25] A. L. Barry, e. al., *Clin Lab Stand Inst* **1999**, *18*, 32.
[26] M. Civan, *Vol. 45*, Academic Press, San Diego, California, **1998**.
[27] R. Chadha, N. Kashid, A. Saini, *Journal of Scientific & Industrial Research* **2004**, *63*, 211.
[28] T. Loftsson, D. Hreinsdottir, M. Masson, *International Journal of Pharmaceutics* **2005**, *302*, 18.
[29] N. Blanchemain, T. Laurent, F. Chai, C. Neut, S. Haulon, V. Krump-konvalinkova, M. Morcellet, B. Martel, C. J. Kirkpatrick, H. F. Hildebrand, *Acta Biomater* **2008**, *4*, 1725.
[30] S. Lepretre, F. Chai, J. C. Hornez, G. Vermet, C. Neut, M. Descamps, H. F. Hildebrand, B. Martel, *Biomaterials* **2009**, *30*, 6086.
[31] K. C. Krogman, J. L. Lowery, N. S. Zacharia, G. C. Rutledge, P. T. Hammond, *Nat Mater* **2009**, *8*, 512.
[32] K. C. Krogman, K. F. Lyon, P. T. Hammond, *J Phys Chem B* **2008**, *112*, 14453.
[33] K. C. Krogman, N. S. Zacharia, S. Schroeder, P. T. Hammond, *Langmuir* **2007**, *23*, 3137.

# Chapter 6 : Conclusion

## Thesis Summary

In twenty eight years, layer-by-layer assembly has become a quintessential tool for the creation of versatile, dynamic nanostructured materials able to dictate cellular behavior through exquisite surface functionality and delivery of bioactive agents. The primary aim of this work was to use layer-by-layer assembly to advance ophthalmic drug delivery modalities post cataract surgery to overcome the challenges of traditional postoperative therapy. Efforts focused on tailored release kinetics and controlled efficacious delivery of appropriate therapeutics. Hydrolytically degradable multilayer films were chosen as a vehicle due to their ability to provide sustained, spatiotemporal drug delivery, while offering valuable yet temporary surface functionality. The establishment of a drug delivery coating for intraocular lenses required key advances in ultrathin film technology. The fundamental understanding of layer-by-layer systems was improved and key challenges were surmounted to build the necessary technological foundation to design a drug delivery coating for intraocular lenses able to prevent complications of cataract surgery.

The design of hydrolytically degradable systems with specified release dynamics requires a fundamental understanding of the influence of polymer structure on release. With this knowledge, release duration can be predicted *a priori* and advance engineered. Though previous research highlighted the ability of different poly(β-amino esters) to change release kinetics, no framework for rational polymer design existed. In chapter two, a structure property relationship study for poly(β-amino esters) in LbL

constructs was conducted.[1] A small library of poly(β-amino esters) varying only in choice of diacrylate monomer used in synthesis was constructed. The growth, release, and degradation properties of films composed of a poly(β-amino esters) and dextran sulfate were examined. This led to the discovery of an unknown phenomenon in electrostatic layer-by-layer films, destabilization due to extreme hydrophobicity. Release duration was found to correlate linearly with the octanol:water coefficient of the diacrylate monomer, providing design rules for this powerful thin film system. The resulting framework was used to tailor drug release in subsequent chapters.

A significant challenge in layer-by-layer is the incorporation and release of small molecule therapeutics with the same characteristic control as macromolecules. Electrostatic layer-by-layer assembly is based on the alternating absorption of polyelectrolytes in aqueous solution. However, 85 % of all FDA approved drugs are small molecules, most of which are hydrophobic and/or uncharged.[2] Previous research has focused on direct drug absorption and a variety of charged drug carriers to overcome this limitation. Yet, all systems suffered from burst release, short release timescales, and/or diffusion based release kinetics. In chapter three, the first ultrathin film system able to deliver a broad range of active small molecule therapeutics with programmable zero order release kinetics through facile aqueous based assembly was described.[3] This system illustrated the first use of polymeric cyclodextrins as carriers for hydrophobic and/or uncharged small molecules. Films constructed from poly(β-amino esters) and poly(carboxymethyl-betacyclodextrin) were shown to deliver nonsteroidal anti-inflammatory drugs for several weeks. Therapeutic release was based on surface erosion and could be modulated through selection of the degradable

polycation. This platform technology for small molecule delivery opened the door for bioactive coatings able to address postoperative inflammation over physiological relevant timescales.

Successful delivery systems hinge on the ability to appropriately regulate cell behavior. However cellular interactions with hydrolytically degradable film had not been previously investigated. The constant aqueous based erosion provides engaging questions about cell adhesion and growth abilities on hydrolytically degradable systems. In addition, the stability of these constructs when subject to cell degradative products has remained a pivotal question in the field and the ability of hydrolytically degradable layer-by-layer films to support cell growth remained unseen. Furthermore, no layer-by-layer construct able to control in situ inflammation over physiologically relevant timescales, days to weeks, had been constructed. In chapter four, the cellular interaction of the hydrolytically degradable small molecule delivery system developed in chapter three was examined. Cell adhesion was reduced on hydrolytically degradable films containing polymeric cyclodextrins. Low cell adhesion is preferable for many systems, including IOLs where adverse cell adhesion and proliferation lead to the formation of a secondary cataract. However, the cells that did adhere proliferated normally and no significant difference existed between hydrolytically degradable films and controls after three days. NSAID containing films suppressed the production of inflammatory cytokines for neighboring cells and those in direct contact for two weeks. The first steps toward a bioactive coating for IOLs were undertaken, by coating IOLs with anti-inflammatory films. Anti-inflammatory films were transparent and maintained the macroscopic optical properties of the IOL. Film release kinetics were unaltered on

intraocular lenses and coatings did not increase the adhesion or proliferation of human lens epithelial cell on intraocular lenses.

In chapter five, the first LbL system able to address infection and inflammation using small molecule pharmaceutics was constructed. Multi-agent films were composed of the previously described anti-inflammatory system and the antibiotic portion was fabricated from a previously described system composed of poly(β-amino esters), natural polymers, and vancomycin in a tetralayer architecture.[3, 4] These dual functional films achieved a variety of concurrent release profiles. Combination devices were constructed by coating bandage, intraocular lenses, and sutures with multi-agent films. These devices were able to control cyclooxygenase enzyme activity while preventing bacterial growth.

## Future Work

Several recommendations can be made to further advance layer-by-layer technology toward the production of multi-functional bioactive thin film assembly. Rational design of hydrolytically degradable polyelectrolyte multilayer films could be enhanced through understanding the role of the amine in poly(β-amino esters). Future efforts should also focus on the design of new charged hydrolytically degradable polymers for multilayer formation. Lynn created polymers whose net charged changed with hydrolysis of pendant groups.[5] These cationic "charge shifting" polymers went from positive to negatively charged in a time dependent manner and allowed for the extended, long term release of plasmid DNA. More hydrolytically controlled charged polymers will expand the capabilities of this unique delivery system. The role of complexation coefficient on release dynamics of cyclodextrin containing films will allow

the full power of this platform technology to be harnessed. A plethora of therapeutic choices will open the door to personalized medicinal coatings for IOLs through tailored drug selection.

Understanding the nature of cell adhesion on anti-inflammatory films containing cyclodextrins may enable the creation of non-adhesive substrates or methods to increase cell attachment. Previous research has focused on control of cell adhesion, proliferation, differentiation, and behavior on layer-by-layer films using chemical and mechanical modulation.[6] The design of bioactive permanent coatings such as, non-fouling or non-adhesive surfaces, under degradable multi-functional drug delivery coatings will allow for additional and improved regulation of cell behavior. While chemical and mechanical properties have been previously investigated as regulators of cell dynamics, cytokine production on polyelectrolyte multilayers and the films' ability to absorb mediators may have a profound effect on cellular behavior and should be investigated.

Barrier layers have been used to prevent interactions in layer-by-layer assemblies.[7, 8] However, most are permanent and interfere with drug release. Research should focus on the development of degradable barrier layers that do not adversely effects drug release dynamics. The use of degradable barrier layer between antibiotic and anti-inflammatory units to form combination films may allow for a broader range of release profiles to be achieved. Multilayer transfer printing, transfer of multilayer thin films onto a surface via contact printing, has enabled the creation of multi-functional thin film systems.[9] Use of printing to combine anti-inflammatory and antibiotic components may limit the system dynamics that interfere with controlled

sustained release capabilities. In addition, other antibiotics should be explored for combination systems such as broad spectrum fluoroquinolones and agents effective against gram negative bacteria. A variety of therapeutic choice will enhance the versatility of this system. Lastly, *in vivo* studies will allow this drug delivery construct to be evaluated in context.

Although this research focused on constructing an ideal coating for intraocular lenses, the potential for infection and inflammation exist for all surgical procedures. The knowledge gained and advances developed here can and should be applied to any implantable device, including biomaterials and tissue engineering constructs. Utilization of the work herein will expand the scope of degradable multilayer films to applications such as microreactors, bioMEMs, agriculture, and basic scientific research while opening the door to personalized nanomedicine coatings and small molecule technologies.

## References


[1] R. C. Smith, A. Leung, B. S. Kim, P. T. Hammond, *Chemistry of Materials* **2009**, *21*, 1108.

[2] D. J. Newman, G. M. Cragg, K. M. Snader, *Journal of Natural Products* **2003**, *66*, 1022.

[3] R. C. Smith, M. Riollano, A. Leung, P. T. Hammond, *Angewandte Chemie-International Edition* **2009**, *48*, 8974.

[4] A. Shukla, P. T. Hammond, *Unpublished work* **2010**.

[5] D. M. Lynn, *Advanced Materials* **2007**, *19*, 4118.

[6] T. Boudou, T. Crouzier, K. F. Ren, G. Blin, C. Picart, *Advanced Materials* **2010**, *22*, 441.

[7] S. Peralta, J. L. Habib-Jiwan, A. M. Jonas, *Chemphyschem* **2009**, *10*, 137.

[8] K. C. Wood, H. F. Chuang, R. D. Batten, D. M. Lynn, P. T. Hammond, *Proceedings of the National Academy of Sciences of the United States of America* **2006**, *103*, 10207.

[9] J. Park, L. D. Fouche, P. T. Hammond, *Advanced Materials* **2005**, *17*, 2575.